Supersaturating oral delivery systems of poorly water-soluble compounds produced by hot melt extrusion

Inauguraldissertation

zur

Erlangung der Würde eines Doktors der Philosophie

vorgelegt der

Philosophisch-Naturwissenschaftlichen Fakultät

der Universität Basel

von

Felix Ditzinger

Basel, 2020

Genehmigt von der Philosophisch-Naturwissenschaftlichen Fakultät

auf Antrag von

Erstbetreuer	Herr Prof. Dr. Georgios Imanidis
Zweitbetreuer	Herr Prof. Dr. Matthias Hamburger
Externer Experte	Herr Prof. Dr. Kyriakos Kachrimanis

Basel, den 17. März 2020

Prof. Dr. Martin Spiess

Dekan

Nothing in life is to be feared, it is only to be understood.

Now is the time to understand more, so that we may fear less.

Marie Skłodowska Curie

Abstract

The field of enabling techniques for poorly water-soluble drugs has been growing over the last decades. Therefore, different formulation strategies and processes have gained relevance within the development of solid pharmaceutical dosage forms for oral drug delivery. A prominent example to manufacture such dosage forms is the process of hot melt extrusion, where mostly combinations of polymers and drugs are melted together and processed to result in an amorphous solid dispersion as a biopharmaceutically enhanced drug delivery system. The final extrudate needs to be further processed downstream for example in a mill or a pelletizer. Processing a drug in an extruded form comes with the advantage of increased apparent solubility and therefore increased amount of dissolved drug available for absorption in the gastrointestinal tract. A crucial quality attribute for this formulation approach is selecting the most suitable polymer in combination with a given drug. To identify the most suitable polymer, a variety of screening approaches can be applied. Some approaches make use of the Flory-Huggins interaction parameter or a comparison of Hansen solubility parameters, while an important experimental alternative is the screening of polymers for amorphous drug stabilization (SPADS) approach. However, a suitable polymer cannot always be found so that a compromise may lead to unbeneficial formulation characteristics. There is current research focusing on the development of new synthetic polymers based on chemical monomer engineering as well as the combination of polymers. Another approach is the addition of a small molecular additive for the stabilization of a drug without the necessary use of a polymer, i.e. so-called co-amorphous systems.

In this work, the interaction of an additive and the modification of the polymer are combined in molecularly designed polymeric matrices consisting of interacting small molecular additives and a polymeric excipient. The key aspect of this development is the specifically targeted molecular interaction between polymer and additive, which alters matrix characteristics thereby leading to possible benefits on the level of processing, amorphous stability and/or aqueous dispersion and drug release.

The first study consisted of establishing a concept of combining acidic co-formers with a basic polymer to improve processablity as well as drug release. In the beginning of this study, the co-former malic acid was identified to be most beneficial for the formulation with the polymer Eudragit E PO (dimethylaminoethyl methacrylate copolymer). Interactions between the additive and the polymer were confirmed by Fourier transform infrared spectroscopy (FTIR) and ^{13}C-nuclear magnetic resonance spectroscopy (NMR). These interactions were also present after the addition of the drug fenofibrate. In the next step, the amorphous stability of the additive-containing formulation was compared with the corresponding non-additive formulation via

atomic force and scanning electron microscopy (SEM). By using energy dispersive X-ray spectroscopy during the SEM measurement, the drug was found to be dispersed homogenously in the malic acid formulation, whereas in the control formulation without additive, drug-rich domains were visible. This finding was supported by an observed phase separation in phasing images of atomic force microscopy using the control formulation.

In addition to the improved stability, the additive formulation showed improved drug release compared to the control formulation and the corresponding physical mixture. Since an extruded formulation requires further downstream processes, such as milling or grinding in a mortar, the powderized extrudate should have sufficient flowability to enable any subsequent processing such as tableting. The modified matrix formulation showed also in this technical aspect better flowability than the control formulation or the pure polymer.

To conclude in this case study on Eudragit E PO, the addition of malic acid to the polymer showed a specific molecular interaction and resulted in different formulation improvements with regards to amorphous stability, downstream processability as well as drug release.

In the second study, a polymer, which is not extrudable in its neat form, was modified in a way to make it applicable for extrusion. Different small molecular additives were investigated each as interacting partner with the polyelectrolyte sodium carboxymethyl cellulose (NaCMC). Studied additives were trometamol, urea, meglumine, and the amino acids lysine, histidine, arginine. These additives were intended to exert strong specific interactions with the macromolecular polyelectrolyte via acid-base-interactions. As manufacturing technique, a combination of solvent evaporation (with and without additive) and subsequent hot melt extrusion was conducted as a two-step process. Such processing served as a model of what an excipient supplier would do to make the modified NaCMC matrix available for a pharmaceutical company to process it together with a drug by hot melt extrusion. Initially, the maximum amount of additive in combination with NaCMC was determined for which an amorphous solid dispersion was still feasible as produced by extrusion. As a result, an excess molar amount of interacting additive was generally needed because amounts of additives below 15 % were shown not to be applicable for improving the extrusion behavior of the polymer. There was on the other hand also a maximum suitable additive concentration given with higher concentrations leading to residual crystallinity after extrusion.

The suitable polyelectrolyte matrices, which showed no indication of crystallinity in the laboratory X-ray diffraction analysis, were further investigated for homogeneity and crystallinity by synchrotron X-ray diffraction. Moreover, possible interactions and melting behavior were studied by hot stage microscopy and heat-assisted FTIR. It was shown that the polyelectrolyte matrices containing either meglumine, lysine, or urea resulted in an amorphous homogenous formulation. This finding was in line with the extrusion performance as well as the heat-assisted FTIR spectroscopy. Therefore, the promising

meglumine and lysine excipient matrices were analyzed further in a subsequent study using a model drug.

In line with the assessment of glass forming ability, the third study was designed for the practical comparison of two crucial enabling techniques i.e. hot melt extrusion and mesoporous silica. Therefore, two drugs, which are instable glass formers, were selected for a stability-based comparison under ICH Q1 accelerated stability conditions. For an increase in measurement sensitivity, the extruded samples were examined at the start of the study and the end using ^{13}C solid-state NMR. This comparison was complemented by drug dissolution studies in biorelevant media at defined time points. In line with theoretical expectations about drugs that are challenging to stabilize in amorphous form, this study confirmed the superior stabilization capabilities of mesoporous silica formulations for which drug was successfully loaded and confined in mesopores. In contrast, the extruded formulations were not able to stabilize the challenging model drugs in their amorphous form over the duration of a three months stability study. These findings were underlined by results of the non-sink dissolution profiles at the defined time points, which showed a comparative decrease in supersaturation for the extruded formulations. The silica formulations, which were lacking the necessary precipitation inhibitor, showed just a "spring-effect" of high supersaturation but they could not sustain it without further excipients to act as a "parachute". There was no decrease in the initial drug supersaturation visible over the duration of the study, which was in line with the solid-state evaluation. In conclusion, this study shows the advantage of mesoporous silica to formulate drugs that have a high tendency to recrystallize so that classical polymeric solid dispersions exhibit a substantial risk of physical instability.

The knowledge gained from the second study formed the basis of the fourth study. The two most promising candidates from the synchrotron study of the modified matrices, which were the lysine and the meglumine formulations, were further investigated regarding their biopharmaceutical properties. Thus, the model drug fenofibrate was selected as quantitative marker for *in vitro* and *in vivo* performance. During the pre-evaluation of the solid state, the amorphous form of both formulations was confirmed via powder X-ray diffraction as well as differential scanning calorimetry. Moreover, a possible interaction was investigated via FTIR.
The *in vitro* non-sink experiments in Fasted Simulated Intestinal Fluid (FaSSIF) showed a higher supersaturation and parachute effect for both formulations compared to the corresponding non-modified matrix without additive. The physical mixture only showed a slight drug release in the beginning, which decreased even more over time. Due to high viscosity, which was measured in separate rheological measurements, there was a 30 min delay in drug release observed in the extruded formulations. These findings agreed with results of the subsequent *in vivo* rat study, which showed a significant difference between the AUCs of the meglumine formulation and the corresponding physical mixture as well as differences in the C_{max} values between both formulations and their physical mixtures. Therefore, this

study showed the beneficial impact of the selected additives on the biopharmaceutical performance of the model drug fenofibrate.

In conclusion, this thesis focused on designing modified polymeric matrices based on targeted molecular interactions of additives and drug carriers. Small molecular additives were used in amorphous solid dispersions with a special emphasis on hot melt extrusion. It could be demonstrated that the careful selection of small molecular additives, which interact with a polymer, could have a beneficial impact on the manufacturing process, the physical stability, and/or biopharmaceutical release properties of a drug from its amorphous form. Different analytical methods supported the view of the intended molecular interactions in the modified matrices but the various technical and biopharmaceutical benefits are currently hard to predict theoretically. While we used molecular simulations occasionally to visualize candidate mixtures for experimental evaluation, a next step would be a more intensive use of *in silico* tools to predict formulation performance and to screen mixtures in the computer.

In line with current research and practice in the pharmaceutical industry, the selection of excipients during the early formulation development is crucial for the successful design of an amorphous drug delivery system on the market. This work showed that the addition of interacting small molecular additives could have a positive impact on the resulting matrix properties and therefore this would broaden the variety of suitable polymer matrices not by any covalent bonds in the synthesis of novel polymers but by virtue of a physical modification of the polymer through the given additive. The presented approach of a modified polymeric matrix therefore holds much promise in future pharmaceutical development of amorphous drug products.

Contents

Acknowledgments

Great thankfulness goes to Professor Georgios Imanidis, who made my PhD at the University of Basel possible. Moreover, he provided me with the support on my scientific capabilities as well as the opportunity to grow in the field of pharmaceutical sciences.

The intense supervision by Professor Martin Kuentz encouraged me to always go further on a scientific path and motivated me to thrive for perfection. I am tremendously happy that he kept motivating me and helped me to become the researcher I am today.

I would like to thank Professor Kyriakos Kachrimanis, who reviewed this thesis as external expert and provided valuable feedback.

The PEARRL network provided me with the irreplaceable opportunity of having 14 fellow PhD students in Europe to collaborate with on various projects. Therefore, I would like to thank my fellow researchers in the PEARRL network with special regards to Daniel, Georgia and Marina as well as my co-supervisors Dr. René Holm and Dr. Brendan Griffin.

I would also like to acknowledge the support of the colleagues at the HPRA in Dublin, Ireland, who provided me with the opportunity to gain insights in the regulatory implications on the pharmaceutical industry.

My gratitude also goes to the amazing colleagues at Merck in Darmstadt, who made the stay at Merck possible. In particular, Dr. Christoph Saal and Dr. Anita Nair need to be mentioned as the driving force of my successful industrial research stay.

Many thanks also go to my colleagues at the University of Applied Sciences and Arts of Northwestern Switzerland, especially Andreas, Kira, Matthias, Uta, Oliver, and Mustafa. Moreover, I am grateful for the time spent with my fellow PhD students working at FHNW and those from other universities, who participated at numerous occasions into scientific as well as non-scientific discussions.

Der Rückhalt meiner Familie hat mich stetig bestärkt. Hierfür danke ich meinen Eltern und meiner Schwester, die sich an Wochenenden, bei Besuchen in Basel oder anderen Anlässen Details meiner Arbeit anhören mussten, ob sie wollten oder nicht.

Introduction

1.1 Background

In the recent years, the poor water solubility of newly developed compounds has presented a major challenge for formulation scientists in the field of pharmaceutical development. There is a great need of exactly identifying the solubility limiting factors as well as techniques to cope with them.

The introduction of a biopharmaceutics classification system (BCS) by Amidon and colleagues [1] provided guidance to point out oral biopharmaceutical performance challenges of such components. The classification was particularly useful to design bioequivalence studies but appeared to address less the needs of scientists in early formulation development. The classification was therefore developed further by Butler and Dressmann, who provided differentiation in the so-called developability classification system (DCS) [2]. In the DCS, the class 2 of the BCS system is further divided in 2a and 2b to highlight the drugs for which solubility enhancement would be favorable to improve oral bioavailability [2]. Substances in class 2a profit mostly from an increased dissolution rate, which can be achieved for example by particle size reduction. In contrast, an increase in solubility would lead to higher bioavailability of class 2b substances [2,3]. The DCS was advanced to the refined DCS or rDCS, which consisted of better integration of weak bases and their salts [4]
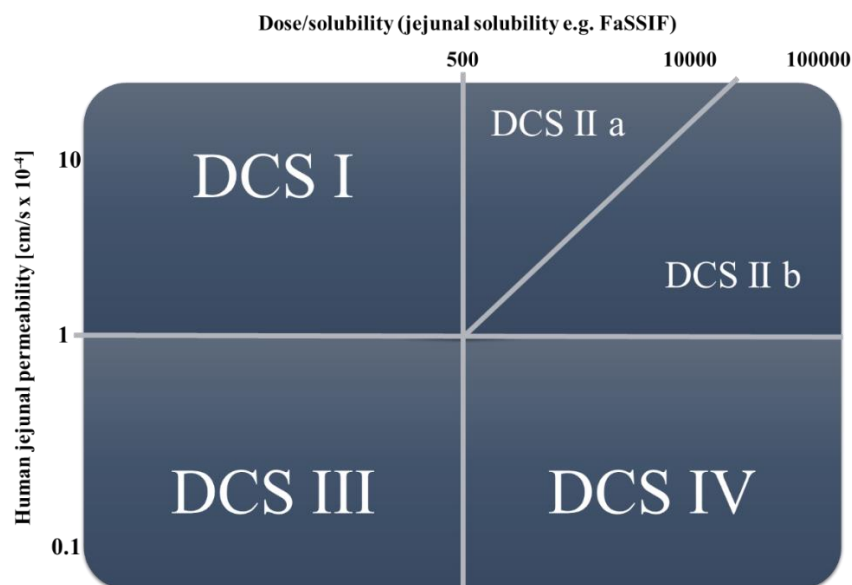

Figure 1.1. Developability classification system according to Butler and Dressman

Limiting factors of the previously mentioned solubility of DCS class 2b substances can be described as solvation and/or solid-state limiting factors [5–7]. Such factors are expressed for example in the general solution equation (GSE) for non-electrolytes (Equation 1) [8].

$$\log S_w = 0.5 - 0.01 \, (T_m - 25) - \log P \tag{1}$$

The GSE presents the aqueous solubility ($\log S_w$) as a function of a compound's crystal lattice energy and lipophilicity expressed as the melting point (T_m, in K) and the octanol/water partition coefficient ($\log P$) and allows an estimation of the solubility based on the before mentioned parameters. High T_m values and moderate or low $\log P$ values are often associated with "brick-dust" characteristics, whereas a substance with low T_m and high $\log P$ values can be referred to as "grease ball". Brick-dust molecules with structural features like aromaticity and rigidity exhibit a solid-state limited solubility as a result of a stable crystal structure with breakdown of the crystal lattice as the most difficult step for the drug release [9]. For grease-ball substances, the molecular features that lead to high partitioning into an apolar phase e.g. as inferred from the Abraham solvation predictors [10,11], have the solvation step in water as the main hurdle for drug dissolution [12,13]. The use of Abraham solvation predictors was recently reported to gain a better understanding of the molecular drug characteristics that drive solubilisation in biorelevant media [14].

It is clear that an improved molecular understanding of solubility limitations would be of great help in the drug discovery phase when designing and selecting drug candidates. General developability criteria other than the DCS, such as Lipinski's rule of 5 [15], could be further refined so there is clearly more research to be done in this field. Novel compounds from drug discovery present frequent issues for formulation development as they often have high T_m and high $\log P$ [16–19]. While T_m is a characteristic of the above mentioned crystal lattice energy, $\log P$, as a partition coefficient, denotes a solvation tendency or a lack of the same. Most importantly, high values of T_m and $\log P$ limit aqueous solubility and consequently often bioavailability when administered orally in conventional dosage forms [5,20,21].

Therefore, such compounds require a bio-enabling formulation approach [22]. A broad variety of formulation approaches exist in the field of pharmaceutical research. Such an approach is a lipid based formulation, where the drug is dissolved or suspended in a lipid and ideally maintained in the solubilised/supersaturated state in the course of lipid dispersion and digestion [20]. This formulation approach comes with the advantage of increasing the gastrointestinal (GI) solvation capacity of drugs [23] as well as leading to drug supersaturation in the intestine by fast digestion and absorption of the lipid [24]. Therefore, lipolysis is an essential part of the in vivo performance of lipid based systems [25].

A further approach is the formulation of a nanosuspension, which can be formed by breaking down larger micron-sized particles down (i.e. top-down approach). These broken down particles are then stabilized by a mixture of polymer and surfactant, as in a wet milling technique [26]. Such an approach is of particular interest when high lattice energy decreases the solubility in any solvent tremendously so that any direct solution formulation as final dosage form becomes hard to achieve [27].

Cyclodextrin formulations can form an inclusion complex with the drug as a result of their hydrophilic outside and hydrophobic cavity [28,29]. Such a complex is an ideal combination, because it can incorporate the hydrophobic drug on the inside, while it can be solubilized upon dispersion in the GI fluids after oral administration, which leads to an increase in apparent drug solubility [30].

Another bio-enabling formulation approach is the transformation of the drug into its amorphous form. This drug form leads to an increase in the apparent solubility of the drug [31], which may lead to different extents of supersaturation upon aqueous dispersion. Different types of amorphous drug formulations and solid solutions were named together under the umbrella term "solid dispersion" by Chiou and Riegelmann [32,33]. Any amorphous solid dispersion (ASD) also comes with the downside of possible recrystallization in the solid state, which means the drug changes to the energetically more favorable crystalline form (Section 2.1.2.1), which has the typical consequence of losing some of the increased apparent solubility.

The variety of formulation strategies reflects the fact that there is not a "one size fits all" approach. It is critical to more rationally select a bio-enabling formulation type based on the given drug properties. Therefore, we developed a decision tree with a focus on amorphous formulation and at what point other formulation techniques should be applied. There are critical drug properties [13,34,35], which greatly affect the successful amorphization as well as determine the process used. Based on the above-mentioned considerations Figure 1.2 describes how the glass forming ability (GFA) (Section 2.1.2.3) and other drug properties can be applied in the process of formulation technique selection.
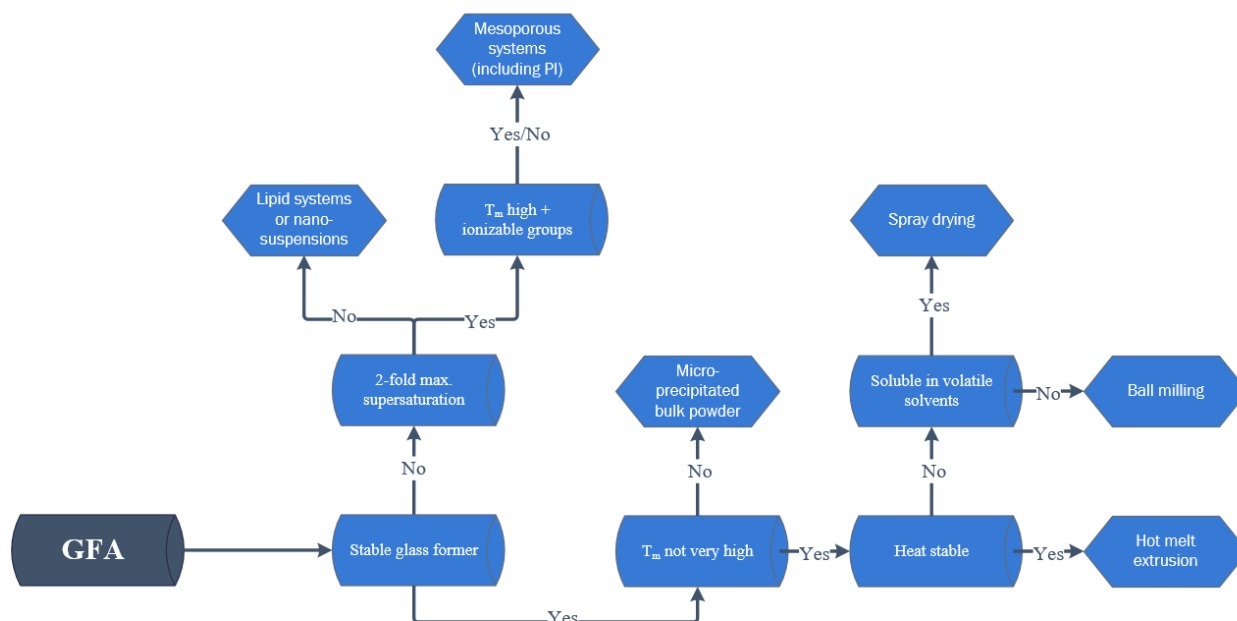
Figure 1.2. Decision tree for the manufacturing technique of an enabling formulation

The developed decision tree starts with the applicability of a specific GFA class for the compound [36], which is commonly determined by scanning differential calorimetry. If such measurement results are not available, GFA can be estimated based on molecular properties by Mahlin and Bergström [34] or Wyttenbach and Kuentz [37]. GFA is about differentiation of non-glass forming compounds (or poor glass formers) vs. glass-formers where the latter can be further differentiated according to the stability of the glass [36,38]. Since poor glass formers tend to show a reduced amount of drug supersaturation [36,38,39], the supersaturation potential needs to be evaluated. The combination of poor glass formation and low supersaturation potential discourages the selection of a solid dispersion and would then lead to a preferable formulation in a lipid system or nanosuspension. For increased stabilization of a supersaturating instable glass former in dependence of high melting point and ionizable groups either micro-precipitated bulk powder (MPB) or mesoporous systems (with a precipitation inhibitor) should be selected. The MPB technology is also an option in case that a stable glass former has a very high T_m. For stable glass formers, which are heat stable and have a moderate T_m, extrusion is a feasible amorphization method. In case that such a substance is not heat stable but soluble in volatile solvents, it can be alternatively processed in a spray dryer or if the solubility in volatile solvents is not sufficient, ball milling could be performed in combination with a small molecular co-former [40].

Figure 1.2 highlights the necessity of a polymer for the majority of formulation approaches. Therefore, such a selection can be crucial for the performance of a bio-enabling drug delivery system. A review of the polymers used in amorphous formulations showed that a small number of polymers is used in marketed amorphous drug products [41], which underlines the need for more polymers. The development of new polymers would come on one side with more options to choose a polymer for a

given drug. On the other side, the implementation of such a newly developed polymer would result in regulatory hurdles to approve the novel excipient, which is particularly demanding when it is a new chemical entity. A possible solution to this challenge is the combination of approved polymers and additives to develop new polymeric matrices. Such an approach of a modified polymeric matrix is based on specifically targeted molecular interactions that are comparatively strong, which is different to an ordinary formulation strategy. The intelligent choice of an additive with the potential to interact may result in technical process benefits, higher amorphous stability of the drug in the modified matrix as well as drug release advantages of the polymeric matrix as well as the possibility of also interacting with the drug and stabilize all components in the formulation.

As shown in Figure 1.3, there are various characteristics necessary for an excipient. These requirements can be divided into aspects like regulatory acceptance for oral use, which are more important for the approval of a drug product, and other properties like stability, miscibility, and molecular interactions regarding a given drug, which are already relevant during early pharmaceutical development. For information on the oral acceptance as well as regulatory implications, the legislations ICH Q6A, USP Chapter 3 and EudraLex Chapter 4 can be used. A practical source of information is the generally recognized as safe (GRAS) list by the FDA. Excipients selected from this list have shown to be safe among qualified experts in the field. Therefore, an additive which is mentioned in the GRAS list can be more easily used in a polymeric matrix even though this does not directly entail regulatory acceptance as pharmaceutical excipient in the different countries. There are other excipient aspects that have more technical relevance for the choice of the amorphization technique. Such properties are primarily about chemical and physical stability at elevated temperatures, which need to be considered depending on the manufacturing process. An excipient with insufficient stability upon heating would not be feasible for example for hot melt extrusion (HME). Moreover, the excipient has to be stable over the duration of a stability study, which means substances that chemically degrade may lead to inacceptable impurities of the final drug product. Closely related to the stability aspect is the hygroscopicity of an excipient. The inclusion of water in the formulation typically leads to physical instability of an amorphous drug because of a massive reduction in the glass transition temperature (T_g) [42]. Moreover, a polymer or additive used in an ASD should have sufficient wettability to ensure appropriate drug release. The drug release is majorly determined by the properties of the polymer used, especially when the drug load in the ASD is comparatively low [43,44]. A recent publication by the group of Lynne Taylor highlighted that the analytical determination of both, drug and polymer dissolution is an important advancement of *in vitro* testing and a synchronized release of drug and precipitation inhibiting polymer is beneficial for the later enhanced absorption.

Such insights into the biopharmaceutical performance of amorphous systems lead to even more excipient aspects to be considered. It underlines the need to have sufficient choice among orally accepted

polymers and opens the discussion towards the modification of existing polymers with generally accepted additives.
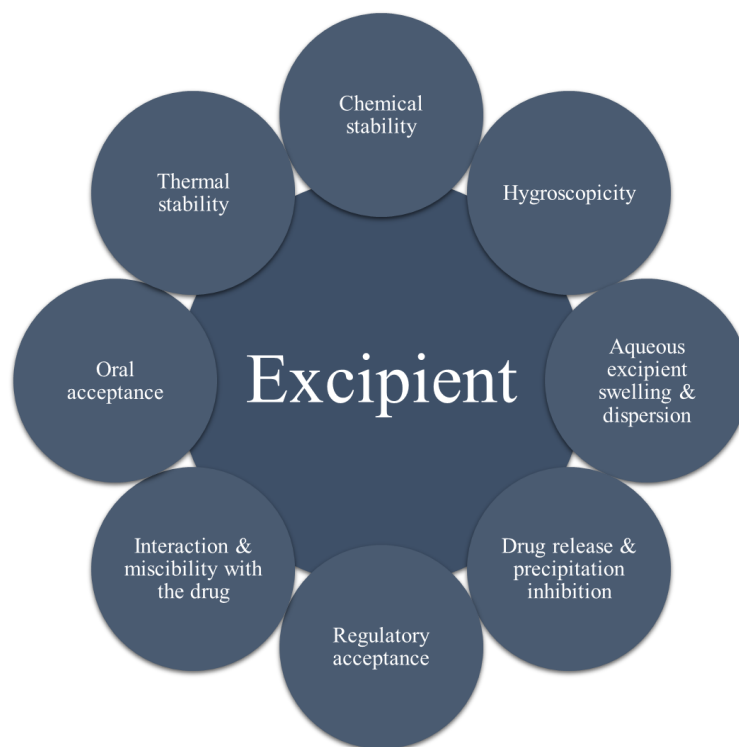
Figure 1.3. Requirements for an excipient used in an ASD

1.2 Objectives

The objective of this scientific work was to investigate beneficial excipient combinations for HME of poorly water-soluble drugs by targeting molecularly designed interactions of polymer and co-formers to obtain modified polymeric matrices and compare those with other solid dispersion formulation techniques. Such an evaluation was based on amorphous stability, dissolution performance including supersaturation potential, and technical feasibility. An important aspect of the latter process performance was the improvement of extrudability with regards to properties of the polymers. Molecular interactions among the components have a critical impact on the before mentioned formulation characteristics. Therefore, the assessment was complemented with the analysis of such interactions by applying spectroscopic techniques reaching from heat-resolved Fourier transform infrared spectroscopy (FTIR) to solid-state nuclear magnetic resonance spectroscopy (SS-NMR) throughout the different studies. Throughout the chapters of this thesis, various polymers in combination with different interacting small molecular additives are studied regarding their applicability in HME.

In the theoretical chapter 2, the important aspects and excipient considerations regarding amorphous solid dispersions are explained. The amorphous state with a focus on drug features like GFA or glass

transition temperature are explained. Furthermore, the manufacturing techniques as well as the analytical and biopharmaceutical implications of the amorphous form are outlined.

The second part of chapter 2 particularly focuses on the manufacturing technique of HME. In this section, the process as well as the restrictions and excipient selection are explained. Since the interactions with a co-former in the formulation are a key component of this work, the last subsection is focused on the application of this novel approach in the field of amorphous solid dispersions regarding increased amorphous stability and the improvement of dissolution performance.

In the third chapter, the concept of a HME formulation containing a polymer, an interacting additive, and a drug was evaluated in comparison to a conventional polymer-drug-extrudate. As a novel component, the co-former was specifically selected to interact with the polymer and therefore led to improved polymer properties focusing on HME. Such investigated properties were an improved processability, increased amorphous stability, and enhanced release behavior. Moreover, the pronounced interaction between the additive and the polymer was demonstrated by NMR and FTIR.

The concept described in the third chapter was applied in the fourth chapter including a broader range of co-formers. The latter small molecules consisted of basic amino acids and three other molecules with proton-acceptor groups. As polymeric counterpart, the polyelectrolyte sodium carboxymethylcelluose (NaCMC) was selected. This is of particular interest because neat NaCMC presents beneficial release behavior upon aqueous dispersion, while due to its degradation at high temperatures, it is unfeasible for extrusion. Therefore, a preliminary solvent evaporation step was applied to produce an extrudable polyelectrolyte matrix. For an increase in resolution and the ability to probe extrudates at different points, the matrices were analyzed with a synchrotron X-ray beam. Favorable compositions as well as additives were identified regarding extrudability and successful amorphization.

As polymeric HME has been applied in the pharmaceutical field for several years, there is a necessity to compare it with new, promising formulation techniques. In chapter five compounds, which are specifically challenging for amorphization methods were used to compare polymeric extrudates with mesoporous silica formulations. The study was designed to show over three months differences in the stabilization of an amorphous active pharmaceutical ingredient (API) under accelerated stability conditions. Moreover, the implications on the biopharmaceutical performance were investigated. These results were complemented with additional solid-state characterization like scanning electron microscopy (SEM) and solid-state nuclear magnetic resonance spectroscopy (SS-NMR).

For the final assessment of bio-enabling capabilities, the most promising polyelectrolyte matrices were used in the development of amorphous formulations containing fenofibrate as model drug. Therefore, in chapter six, the formulations consisting of NaCMC/lysine/fenofibrate and

NaCMC/meglumine/fenofibrate were evaluated *in vitro* and *in vivo*. In these studies, the physical mixtures of the formulations were compared with the corresponding formulations in FaSSIF non-sink dissolution as well as a rat study. Additional solid-state characteristics were applied to confirm the amorphous state of the formulations and viscosity measurements should provide insights in the stabilization properties of the polyelectrolyte upon aqueous dispersion.

Theoretical section

2.1 Amorphous solid dispersions

2.1.1 General consideration

The formulation approach of amorphous solid dispersion was introduced by Chiou and Riegelmann in 1969 because of an increasing number of poorly water-soluble compounds that required a new formulation perspective [32]. Since then this approach has been common practice for solubility enhancement [32] of poorly water-soluble drugs [31]. As mentioned in Section 1.1, drugs with limited bioavailability as a result of poor solubility can potentially benefit greatly from an increase in their apparent solubility through amorphization.

In a recent review, Wyttenbach and Kuentz highlighted the thriving need of amorphous formulations. Currently there are 17 drugs formulated as amorphous solid dispersions and 5 drugs in their amorphous form available in internationally marketed products [41]. As highlighted in Table 2.1, most of the amorphous formulation are manufactured via HME or spray drying.

Solid dispersions can be categorized according to the physical state of the given phases [33]. The first dispersions were often eutectic mixtures, which were miscible in the molten state. A disadvantage of the eutectic systems is that recrystallization occurs at the characteristic eutectic temperature, which typically takes place during the cooling process. Pioneer solid dispersions were prepared with a water-soluble carrier like citric acid, and a poorly water-soluble drug (e.g. griseofulvin) [32]. Depending on the individual composition it is possible to obtain an amorphous solid solution, where a compound is dispersed molecularly in the amorphous carrier [45]. Leuner and Dressman pointed out that solid solutions can be continuous versus discontinuous or substitutional versus interstitial. Systems with an amorphous carrier are generally called glasses where glass solutions can be differentiated from glass suspensions depending on the physical state of the drug and whether one or two phases are present in the system [45].

Table 2.1. Marketed amorphous formulations (adapted from [41])

Compound	Carrier	Manufacturing technology	Dosage form
Etravirine	HPMC	Spray drying	Tablet
Everolimus	HPMC	Spray drying	Tablet
Fenofibrate	PEG	Spray melt	Tablet
Griseofulvin	PEG	HME	Tablet
Itraconazole	PVPVA 64	HME	Tablet
Ivacaftor	HPMCAS	Spray drying	Tablet
Lopinavir / Ritonavir	PVPVA 64	HME	Tablet
Nabilone	PVP	HME	Capsule
Nifedipine	PVP	Melt/absorb on carrier	Tablet
Nilvadipine	HPMC	n/a	Tablet
Nimodipine	PEG	Spray drying	Tablet
Posaconazole	HPMCAS	HME	Tablet
Ritonavir	PVPVA 64	HME	Tablet
Tacrolimus	HPMC	Spray drying	Capsule
Telaprevir	HPMCAS	Spray drying	Tablet
Troglitazone	PVP	HME	Tablet
Vemurafenib	HPMCAS	Co-precipitation	Tablet
Verapamil hydrochloride	HPC/HPMC	HME	Tablet
Neat amorphous drugs			
Cefuroxime axetil	-	-	Tablet
Nefinavir mesylate	-	-	Tablet
Quinapril hydrochloride	-	-	Tablet
Rosuvastatin calcium	-	-	Tablet
Zafirlukast	-	-	Tablet

Since solid dispersions have a long tradition, different generations of formulation types have been in use. These different generations were described in detail by Vo et al. [46]. Main differences are given in the types of excipients selected during the pharmaceutical development of solid dispersions (Figure 2.1.).
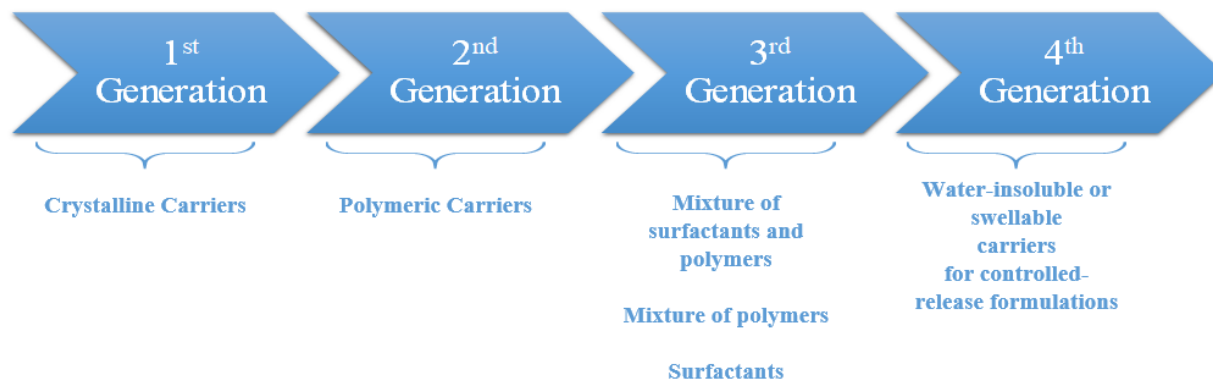
Figure 2.1. Generations of solid dispersions

In the first generation of solid dispersions, crystalline carriers (i.e. mostly small molecular additives) were used for dispersing the drug homogeneously in the solid state, which had the disadvantage that a rather fast drug precipitation was often observed upon aqueous dispersion. Therefore, a second generation of improved formulations was proposed. These formulations were based on polymeric carriers, which were advantageous regarding the biopharmaceutical fate of the drug. Such solid dispersions typically showed a dissolution rate that was widely controlled by the hydration and dissolution of the polymeric matrix [47]. The third generation of solid dispersions consisted mainly of polymeric carriers combined either with each other or with surfactants to improve the aqueous dispersion following oral administration. Interesting is here a combined functionality like, for example, the BASF polymer Soluplus®, which represents a polymer (polyvinyl caprolactam-polyvinyl acetate-polyethylene glycol graft copolymer) with significant amphiphilic characteristics of a surfactant.

General aspects have to be considered for a successful formulation of an ASD (Table 2.2). Such considerations in the early development can be divided in solid state and dissolution performance related.

Table 2.2. Aspects to be considered during the development of ASDs (adapted from [48])

	Aspect	Recommendations
Solid state	Polymer-drug ratio	Selection of sufficient amount of polymer to ensure amorphous stability in the solid state over the shelf life
	Miscibility	Assessment of miscibility to avoid phase separation, which could later lead to recrystallization
	Amorphization process	Determination of a process with a focus on the API (thermal stability for HME or solubility in volatile solvents), but also suitable the used excipients
	Hygroscopicity	Highly hygroscopic materials could lead to water uptake in the ASD, which decreases T_g. This could lead to potential recrystallization.
Dissolution	Dissolution apparatus including media selection	Apparatus selection as well as media selection should simulate the physiological conditions and must be adequate for the given dosage form.
	Sink or non-sink conditions	Both aspects have to be investigated. Sink dissolution may be used as quality test for batch release, whereas non-sink dissolution enables analysis of drug supersaturation/precipitation and can be coupled with a permeation test.

2.1.2   The amorphous form

The amorphous form comes with distinctive structural properties that are different to the crystalline counterpart. An amorphous solid is lacking the long-range order, which leads to a rather random orientation of molecules more in the sense of a frozen liquid with no symmetry operators present [49]. This can be experimentally verified by the absence of distinct Bragg peaks in the X-ray diffraction, which results in a distinctive halo of an amorphous substance (Section 2.1.4). Such a solid has the properties of a liquid on the molecular level and the properties of a solid on the macroscopic and rheological level [50,51]. Current research has highlighted the fact that the amorphous form is most likely not completely amorphous and organized in a random manner. It is rather the case that even in an amorphous formulation, some order is given as smaller short-range clusters. However, in contrast to the crystalline material, such clusters are too small to present crystalline properties [52].

2.1.2.1 Thermodynamic implication of the amorphous state

From a thermodynamic viewpoint, an amorphous state has generally higher Gibbs free energy than a crystal. Therefore, an amorphous state is considered metastable with a considerable risk of crystallization in a non-stabilized amorphous solid dispersion.

Figure 2.2. emphasizes the differences in Gibbs Energy between an amorphous and crystalline material [53]. Moreover, it shows the changes in this energy with increasing temperature, going from the glassy to a possible rubbery state in case of the amorphous form and from the crystalline to the molten state in case of the crystalline form. The two temperatures in Figure 2.2. mark the transition of an amorphous and a crystalline state. The T_g represents the alteration between a glassy state and a rubbery state, whereas the other change in the solid state of crystalline material can be observed at T_m, when the crystals melt.
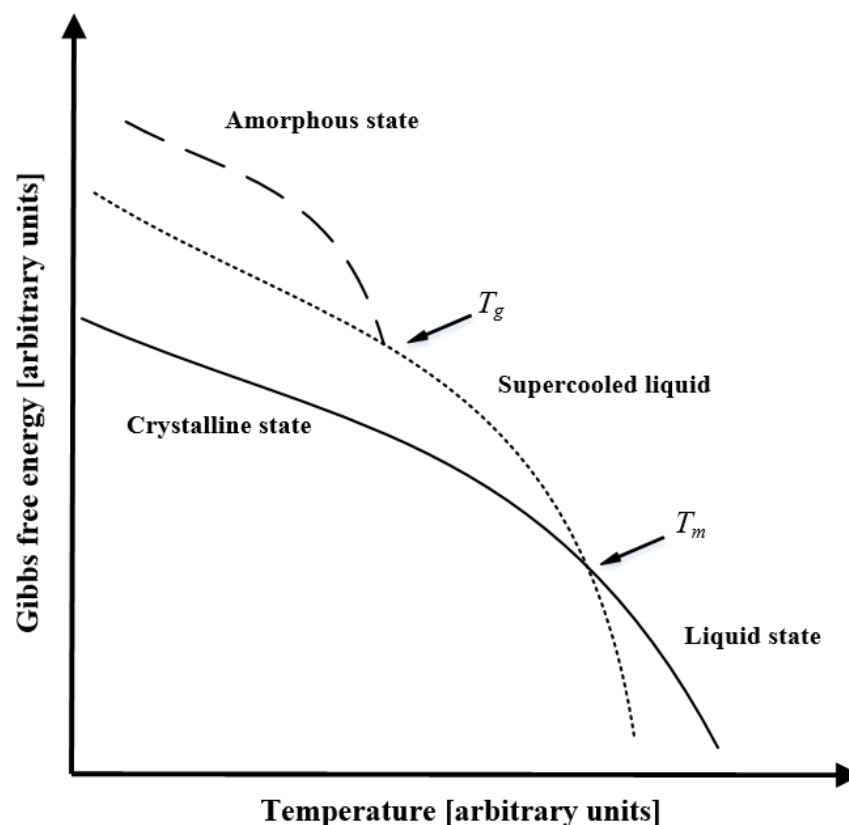
Figure 2.2. Gibbs Free Energy of amorphous and crystalline material (Reprinted with permission of Elsevier [53])

Furthermore, the difference in Gibbs free energy shown in Figure 2.2. results in an enhanced apparent solubility compared to the crystalline form [54]. This so-called amorphous solubility advantage was coined by Hancock and Parks, who associated the difference in free energy to the difference in apparent solubility according to equation 2 [55].

$$\Delta G_T^{a,c} = -RT \ln\left(\frac{\sigma_T^a}{\sigma_T^c}\right) \qquad (2)$$

The different solubilities of the amorphous and the crystalline drug at a fixed temperature are represented by σ_T^a and σ_T^c, respectively. Consequently, $\Delta G_T^{a,c}$ is the difference in free energy at a given temperature. A higher difference in free energy can be associated with a larger solubility advantage of the amorphous form over the crystalline form [55]. Such increased apparent solubility has to be balanced with the general drawback of potential physical instability of an amorphous form.

Since the crystalline form has lower chemical potential, possible drug crystallization to the original crystal form or any other polymorph has to be monitored by adequate solid-state analysis. Such recrystallization can be described by the two kinetic processes of nucleation and growth. Thus, small crystalline nuclei in an amorphous formulation can grow over time to manifest a macroscopic crystallization [56].

On a molecular level there can be certain kinetic factors identified that lead to recrystallization. One of such kinetic influences is the presence of foreign particles, which are insoluble in the undercooled melt and act as a site of heterogeneous nucleation [56,57]. Other sources for increased recrystallization are the plasticizing behavior of water, which introduces a reduced glass transition with a general increased molecular mobility thereby enhancing nucleation kinetics [13].

2.1.2.2 The glass transition

Amorphous materials, as discussed in the previous section, are lacking the well-defined lattice of a crystal. Crystallinity comes with a specific melting point for every drug and its polymorphs, whereas amorphous materials show a glass transition at which the material goes from metastable equilibrium to a frozen-in non-equilibrium state (Figure 2.2) [58]. As a result of the formation of a non-equilibrium state, the glass transition is not a thermodynamic phase transition like for example melting and can therefore not be categorized according to the Ehrenfest definition of thermodynamic phase transitions [58,59].

A T_g can vary depending on the cooling rate and hence possibly the manufacturing method [60,61]. Based on the given variations of this critical temperature, it is more accurate to refer to a glass transition range rather than a clearly defined point [61,62].

Below the measured glass transition, the viscosity increase is limiting molecular movement in the formulation. Relaxations within the amorphous formulation are considered as major factors for instability, which lead to recrystallization. Such molecular movements can occur as α relaxations, which represent a global mobility and are rarely present below T_g. This is why in a recent publication, this T_g was referred to as $T_{g\alpha}$ [62]. In contrast, the so-called Johari-Goldstein β relaxation is associated with local mobility within the molecule and can still occur below $T_{g\alpha}$. The reason for this is the lower activation energy of the β relaxation compared to the cooperative α relaxation [63]. Therefore, recent

publications investigate the temperature at which the β relaxation is massively reduced to possibly avoid recrystallization in ASDs [62]. For general stability consideration, it is favorable to reduce such relaxation in amorphous drug delivery systems [64–66] by storing the formulation at sufficiently reduced temperatures and low humidity. Introducing water into the system through humidity leads to an increase of the drug's mobility as it acts as a strong plasticizer decreasing the T_g [67]. Recrystallization certainly can occur above but might also happen below T_g [68], which means that storing the amorphous formulation below T_g cannot guarantee sufficient stability. A classical rule of thumb is to target a T_g that is at least 50 °C above the storage temperature to result in sufficient stability because of the additional reduction of β relaxation.

Due to the practical importance of a glass transition, several methods have been proposed to measure T_g, such as: differential scanning calorimetry (DSC), atomic force microscopy, dynamic mechanical thermal analysis, thermally stimulated current spectroscopy, density, and inverse gas chromatography [69]. Most abundantly employed in the pharmaceutical industry as well as in academia is the DSC method.

2.1.2.3 Glass forming ability

The characteristic glass forming ability (GFA) is generally described as the ease of vitrification of a liquid upon cooling [70]. Before the definition of classes, it was proposed that a differentiation could be applied in compounds that prefer to be in a crystalline state and drugs being stable in their amorphous form. For such a differentiation, temperature dependencies of the nucleation rate and growth velocity were used [71] in a diagram which would be today applied as a time-temperature-transformation diagram to access the glass forming ability of drugs [72]. Based on these diagrams, fast crystallizing compounds exhibit nucleation and growth occurring in an overlap region, while stable glass formers do not cross such a crystallization region for most practically accessible cooling rates [61].

Baird and coworkers applied the concept of glass forming ability and proposed a more accessible solution of the definition in classes [36]. In their publication, the researchers defined three groups of drugs based on their recrystallization behavior in a heating-cooling-heating DSC experiment. Such experiments provided an initial assessment of GFA. However, the heating and cooling rates during the DSC experiments have an impact on the recrystallization of the drug. This is hardly critical for GFA class I and GFA class III drugs, since their differentiation is robust in a wide range of typical cooling rates from the undercooled melt. However, GFA class II drugs might be categorized differently because of variations in the given measurement protocol. Therefore, Blaabjerg and coworkers proposed the categorization based on critical cooling rates of the melts (Table 2.3.). Their definitions reached from GFA I compounds, which require heating rates higher than 750 °C/min to GFA III compounds, which can be cooled with 1 °C/min and still enable the vitrification of the drug [72]. However, like any simplified classification also this proposal includes an element of arbitrary group assignment.

Table 2.3. Glass forming ability definitions

	GFA I	GFA II	GFA III
Baird et al. [36]	Recrystallization after cooling of the melt	Recrystallization after reheating the cooled melt	No recrystallization
Blaabjerg et al. [72]	Cooling rate > 750 °C/min	Cooling rate 10 – 20 °C/min	Cooling rate 1 °C/min

It has to be noted that the GFA can be used as predictor of amorphous stability in the development of new formulations [34,73]. However, by applying this concept, the influences of the additional compounds like polymers have to be taken into consideration. Unbeneficial properties such as insufficient miscibility with the polymer or an extensive drug load can still lead to recrystallization of otherwise stable glass formers (GFA III) [74].

2.1.3   Manufacturing techniques

There are numerous formulation techniques in the field of ASDs with spray drying and HME being the most common. More generally, the production of amorphous formulations can be mainly divided into melt-based and solvent-based methods [54]. This is critical since the preparation has a substantial effect on the physicochemical characteristics, stability and therefore performance of solid dispersions [75]. Considering the marketed solid dispersions, it is interesting to see that a rather limited number of polymeric carriers and production techniques have been used [41]. While the choice of the formulation components is generally based on physical and chemical considerations and long series of experiments during development, the production methods are often more arbitrarily selected depending on available technological knowledge and equipment [76]. The selection of the manufacturing method based on the physicochemical drug properties could accelerate process development and should finally result in a robust manufacturing of drug product.

Different melt and fusion techniques represent the classical methods to prepare drugs in their amorphous form [76,77]. For the melting of the API and a carrier, temperatures should be above the T_m of the API [78]. Raising the temperature above the T_g of the mixture creates adequate molecular mobility for the API to be incorporated in the carrier [76]. Although a variety of methods and modifications have been introduced throughout the years, solid dispersions containing APIs with high T_m values (e.g. quercetin) typically encounter issues of lacking temperature stability of the carrier. These high-melting APIs therefore only have a limited range of available polymers that can be used at the needed process

temperatures. Moreover, high shear forces in a process of HME may facilitate the removal of oxygen and moisture, besides the vigorous mixing and the desirable dispersion of the API in the carrier [46,79]. This enables the incorporation and usage of APIs that are sensitive to oxidation. However, high shear forces may also compromise the stability of thermo-sensitive APIs, due to possible local high temperatures [79].

An alternative to any melt method is to prepare a solution of drug and carrier in a solvent. The fate of the solution may vary, from solvent evaporation to amorphous precipitation. The solvent evaporation method includes first the dissolution of API and carrier in a common organic solvent (or solvent mixture) and the subsequent removal of the solvent by heating, spray drying or freeze-drying [80]. The choice of a common solvent for the API-carrier systems may prove to be limiting, as it is challenging to identify a solvent for combinations that vary significantly in polarity [80]. Generally, thermal degradation is not a common limitation in the solvent evaporation methods, as temperatures are kept low. Specifically for thermo-labile compounds, a freeze-drying method is of interest, where the API-carrier solution is frozen and the solvent or solvent mixture is sublimated at temperatures below the T_g of the mixture [76]. A sublimation above this critical temperature comes with increased molecular mobility that can facilitate recrystallization. Consequently, APIs with extremely low T_gs may not be suitable for this method. In addition, during the removal of the solvent by heating, molecular mobility is critical, as elevated temperatures (above T_g) may facilitate API diffusion from the carrier, thereby creating a phase separation and subsequent crystallization. This suggests that this method may be less suitable for APIs with a T_g below the boiling point of common organic solvents (e.g. methanol, ethanol, acetone ~60-70 °C).

An innovative technique applied in the amorphization of a commercial product is micro precipitation. This technique was invented by Roche and first applied as amorphization technique of Vemurafenib (Zelboraf®). The high melting point as well as the insufficient solubility in volatile solvents made this compound impractical to be processed by either spray drying or HME. The process of micro precipitation starts with dissolving the polymer and drug in a solvent with high boiling point, which would not be feasible for spray drying. Afterwards, an anti-solvent is added to result in a solvent-controlled precipitation of the amorphous drug in the polymer [81,82].

2.1.4   Analytics

Due to the high relevance of identification and quantification of amorphous drug in a solid dispersion, there several methods are commonly applied. These methods are on one side based on solid-state characterization, which are mainly used for the structural characterization and stability monitoring. On the other side, analytical methods investigate the biopharmaceutical performance of the formulations by conducting dissolution experiments in different setups, which mostly simulate *in vivo* release and sometimes include also a permeation step to mimic absorption in the human GI tract.

Table 2.4. Solid-state analytical methods for ASDs

Analytical method	Measurement	Considerations for ASDs
Powder X-ray diffraction	X-ray counts at various detection angles	Application in the detection of polymorphic forms and the absence of crystalline structures
Pair distribution function	Derived from Fourier transform X-ray patterns Describes the probability of finding two atoms at a defined interatomic distance	Assessment of specific configurations in a polymeric system
Differential Scanning Calorimetry	Heat flow changes of the sample over a defined temperature range	Various thermal events can be detected as well as different heating programs applied to increase sensitivity or differentiate.
Fourier transform infrared spectroscopy	Measurement of absorption or transmission of a drug in the infrared region	Such a measurement can be also combined with a microscope to scan in specific areas for predefined wavenumbers.
Raman spectroscopy	Detection of Raman scattering over a defined region of wavelengths	Evaluation of interactions and amorphous content. Not well applicable with substances showing fluorescence. Same possible combination with a microscope like with IR.
UV/Vis spectroscopy	Absorption at a defined wavelength within the UV/Vis spectrum	This method is widely applied as stand-alone instrument or integrated into an LC system for the quantification of UV-active samples
Nuclear magnetic resonance spectroscopy	Detection of nuclear spin energies in a high magnetic field with additional inductive magnetic fields in the range of radio frequencies [83,84]	Can be applied in the solid and liquid state as well as specifically detect spins of various nuclei (^{1}H, ^{13}C, ^{15}N, ^{19}F, ^{29}Si, and ^{31}P)

A widely used solid-state technique is powder X-ray diffraction (PXRD), which is based on the measurements of X-ray scattering over a range of scattering angles [85], where an amorphous form shows a halo and absence of any Bragg peaks [86] over the 2θ angles (usually between 2° and 40°). This is a result of the lack of long-range order in an amorphous solid [49]. The resolution of such measurement is highly dependent on the X-ray source used. This fact is further highlighted in the calculation of the Q-value, which can be used in the diffractogram, where the intensity of the scattering is displayed on the y-axis and the Q-value on the x-axis.

$$Q = 4\pi \sin \theta/\lambda \tag{3}$$

Common measurement setups consist of a copper X-ray source, which provides Q_{max} values of 8 Å^{-1}. In case a laboratory diffractometer is not sufficient for needed resolution, a measurement at a synchrotron facility can be performed, which has Q_{max} values of 20 Å^{-1}. Such measurement comes with higher resolution, increased sensitivity to small amounts of crystallinity, and the possibility of probing the sample by focusing the beam at different areas. The X-ray measurement is of particular interest for the measurement of the local structure in an amorphous solid by pair distribution function (PDF). This function can be obtained by Fourier transformation of information from a regular X-ray diffraction pattern. For the information content of a PDF, it is highly beneficial to use synchrotron radiation [85]. Another common method is DSC, where the absence of a melting endotherm and the presence of a T_g indicate an amorphous state. In such a measurement, the sample is put in a crucible, in which it is typically first heated then cooled and heated again. During these measurements, the solid state of the sample is monitored by measuring the heat flow through the sample over a defined temperature range. As a result, thermal events like melting peaks, recrystallization peaks or glass transitions give indications about the initial solid state of the sample. During the first heating, the current state of the samples is recorded. In the subsequent cooling and the following heating, the amorphous stability as well as the miscibility in case of a mixture can be assessed. This was also used for the determination of the GFA (Section 2.1.2.2.). The T_g of mixtures can be estimated by the classical Gordon Taylor or the Kwei equation, which both combine the T_gs of the substances in the calculation. A major advantage of the Kwei equation is the introduction of an interaction parameter to predict T_gs more reliably [87].

Depending on the heating rate, the sensitivity can be adjusted, although this has to be applied with caution. A higher heating rate comes with higher peak intensity, but it also leads to a shift of the thermal events. Therefore, for the comparison of samples, the same heating rate should be selected. For the differentiation of thermal events, which occur at similar temperatures, modulated DSC can be applied. During such modulated measurements, the heating rate is modulated and a subsequent transformation of the thermogram leads to the differentiation in reversed and non-reversed heat flow. More details on modulated DSC can be inferred from the literature [88].

The most widely applied spectroscopic method is FTIR which can be used for the identification of substances by the absorption in the infrared spectrum reaching from wavelengths of about 2.5 to 50 μm and wavenumbers of 4000 to 200 cm^{-1}. In the research field of ASDs, the spectra are more commonly used to identify interactions between molecules through changes, which are visible in the mixture but not in the spectra of pure substances. Examples for such changes can be found in the absorption range of 1750 cm^{-1}, which corresponds to the C=O functional group and can be impacted by direct hydrogen bonding or molecular interactions of neighboring atoms. This evaluation should always be performed with the physical mixture and the given formulation, because dilution effects of mixing between excipients and drug can result in reduction of peak intensities making such a control experiment necessary. Moreover, the samples should be dried because water reduces the detectability of peaks at higher wavelength areas. FTIR measurements are usually conducted in the attenuated total reflection mode, which comes with the benefit that the sample can be placed in its neat form on the sample holder and measured without further preparation. Another sample preparation involves the compression of the sample with KBr.

Table 2.5. Microscopic analytical methods for ASDs

Analytical method	Measurement	Considerations for ASDs
Polarized light microscopy	Microscopic Images with polarized light resulting in bright appearance of birefringent crystalline structures	Since nucleation can randomly occur, the complete sample should be assessed to identify possible sites of crystallization.
Atomic force microscopy	Topographical measurements	Small amounts of phase separation or crystallization can be monitored in phasing images or simple surface measurements.
Scanning electron microscopy	Monochromatic images of morphological features on the surface detected through backscattered electron detection	Crystal structures and morphological features can be analyzed. However, the clear identification of crystals might not be possible.
Energy dispersive X-ray detection	Elemental information on electron microscopy images can be gathered	The color coding of different elements can be used to map the distribution of a drug, if a detectable element is available

Closely related to FTIR for probing molecular vibrations as well is the Raman spectroscopy, in which Raman scattering of an incident laser light is detected following adequate filtering of Rayleigh scattering. Fiber optical connections enable in-line Raman probes that can be used to monitor recrystallization and amorphization processes during HME [89]. Another application is the analysis of precipitates during dissolution experiments, because Raman spectroscopy is less disturbed by water than FTIR and has the ability to differentiate between dissolved drug and precipitated compound [90]. In line with FTIR, Raman measurements can also be used to investigate interaction in an ASD in the solid state [91].

Optical methods can be used as well for the investigation of ASDs. Such methods reach from the simple visual inspection to more complex methods like atomic force microscopy (Table 2.5). The method commonly applied for the detection of crystals is polarized light microscopy. In contrast to DSC and PXRD in a normal setup, the polarized light microscopy can detect smaller amounts of crystallinity in transparent or slightly opaque samples. Through the polarization of the light, crystalline features can be detected as shining objects in the sample. However, this analysis has to be carefully applied, because the measurement of artifacts is also possible.

Another microscopic measurement method is the imaging via scanning electron microscopy. In this method, monochromatic images are taken by the detection of backscattered electrons. Depending on the instrument, high magnifications can be reached. Of great interest for the analysis of ASDs is the combination with electron dispersive X-ray detection. This measurement setup allows for the detection of different chemical elements on surface of the sample. Therefore, the distribution of an API like fenofibrate, which contains a chlorine atom, can be detected. Unequal distribution of a drug, which could lead to stability issues, can be identified as well [92].

Table 2.6. Dissolution methods for ASDs

Analytical method	Measurement	Considerations for ASDs
Sink dissolution	Measurement of complete drug content, which is released by the investigated formulation over time	The conditions are defined in regulatory documents to assure consistent measurements. Measurements can be conducted at various conditions to simulate different parts of the GI tract.
Non-sink dissolution	Quantification of the drug concentration released over time at oversaturated starting conditions	Precipitation and supersaturation in biorelevant media can be detected to show the solubility advantage of an amorphous formulation

Atomic force microscopy presents a method which is used for the detection of morphological sample features by using a cantilever, which scans the surface of the sample. With this method, phase separation on the surface of sample can be monitored even before recrystallization occurs [88,93]. Therefore, stability issues can be spotted at an early stage. However, the measurement setup should be in a mechanical resonance-reduced area, since minor vibrations can lead to artifacts in the measurement.

The initial biopharmaceutical evaluation of a newly developed formulation is usually done in a dissolution apparatus. In this measurement, the release of drug is monitored over a defined period of time at constant conditions. Different types of dissolution equipment are described in the pharmacopeias and test conditions for drug release of marketed products are defined in various regulatory documents for different types of drug release products to ensure comparable testing conditions [94]. The research on biorelevant dissolution testing procedures has further improved the conditions reaching from the apparatus to the release media used. This development led to such *in vitro* experiments becoming more comparable to the human GI tract. Different media were developed for a standardized biorelevant comparison at fasted or fed state release of drugs [95]. The generally most applied dissolution equipment is the paddle apparatus (USP 2) in combination with dissolution media defined in the pharmacopeia (Ph.Eur. or USP). This apparatus also enables the previously mentioned detection of drug precipitation from supersaturated formulations through the use of Raman inline probes. Other instruments are used as well with regards to different dosage forms. Moreover, the pH and other changes during the GI transit can be evaluated through media changes in the standard dissolution vessel (as described in the American pharmacopeia; apparatus USP 1 and 2) or the flow through cell (USP 4). Such more elaborate dissolution testing is typically used for the development of controlled release formulations or in a later stage of formulation development.

The experimental condition in which the drug can be released completely according to its solubility is called sink dissolution (Table 2.6). In this experiment type, it is possible to monitor when certain percentages of drug release are reached. The previously mentioned USP 2 apparatus provides a typical vessel for sink dissolution experiments. However, phenomena like supersaturation, which occur at concentrations higher than the equilibrium solubility, can hardly be investigated with the described setup. Therefore, smaller volumes can be used, which are not sufficient to solubilize the complete amount of drug in the formulation. Especially for ASDs, this is essential, because important factors like supersaturation and precipitation can be easily detected and are expected to provide a more realistic simulation of the events occurring in the GI lumen. In pharmaceutical research, such experiments can be conducted on a small scale to get a first idea of the supersaturation potential of the formulation. Moreover, these experiments can be used to investigate the precipitation of drug in the presence of different polymers. In these experiments, a polymer is pre-dissolved in the dissolution medium and afterwards a drug solution in an organic miscible solvent is added [96]. For polymers with poor drug

stabilization properties of a supersaturated solution, recrystallization can be detected, whereas polymers with sufficient drug stabilization would sustain drug in a supersaturated state.

2.1.5   Biopharmaceutical implications

After the oral administration of an ASD, the amorphous drug is exposed to the digestive fluids in the GI tract. Upon this aqueous dispersion, different species are formed. Friesen and coworkers described 7 of those species: free or solvated drug, drug in bile-salt micelles (2 to 20 nm), free or solvated polymer, polymer colloids (10 to 20 nm), amorphous drug/polymer nanostructures (20 to 100 nm), nanoaggregates of amorphous drug/polymer nanostructures (70 to 300 nm), and precipitates (> 500 nm) [97]. The drug is kept in amorphous form in the nanostructures and their aggregates. Therefore, these species have the greatest impact on the amorphous solubility advantage and the related enhanced bioavailability [97].

One of the reasons for the enhanced bioavailability is the formation of a supersaturated state in the intestinal fluids, which is exceeding the solubility of the crystalline drug (Section 2.1.2.1) [45,55]. This formation of the supersaturated state in aqueous media is described in the spring and parachute model by Guzman [98]. In this model, the drug is quickly released and stays in a state exceeding equilibrium solubility as result of the amorphous solubility advantage. The duration and therefore the parachute of such supersaturation is highly dependent on the stabilization through excipients acting as precipitation inhibitors (Figure 2.3). An example is the embedment of a drug in mesoporous silica without any precipitation inhibitor. Due to the non-crystalline state of the API, a spring (i.e. high initial supersaturation) is obtained. However, since mesoporous silica alone is unable to stabilize drug supersaturation, the drug typically precipitates quickly due to the lacking parachute effect, and the solubility decreases to the equilibrium solubility. If balanced carefully, the supersaturation over the absorption window within the human GI tract can lead to improved absorption properties of a solubility-limited drug. As a reference, the dissolution of a crystalline material is shown in Figure 2.3, which slowly dissolves until it reaches the equilibrium solubility. Depending on the drug and the dissolution medium, slightly higher concentration that the equilibrium solubility might be reached even here, because of surface amorphization or solubilization by micelle containing biorelevant media [99].

During the dissolution of an ASD, the amorphous solubility, as shown in the spring and parachute behavior depicted in Figure 2.3, can lead to such high concentrations resulting in a liquid-liquid phase separation (LLPS) in a drug-rich and a drug-poor phase in solution if the drug stays in the non-crystalline state. LLPS is expected to have a positive implication on the bioavailability enhancement of poorly water-soluble drugs [44,100]. An important implication of the LLPS is, however, that drug permeation can only be driven by the free fraction of drug that is lower than drug of the apparent concentration since there is a drug reservoir in colloidal droplets. The group of Lynne Taylor showed further that there is an

apparent sweet spot in the dissolution of ASDs. This sweet spot is specific for each individual drug and formulation as it is about a synchronized release of drug and polymer from the surface and thereby enabling the desired sustained drug supersaturation without particular enrichment of the drug occurring on the surface [44]. This led to the conclusion that low drug loadings would be beneficial with regards to drug dissolution from ASDs, which would lead to high supersaturation and eventually the formation of non-crystalline liquid-liquid phase separated colloidal species upon aqueous dispersion [44]. Such balanced release of drug in relation to hydration of the polymeric matrix should become an important biopharmaceutical objective for formulators of ASDs.
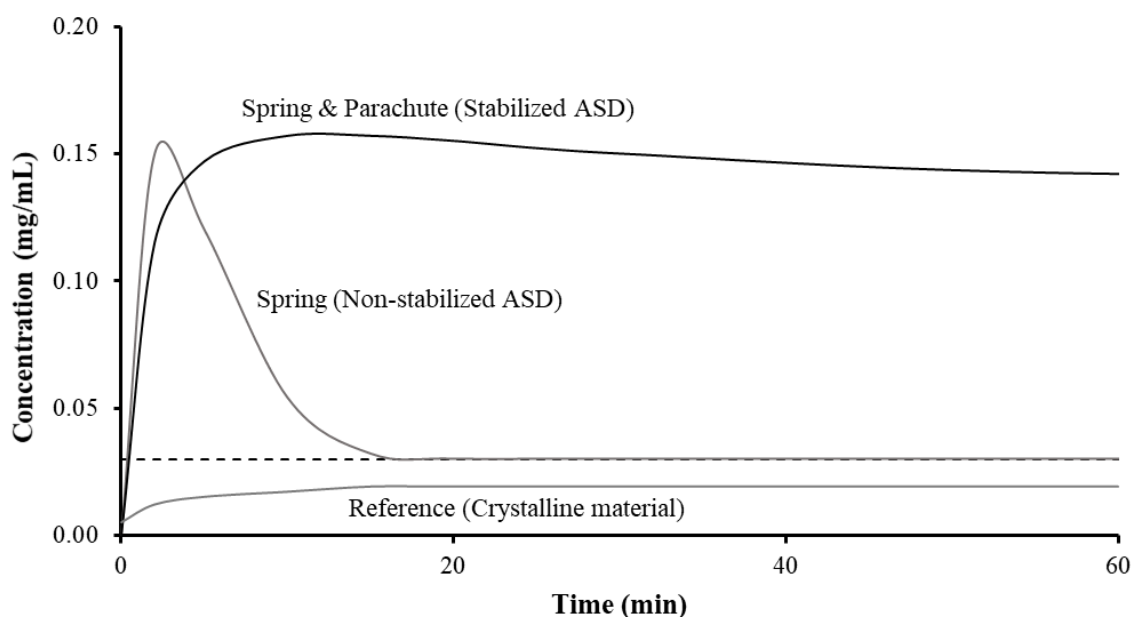

Figure 2.3. Drug release profiles of a stabilized ASD, a non-stabilized ASD, and a crystalline reference in non-sink dissolution. The terms of spring and parachute effects are explained in the text.

Moreover, it was highlighted by Neman et al. in an overview of ASDs that such a formulation approach increases the oral bioavailability in 82 % of the investigated solid dispersions, whereas in 8 % of the cases even a decrease in oral bioavailability was evidenced compared to a reference drug [48]. It is therefore important to study biopharmaceutical properties of ASDs early on in their development. Drug release is usually first evaluated using a biorelevant medium to simulate the release behavior in the GI tract [95,101]. In this context it might be an advantage to apply a non-sink dissolution testing, since events like precipitation and supersaturation, which are highly relevant for the biopharmaceutical performance of any supersaturating formulation such as ASDs [102], can be monitored more precisely [103]. Afterwards, promising formulations can be evaluated in the animal model.

An alternative to this approach prior to an animal study is the application of an experimental setup, which allows the evaluation of the dissolution as well as the drug permeation. Such an experimental setup was recently published by Sironi and colleagues, in which a tubing loop was linked to a biomimetic

membrane (i.e. PermeaLoop™) to simulate physiological dissolution coupled with an absorption step. The described setup has the benefits of increased area-to-volume ratio and the capability of showing how dissolution can be rate limiting [104]. Such dissolution testing using a biomimetic membrane with an absorption compartment bears much potential for the testing of ASDs. It allows to mimic an absorption process from supersaturation occurring in the donor compartment of the dissolution test. However more research is needed in the future to finally assess how predictable such an *in vitro* test is for the *in vivo* situation.

2.2 Hot melt extrusion

2.2.1   Process

The process of HME was first developed in the manufacturing of plastics in the 1930s, only later in 1971 was it initially applied in pharmaceutical formulation design [105]. The increasing need of formulation techniques for poorly water-soluble drugs encouraged this processing step to be applied in the formulation development and later in the manufacturing of drug products. A particular advantage is that it is free of a solvent and the footprint of the equipment in a production floor is comparatively low. Moreover, HME can also be applied for other purposes than the increase of apparent solubility, such as controlled drug release, taste masking, and to achieve particularly shaped drug delivery systems. Depending on the equipment and requirements used, common shapes are patches, granules, powder, spheres or films.

In general extruders consist of a hopper, a mechanical motor, a control panel, a barrel, a temperature regulating system, one or two screws, and a die (Figure 2.5).
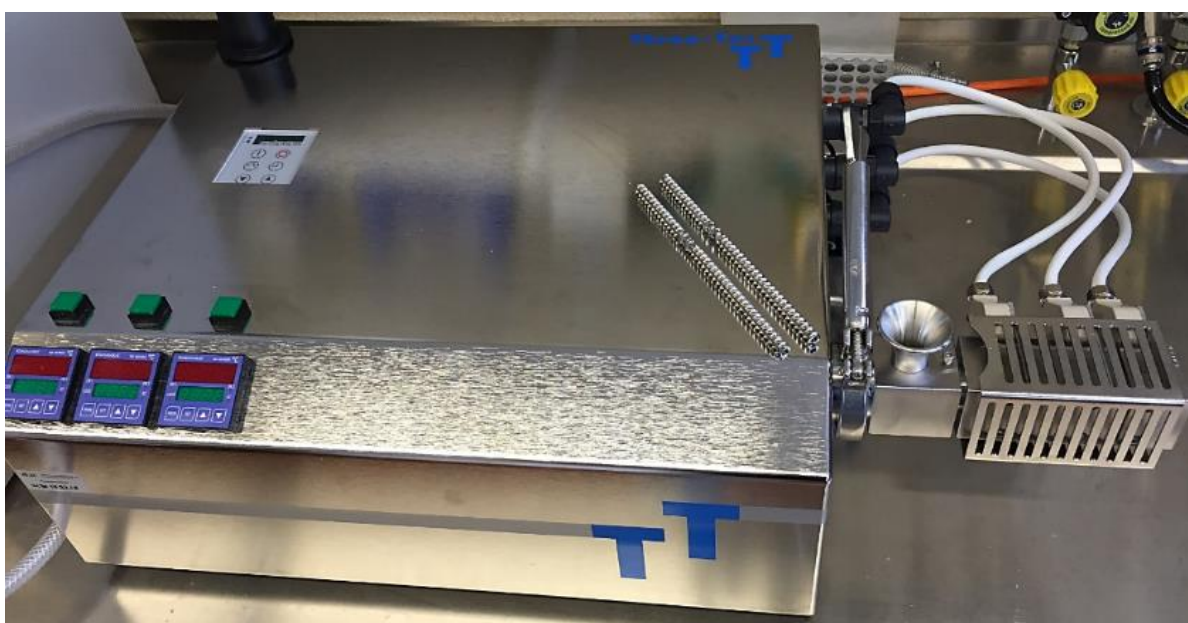

Figure 2.4. Example of a twin-screw hot melt extruder for compounding on a relatively small scale

In a modern extrusion setup, the hopper is connected to a feeder, which ensures a constant flow of material. Such a feeder can be further equipped with a mixing device to prevent the powder mixture from separating prior to extrusion. The feeding has to be accurate to ensure adequate content uniformity, which goes hand in hand with a constant filling of the barrel to ensure sufficient mixing and a constant pressure at the die. The motor of the extruder determines the torque, which is applied on the screws. It drives the rotation speed as well as the direction of the rotation. The motor of a twin-screw extruder further determines whether the screws are co- or counter-rotating. Since counter-rotating screws are only beneficial when higher shear forces are necessary and show limited mixing capabilities in comparison co-rotating screws, the setup of co-rotating screws is mostly applied in the pharmaceutical industry [106]. The barrel, which is visible at the right side of Figure 2.4, primarily ensures the smooth running of the screws and the equal heat distribution throughout the full length the extrusion. Different sizes of heating segments and split barrels can be used to adapt the heat uptake and facilitate the cleaning of the barrel, respectively. Furthermore, it can be equipped with additional openings for the application of analytical in-process probes or additional feeding ports. The given software-controlled panel can be used for the control of the whole process. In a basic setup, the parameters of the temperature regulating system and the screw speed can be adjusted. More sophisticated machine setups with more complex control panels can inform about for example the torque generated at the end of the extruder. Such information can be critical, since fluctuations are an indicator of insufficient barrel filling or unpredicted changes in the material. For the temperature control, heating cartridges around the barrel are used and monitored by thermocouples.

The screws play an essential role in the extrusion. Extruders can be either equipped with one or two screws, which can be either counter- or co-rotating. As mentioned above, a typical formulation development makes use of twin-screw extruders, which do not rely as much on shear forces as single screw extruders. Furthermore, they have only a minor problem with the formation of agglomerates and show more sufficient mixing as well as better conveying. The two screws, which are a key part of the extruder, can be adapted to fit different purposes or process requirements.
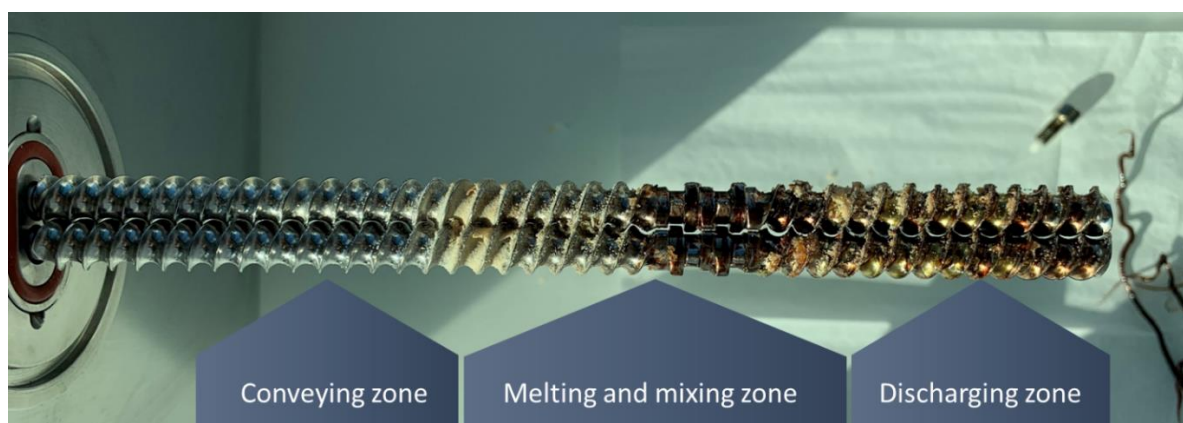

Figure 2.5. Example screws of a 9 mm hot melt extruder

The screws can be equipped with different elements, like conveying, mixing, and kneading parts. Such elements can vary in their staggering angle and disk widths. These features can be adapted to intensify the heat impact and mixing efficiency of the extruded formulation [107]. Usually at the end of the screw, where the feeder is located, the flights have a deeper pitch, which makes the conveying along the barrel easier. At the melting and mixing zone, the pitch is reduced and kneading elements can be applied to increase the pressure and ensure homogeneous melting. Throughout the transition along the discharging zone, a constant flow of material has to be created to enable further downstream processing or collecting of the extrudate. Figure 2.6 depicts the typical geometry of a conveying element. Moreover, there are screws consisting of changeable screw elements which can be stacked on a template screw to achieve specific extrusion parameters. The screws are normally defined by their diameter in mm, which means an extruder with 9 to 12 mm can be used for first extrusion trials during early pharmaceutical development with later scale-up options. Extruders of that size can produce amounts of 60 to 600 g/h. In contrast, production scale screws in the pharmaceutical industry can have dimensions up to 50 mm in diameter with a flow rate of 150 kg/h. These extruders are used in continuous manufacturing and are able to be operated over a longer period of time, while being switched off only for cleaning purposes.
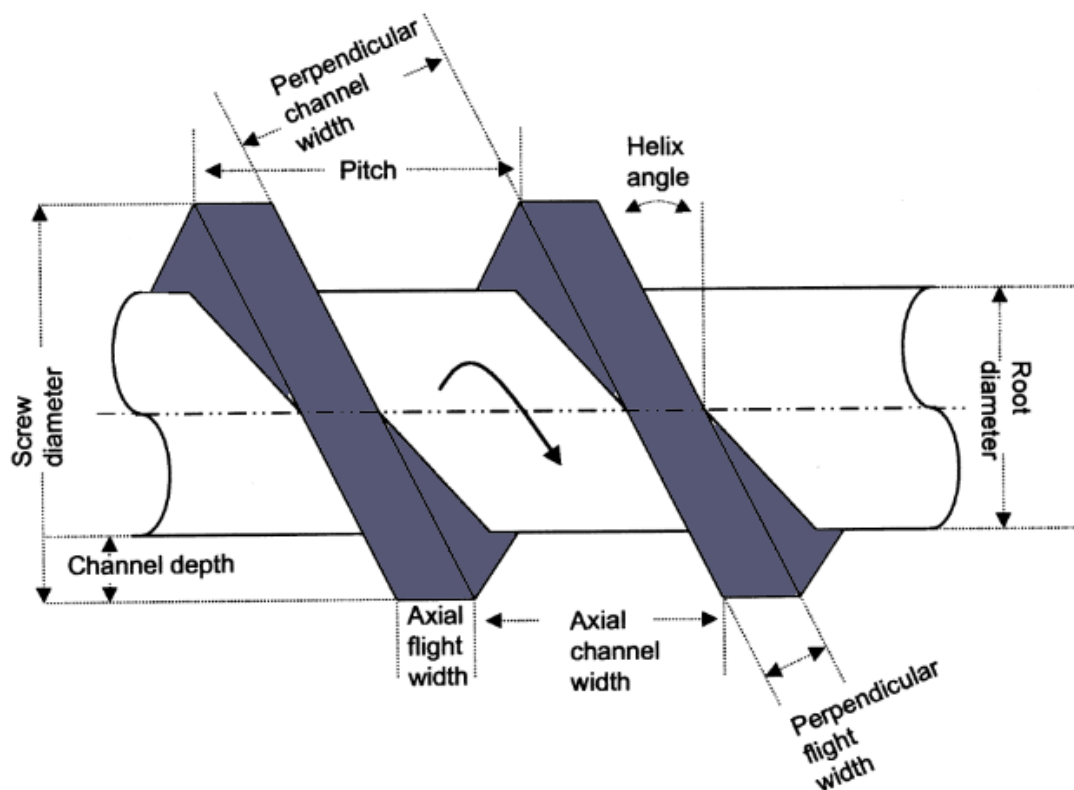

Figure 2.6. Geometry of an extruder screw (Reprinted with permission of Elsevier from [106])

At the end of the extruder as downstream processing units, equipment like chill rolls and pelletizers are required to transform the extrusion strand into a powder, which can be pressed into tablets or filled into

capsules. Another processing option is the direct shaping after extrusion. Extruded products are available in a broad variety of shapes for different applications ranging from ophthalmic to vaginal [108].

With the application of continuous manufacturing in the field of HME, process analytical technology (PAT) tools gained a major interest. Therefore, in-process controls (IPC) to monitor the performance were developed and encouraged for application of the quality by design approach by regulatory authorities [109,110]. Crucial parameters with a great impact on the formulation are processing temperature, screw configuration, screw speed, torque, transition time, and solidification properties at the outlet [111]. In a modern continuous manufacturing extrusion setup, parameters like feeding rate and barrel temperature can be adjusted during the process, whereas parameters like torque, material temperature, pressure at the die and other PAT parameters are monitored. Newly developed PAT tools, which enable in-line measurements, consist of spectroscopic measurements at the die. Such measurements can be performed by near infrared (NIR) probes, which monitor chemical as well as physical changes in the sample [79]. More specific with the inclusion of a Raman probe, properties like the concentration of a certain substance and the crystallinity can be determined, which is essential considering the fact that extrusion is widely used in the manufacturing of amorphous drug products [79]. Moreover, optical sensors can be used to determine mean residence time by detecting the change in color of a marker that was added to the formulation at the end of the barrel.

Versatile applications and scale-up options of extrusion in the pharmaceutical industry range from the field of bio-enabling drug delivery to taste masking and controlled drug delivery, which led to a broad implementation of the extrusion technology within pharmaceutical development. With further development of continuous manufacturing and PAT tools, HME has the potential to be even more applied in the future within the pharmaceutical industry.

2.2.2   Restrictions and benefits

Since there is a variety of amorphization techniques applied in the field of pharmaceutical development and manufacturing, the adequate selection of the amorphization method is crucial for a successful formulation. Therefore, this section describes the applicability of HME by highlighting advantages and possible disadvantages, which would make the process either preferred or unfavorable.

One of the advantage and reason why HME is broadly applied in the pharmaceutical field of enabling formulations is the increase in apparent solubility (Section 2.1.1 and 2.1.5.), which comes with the successful amorphization of the drug substance. Although this can also be achieved with other techniques like spray drying or micro precipitated bulk powder, a unique advantage of the before mentioned technique is that it is a solvent-free process and it reduces the oxygen exposure during

formulation compounding [112]. This is particularly relevant when a drug is not stable in contact with a solvent or feasible solvents for the formulation are unavailable due to safety or other restrictions. Moreover, an extruder can run in a continues operation, while being monitored through process analytical tools (Section 2.2.1.) because of the robustness of the process [113]. In addition, complex downstream processing like tableting can be avoided for example by direct shaping. The process is highly adaptable and can be used for different applications from immediate to controlled release as mentioned before. In addition, different routes of administration are possible with such systems. Extruded formulations can be used for example transdermal, oral, transmucosal or subcutaneously.

The major disadvantage of extrusion is the heating of the compounds. Therefore, compounds with insufficient thermal stability are not available for HME. Furthermore, it presents a more complicated and expensive formulation technique in comparison to common techniques like tableting. With the formulation of the drug in its amorphous state (Section 2.1.2), this formulation approach comes with the risk of recrystallization, which has to be avoided over the shelf life of the drug product. Another practical restriction is the processing of molecules with high melting points as highlighted in Section 1.1. Although high melting drugs might dissolve in the molten polymer, if melting of such drug is required, HME might not be the most feasible formulation technique.

2.2.3   Excipient selection

Typical compounds for an extruded formulation are one or more thermoplastic polymers, which are used as a carrier system to embed and stabilize the drug in its amorphous form [114,115]. Another advantage of the polymer is the stabilization of the drug in the supersaturated state upon aqueous dispersion as mentioned before [116]. Therefore, the selection of the polymer in the formulation is one of the most important decisions to be made during the design of a formulation [117]. As a consequence, to encourage a rather rational decision in contrast to a trial and error approach, the screening of polymers for amorphous drug stabilization (SPADS) approach was introduced by Wyttenbach and colleagues [118]. In this approach, combinations of polymer and drug are screened in various compositions with regards to supersaturation potential, amorphous stability and molecular interactions of drug with the matrix. Other functional excipients are needed to act as plasticizers during the extrusion and therefore reduce the necessary processing temperature [119]. Further excipients include surfactants for an increase in wettability, antioxidants to increase the stability, pH and release modifiers regarding the pharmacokinetic needs of the drug and additional excipients to facilitate further downstream processing [113]. Depending on the required drug delivery system, further parameters play an important role such as T_g, T_m, melt viscosity, thermal stability, solubility parameters, solubility, hygroscopicity, lipophilicity, hydrophobicity [113]. Additionally, when a specific molecular interaction within the extrudate is targeted, the hydrogen donor acceptor moieties as well as ionizable groups can play an important role.

Such an interaction can be formed during the extrusion and result in beneficial mixing, stability and release properties [120–122].

2.2.3.1 Miscibility considerations

As described in the previous sections, the miscibility of the components of an amorphous solid dispersion is crucial for the performance. Therefore, different concepts were developed to predict and assess the miscibility and maximum drug load in homogenous mixtures. Miscibility or solubility considerations are mostly based on the principle of "like dissolves like". However, this concept is not theoretically applicable without any numerical values. Therefore, the first concept of a solubility parameter was introduced by Hildebrand and Scott in 1950 [123]. This model calculated the solubility of a specific material in another material by means of the introduced concept of the solubility parameter that is the square root of the cohesive energy density [124], which can be also expressed as the energy needed to remove solvent molecules for creating an ideal cavity for solute [125]. The described cohesive energy (E_{total}) can be divided further into the dispersive energy from for example Van der Waals forces, which represent the atomic nonpolar forces (E_d); the energy based on polar forces (E_p), and the energy contributed by hydrogen bonding (E_h).

$$\frac{E_{total}}{V_m} = \frac{E_d}{V_m} + \frac{E_p}{V_m} + \frac{E_h}{V_m} \tag{4}$$

The division of these energy contributions by the molar volume results in the partial solubility parameters, which can be added to the total Hansen solubility parameter [126].

$$\delta_{total}^2 = \delta_d^2 + \delta_p^2 + \delta_h^2 \tag{5}$$

Such solubility parameter can be derived from various analytical methods such as solubility evaluation in solvents with known cohesive energy or by inverse gas chromatography [124,125]. Another common approach to estimate solubility parameters is their *in silico* calculation, for which novel methods are particularly encouraging [127]. The comparison of calculated solubility parameters is a common method for the theoretical evaluation of the miscibility between polymer and drug during the development of an ASD. The assessment of miscibility here is based on the difference between the solubility parameter of the API and the polymer. Apart from the mentioned calculation approach, classical group contribution methods can be applied as well [125]. The Van Krevelen method and calculation of the total solubility parameter by summation of the functional group contributions, which provide the partial solubility parameters in equation 5, is well established in the field of research [126]. To finally evaluate the miscibility of polymer and drug, the difference between the solubility parameters should be below 7 mPa$^{1/2}$. If the difference is below 2 mPa$^{1/2}$ the compounds might form a solid solution. In contrast, if

the difference is more than 10 mPa$^{1/2}$ the compounds are most likely not miscible [124,128,129]. Consequently, a different polymer in the case of an ASD should be selected.

The solubility parameter derived from the methods described above can be used in the thermodynamic evaluation of mixing for the calculation of the interaction parameter in the Flory-Huggins theory, which was developed to describe the dissolution of crystalline material in a solvent [130–132]. According to this theory, the free energy of mixing can be calculated as shown in equation 6.

$$\frac{\Delta G_{mix}}{RT} = n_d \ln \varphi_d + n_p \ln \varphi_p + \chi_{dp} n_d \varphi_p \qquad (6)$$

The entropic contributions to the mixing are represented on the right side by the two first terms, which not only include the molar amount of the drug (n_d) and of the polymer (n_p), but also the volume fractions of these components ($\varphi_{d,p}$). The enthalpic contribution as the third term on the right hand side of the equation determines whether the result is a negative free energy of mixing and therefore thermodynamically favorable. A major contribution to that last term is the previously mentioned Flory-Huggins interaction parameter χ_{dp}. In case this parameter is negative, the adhesive forces between drug and polymer should be greater than the cohesive forces between drug-drug and polymer-polymer, respectively. It has to be noted that the interaction parameter depends on temperature, composition and chain length of the polymer [124]. A major limitation of the described theory is the inability to take interactions like hydrogen bonding into account. Moreover, like any consideration of mixing, it does not consider crystal lattice energy break and therefore assumes the mixing of the drug and the polymer in the amorphous form [133].

A phase diagram based on the energy of mixing derived from the Flory Huggins theory can be applied for the determination of stable regions at specific polymer-drug ratios [97,132,134,135]. Another method to predict either miscibility or the solubility of an API in a polymeric system is the perturbed-chain statistical associating fluid theory (PC-SAFT), which is based on the perturbation theory with regards to chain molecules and evaluates the interactions between molecular chains by reducing them to spherical segments [136,137]. This comparatively more elaborate thermodynamic method is widely applied in pharmacutics by the group of Professor Sadowski to for example estimate the stability of drugs in polymeric amorphous solid dispersions [138,139].

The phase diagram divides the different states of an ASD based on the temperature and the composition of drug and polymer. The space under the phase separation curve on the right hand side describes states of the ASD, at which spontaneous separation in drug-poor and drug-rich phases could occur spontaneously above and below the T_g [140]. In the area between the solubility line and that of the phase separation, the ASD can be kinetically stabilized in its supersaturated state by a polymeric compound. Destabilization in those areas requires a certain activation energy so those systems are much more stable

when stored sufficiently below their T_g. Although the areas above the solubility line lead to the best stability, such low concentration are mostly not feasible for the formulation of a poorly water-soluble drug.
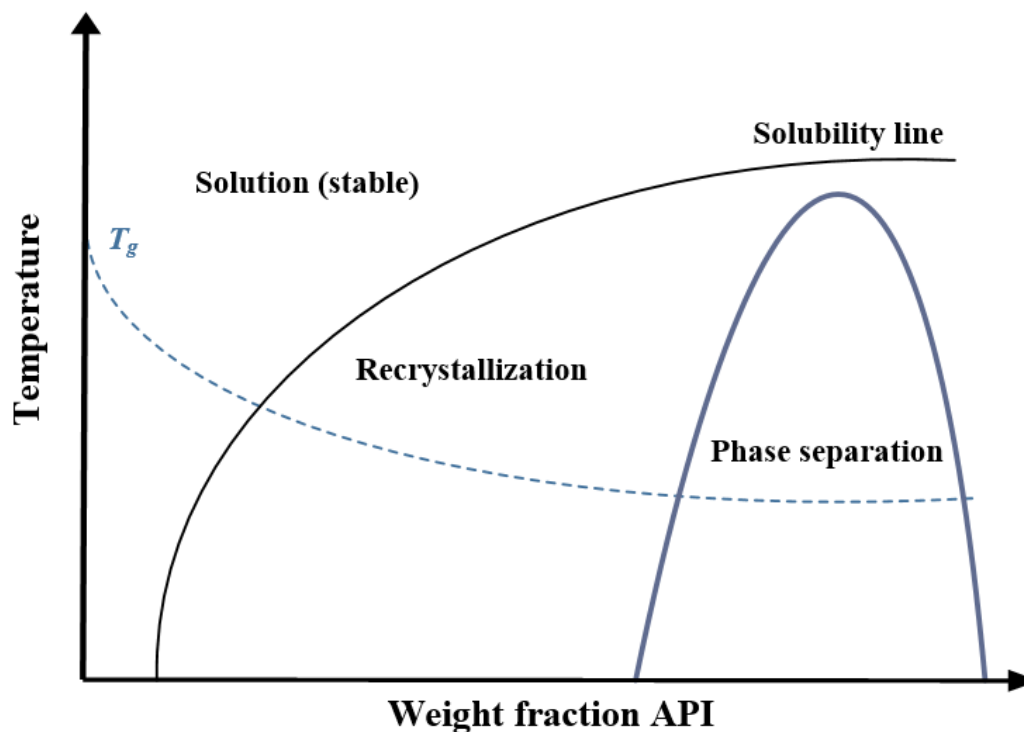

Figure 2.7. Theoretical phase diagram of a polymer drug mixture constructed using the PC-SAFT theory with the combined glass transition temperature (dashed line) [139].

More recently molecular dynamics and docking have been used for the screening of applicable excipient combinations and the interaction between them [141–143]. These studies have shown that for example a T_g and the effect of a plasticizer on this property can be estimated by molecular dynamics. Moreover, such simulations have been shown to enable the simulation of HME by a simulated annealing step, which was further used for the evaluation of miscibility of the compounds used.
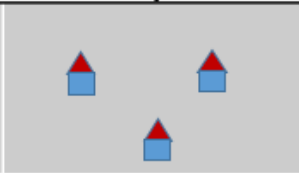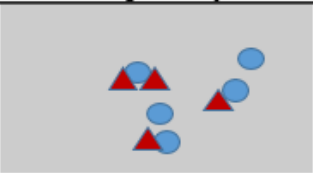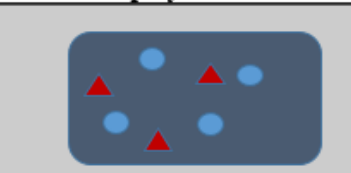
2.3 Co-former in amorphous solid dispersions

2.3.1   General considerations

In an amorphous drug delivery system, excipient characteristics are particularly critical for the formulation performance like miscibility of the components, aqueous solubility, supersaturation behavior, and stability of the amorphous form as outlined in the previous sections. Since the need of viable multifunctional excipients has outgrown the number of available pharmaceutical polymers,

different research groups presented the concept of introducing small molecular additives, which interact specifically either with the drug [40,144–147] or with the polymer [122,148,149]. The important difference to the simple combination of two polymers in a blend and the systems described in this section is that a specific interaction between the components is targeted already through the selection of the additives. Such systems can be differentiated in either modified polymeric matrix systems [122], co-amorphous systems [150], or co-crystals [151]. The intended molecular interaction has at least for co-crystals not always been a characteristic aspect but it is these days common in modern crystal engineering [152]. The co-amorphous and modified matrix systems are more recent formulation options and come generally with the engineering approach of targeting the interactions. The major differences between these systems are described below and highlighted in Table 2.7.

Table 2.7. Overview co-former systems

	Co-crystals	Co-amorphous systems	Modified polymeric matrix
Solid state	Crystalline	Amorphous	Amorphous
Composition	Co-crystal former + drug	Additive + drug	Additive + polymer + drug
Interaction	Hydrogen bonding	Mostly hydrogen bonding or salt formation	Hydrogen bonding between the additive and polymer. Interactions between polymeric matrix and drug are possible
Primary objective	• Improved drug dissolution	• Improved amorphous stability • Improved drug dissolution	• Technical processing benefits • Improved amorphous stability • Improved drug dissolution

The polymeric matrix systems mostly focus on altering polymer properties as described in section 3 by mainly targeting the interaction between the co-former and the polymer rather than the interaction with the drug [122,148]. Co-amorphous systems are mainly investigated with regards to the sole interaction between a drug and a small molecular additive and have been proposed to be feasible without the addition of a polymer [40,153]. The third option when combining small molecular additives with APIs is the formation of a co-crystal, which describes a crystalline structure of the additive and drug. The absence of ionic interactions makes here a difference to drug salts. Whether a drug forms a co-crystal or a co-amorphous system has to be determined experimentally. There are efforts to identify co-formers

that rather form a co-crystal than a co-amorphous complex [154]. However, this highly depends on the components as well as the composition of the mixture. Moreover, it is possible for co-amorphous systems to be used as an intermediate during the formation of a co-crystal [155].

As highlighted in the previous sections, besides the stability of the amorphous form, the ability to form a supersaturated state upon aqueous dispersion is pivotal for an amorphous drug delivery system. This is particularly important when co-formers with limited water solubility are used to increase the stability, because the strong interaction within the formulation has to be balanced with the intended release of the drug. Therefore, the majority of co-formers in amorphous formulations are amino acids, which are ionized upon aqueous dispersion and as a consequence present a sufficient solubility in water. However, other compounds like dicarboxylic acids [122] or highly water-soluble substances like urea or meglumine [148] have also shown beneficial properties in the application as a co-former. The highly water-soluble co-formers come, however, with the drawback that it is difficult to find a common solvent with a poorly water-soluble drug. If neither a solvent-based method nor HME is an option, the only feasible production process is co-milling [91,154].

In review articles, several authors suggested different approaches for the selection of additives in amorphous drug delivery systems [140,156]. The two crucial factors for the successful selection of a co-former in an amorphous system are miscibility and molecular interaction with a compound in the formulation.

The classical approach to select additives case-by-case on a trial and error basis is still often pursued but should be replaced by designing formulations. Such a concept was reported by Pajula and colleagues, who applied computational docking to identify promising candidates for the inhibition of drug crystallization [157]. In their studies, they reported that molecules with a higher free energy of binding than the reference molecule showed experimental inhibition of crystallization.

Several reviews were published over the last years, which highlight the selection of co-formers as well as the evaluation of co-formers in amorphous solid dispersions [91,140,147,150,158,159]. Moreover, an overview of co-formers used in amorphous formulations is provided in table 2.8.

In summary, all of the three described systems can be applied for their specific pharmaceutical application. The co-crystals might not reach similar apparent solubility increase and drug dissolution when compared to the two other amorphous systems. However, a co-crystal does not come with the stability issues of an amorphous formulation. Co-amorphous system and polymeric matrices come with the difficulty of physical stabilization as mentioned above. Although they show tremendous improvement in drug release, the future will show how broadly they find application in industrial developments of drug products.

Table 2.8. Co-former used in amorphous solid dispersions

Co-former	Side chain	Physiological charge	Melting point/ degradation	Typical interactions
Amino Acids				
Lysine [144]	-NH$_2$	+1	224.5 °C	Acid/Base or H-bonding
Arginine [144]	-NH$_2$-NH-NH$_2$	+1	244.0 °C	Acid/Base or H-bonding
Histidine [148]	-NH-	0	287.0 °C	H-bonding
Phenylalanine [144]	Benzene ring	0	283.0 °C	Hydrophobic or π-π
Tryptophan [160]	Indole ring	0	290.5 °C	H-bonding or π-π
Serine [144]	-OH	0	228.0 °C	H-bonding
Aspartic acid [144]	-COOH	-1	270.0 °C	Acid/Base or H-bonding
Glutamine [144]	-CONH$_2$	0	185.5 °C	H-bonding
Threonine [140]	-OH	0	256.0	H-bonding or hydrophobic
Other Acids				
Citric acid	3x –COOH & -OH	-3	153.0 °C	Acid/Base or H-bonding
Succinic acid [161]	2x -COOH	-2	188.0 °C	Acid/Base or H-bonding
Tartaric acid [161]	2x -COOH & 2x -OH	-2	206.0 °C	Acid/Base or H-bonding
Malic acid [122]	2x –COOH & -OH	-2	130.0 °C	Acid/Base or H-bonding
Other Co-former				
Saccharine [149]	-NH-SO$_2$ & Benzene ring	-1	224.0 °C	Acid/Base or H-bonding or π-π
Meglumine [148]	5x -OH & -NH-	1	128.5 °C	H-bonding
Quercetin [162]	5x -OH & Benzene rings	-1	316.5 °C	H-bonding or π-π

2.3.2   Application of co-formers in polymeric amorphous drug formulations

The concept of modifying existing polymers by combining them was broadly used in current research to result in desirable polymer properties [163,164]. While this concept also targeted the interaction between the polymers, it most commonly utilized only polymer-polymer combinations. The combination of a small molecular additive to target specific interactions with the polymer, which could result in comparable beneficial processing parameter and better stabilization of a drug in its amorphous form, was rather new to this field.

The basis of small molecular additives interacting with a polymer in an ASD was first proposed by Higashi and colleagues, who milled a ternary mixture of probucol, saccharin, and Eudragit E PO in a cryomill. The resulting mixtures showed interactions between probucol and Eudragit E as well as between saccharin and Eudragit E. Moreover, these interactions led to improved release properties in comparison to the mixtures without saccharin and an improvement in amorphous stability of the drug. In contrast to the co-amorphous systems mentioned in the previous section, the system described by Higashi and colleagues also targeted the interaction between the polymer and the additive to stabilize the drug through further interactions [149].

On the basis of a polymer in a ternary mixture with an additive and a drug, the amorphous drug delivery system of modified polymeric matrices (Table 2.7) was developed. In this concept, instead of the interaction between additive and drug, only the interaction between the additive and the polymer is addressed. A new polymeric matrix is targeted in this case that could be used for different drugs. Therefore, this excipient interaction primarily alters the characteristics of neat polymer but further interactions with drug are desired regarding formulation performance. Prior to the practical formulation development, the molecular interactions should be targeted based on a molecular rationale. Such a modified polymer matrix is produced in a two-step process, which consists of the manufacturing of a polymer-additive matrix and the combination of such systems with a drug in a separate step. The pre-processing of the polymer with the additive can lead to a broader range of processing options for the later manufacturing of a drug- containing ASD. If this approach is applied carefully, polymeric compounds, which would otherwise not be feasible for HME, can be easily extruded [148]. This is of particular interest if HME is the most promising amorphization technique for the selected API.

The desired improvements of a modified polymeric matrix are in line with the co-amorphous systems, which may provide an increase in amorphous stability as well as supersaturation upon aqueous dispersion thereby resulting in a likely higher absorption *in vivo*. The advantages of a modified matrix would have to be assessed specifically for a given drug.

Another aspect of such a system is the practical use for an excipient manufacturer, who is able to produce for example a proprietary modified polymeric matrix to sell it to the pharmaceutical industry.

Consequently, the modified polymeric matrices present a valuable option in the development of modern ASDs. This formulation approach is especially attractive if no suitable polymer is available and the biopharmaceutical properties require drug formulation in an amorphous form.

Chapter 3

Modified polymer matrix in pharmaceutical hot melt extrusion by molecular interactions with a carboxylic co-former

Summary

Hot melt extrusion (HME) has become an essential technology to cope with an increasing number of poorly soluble drug candidates. However, there is only a limited choice of pharmaceutical polymers to obtain suitable amorphous solid dispersions (ASD). Considerations of miscibility, stability, and biopharmaceutical performance narrow the selection of excipients, and further technical constraints arise from needed pharmaceutical processing. The present work introduces the concept of molecularly targeted interactions of a co-former with a polymer to design a new matrix for HME. Model systems of dimethylaminoethyl methacrylate copolymer, Eudragit E (EE), and bicarboxylic acids were studied, and pronounced molecular interactions were demonstrated by ^{1}H, ^{13}C NMR, FTIR spectroscopy, as well as by different techniques of microscopic imaging. A difference was shown between new formulations exploiting specifically the targeted molecular interactions and a common drug-polymer formulation. More specifically, a modified matrix with malic acid exhibited a technical extrusion advantage over polymer alone, and there was a benefit of improved physical stability revealed for the drug fenofibrate. This model compound displayed greatly enhanced dissolution kinetics from the ASD formulations. It can be concluded that harnessing molecularly designed polymer modifications by co-formers has much potential in solid dispersion technology and in particular regarding HME processing.

3.1 Introduction

Poor water solubility of new drug candidates is a main pharmaceutical challenge to avoid erratic and highly variable absorption following oral administration. To facilitate effective and safe medications, bio-enabling formulations are needed and much research has centered around amorphous drug delivery systems [55,165–167]. There are a few methods available for drug amorphization; however, a recent overview of oral drug products on the market based upon amorphous drug delivery systems clearly demonstrated that spray drying and hot melt extrusion (HME) were the most abundant industrial manufacturing processes [41,165].

For physical stabilization of drugs in an amorphous form, there are some pharmaceutically accepted polymers available. However, specific process demands of spray drying or HME manufacturing define some limitations to this choice. This is also reflected by the use of few different polymers in the compositions of marketed solid dispersions [41]. Hence, new chemically engineered polymers would be desirable. However, the development and regulatory requirements [168] of a pharmaceutical excipient results in lengthy and costly processes. Another hurdle of chemical excipient modifications is the resulting permanent character. This permanent modification could lead to advantages regarding processing and physical stability, which may not always go along with the situation upon formulation hydration followed by a suitable drug release and supersaturation. Consequently, a non-permanent modification would be beneficial to overcome the previously mentioned difficulties.

Therefore, another approach to broaden the excipient landscape would be the combination of already approved polymers with interacting pharmaceutically acceptable small molecular compounds to obtain specifically designed matrices by co-processing. This could generate advantages with respect to dry formulation as well as improving the biopharmaceutical properties. This scope differs from classical addition of small molecular process aids that typically interact non-specifically without a clear molecular rationale [169]. Previous work on additives was either rather of an exploratory nature or it was, for example, intended to generate a pH microclimate upon release, which is a specific approach in its own right [91]. Different from the present study aims are further co-amorphous systems because the targeted interactions are directly between additive and active pharmaceutical ingredient (API) [145,170].

It was recently identified by Higashi and co-workers [149] that the creation of molecular interactions between a model drug and dimethylaminoethyl methacrylate copolymer, Eudragit E (EE) together with saccharine, as a small molecular additive, led to an improved drug dissolution behavior. The authors argued that saccharine was interacting via ionic or hydrogen bonding with the polymeric amino group. Drug interactions were in this case rather given by the hydrophobic side chains of the polymer. This was in line with a recent study, which suggested that even basic drugs can exhibit great solubility enhancement with EE [171,172]. This may appear counter-intuitive given the same charges of drug and

polymer at physiological pH. However, NMR data indicated that hydrophobic interactions of the drug with polymer were likely involved in the observed solubility increase. While the amino group can be beneficial for direct interactions with acidic drugs [172], it might be in other cases better masked or changed by specific additives.

Encouraged by finding an additive hydrophobic interaction of EE with lipophilic drugs, [171] a change of the amino group in EE could lead to a modified matrix that retains its ability to interact with hydrophobic compounds. A concern of this approach may be that masking of the hydrophilic amino group possibly decreases hydration and solubility of the modified polymer; hence, an optimal interacting component may need to have an additional hydrophilic group to compensate.

Therefore, the aim is to use small-molecular additives to change specifically functional polymer groups. In this context it is possible to profit from analytical advancements and excipient screening in the science of co-amorphous formulations, even though the latter field is quite different from that of modified matrices as the scope of co-amorphous complexes is to alter drug properties directly, for example regarding glass forming ability [91,173].

In contrast to previous co-amorphous studies [144,145,147], the idea to design a modified polymer matrix by small-molecular additives is a new approach and improvements regarding processing, stability, or biopharmaceutical performance can origin from such a co-processed system [91]. This work targets specific interactions of small molecular bivalent acids with the amino group of EE. In line with the above-mentioned considerations, bivalent acids mask the amino group of EE, while the second carboxyl group is meant to retain sufficient polymer swelling and solubility. The hypothesis is whether such an approach is technically feasible and if it is possible to obtain clear benefits for amorphous solid dispersions of a poorly water-soluble model drug (i.e. fenofibrate).

3.2 Materials and Methods

3.2.1 Materials

EE was kindly provided by Evonik Industries (Essen, Germany); malic acid (MA) and the model drug fenofibrate (FE) were bought from Sigma-Aldrich (St. Louis, MO, USA). All compounds were used as received either in the initial co-processing of polymer and MA or for an alternative direct extrusion of all components by hot melt extrusion. The different compositions of the formulations as well as reference mixtures are outlined in Table 3.1. For a reference of the physical mixture, crystalline FE was used.

3.2.2 Methods

3.2.2.1 Process of hot melt extrusion (HME)

The different solid dispersions were prepared by using the co-rotating twin-screw extruder ZE9 ECO from Three-Tec (Birren, Switzerland). A pair of screws with a diameter of 9 mm, a length of 180 mm was used that consisted of conveying as well as mixing elements. Prior to extrusion, all ingredients were pre-mixed in a beaker to then manually fill the extruder with a spatula. The three heating zones of the extruder were set to 130 °C and a screw speed of 80 rpm was applied. After extrusion, the extrudates were cooled to room temperature and stored at ambient conditions in falcon tubes. The formulation called 'matrix extrusion' was manufactured by an initial extrusion of the polymer with additive (EE / MA) to obtain a co-processed matrix ('matrix extrusion') that was vibrational milled at 30/s for 1 min. A subsequent extrusion with addition of the model compound FE provided the final drug product. All other formulations (FE / EE / MA 'direct extrusion', and FE / EE) were manufactured in the process described by a single extrusion step. The physical mixture was obtained by mixing and consecutive milling (Table 3.1). All milled powders were sieved (mesh size = 150 μm) to achieve a comparable particle size distribution.

Table 3.1. Composition of the different extrudates and of physical mixture for comparison

	Content MA [%]	Content EE [%]	Content FE [%]	Manufacturing[a]
Matrix	32.4	67.6	-	Extrusion, milling
Direct extrusion	27.5	57.5	15	Extrusion, milling
Matrix extrusion	27.5	57.5	15	Extrusion, milling, extrusion, milling
FE / EE extrusion	-	85	15	Extrusion, milling
Physical mixture	27.5	57.5	15	Milling

[a] The described processing steps were applied in the order mentioned

3.2.2.2 Molecular interaction studies

3.2.2.2.1   Attenuated total reflectance Fourier-transform infrared spectroscopy (ATR-FTIR)

The FTIR spectra were measured by a Cary 680 Series FTIR spectrometer (Agilent Technologies, Santa Clara, USA) equipped with an attenuated total reflectance accessory. A scanning range of 4000–600 cm^{-1} was selected with 32 scans and a resolution of 4 cm^{-1}. The spectra were evaluated using the software ACD/Spectrus Processor 2016.1.1 (Advanced Chemistry Development Toronto, Canada).

3.2.2.2.2 Nuclear magnetic resonance spectroscopy (NMR)

The ^{13}C-NMR spectra were recorded at ambient conditions on a Bruker Avance III 400 NMR spectrometer (Bruker BioSpin AG, Fällanden, Switzerland) fitted with a 5 mm i.d. BBO prodigy probe and operating at 100.61 MHz. The number of scans was set to 1024. The samples were dissolved in deuterated DMSO, and for processing the spectra, the software TopSpin 3.5pl7 from Bruker was used. Deuterated DMSO was selected, because it would not interfere with the investigated interaction [120]. The solvent peak of DMSO served as reference for comparison of the spectra. Peaks were assigned using 2D heteronuclear single quantum coherence spectroscopy (HSQC) NMR measurements. Moreover, the influence of molecular interactions between additive and polymer were also simulated by the software ACD/C+H NMR Predictors 2016.1.1 (Advanced Chemistry Development Toronto, Canada) to support interpretation of the NMR spectra.

3.2.2.3 Stability assessment and drug dissolution

3.2.2.3.1 Powder X-ray diffraction (PXRD)

The analysis of an amorphous form by PXRD was performed on a D2 Phaser diffractometer (Bruker AXS GmbH, Karlsruhe, Germany) with a 1-D Lynxeye detector. The instrument was equipped with a 1.8 kW Co KFL tube providing X-ray radiation at a wavelength of 1.79 Å. During the measurements, a voltage of 30 kV and a current of 10 mA were used. The increment and time per step were set to 0.02 ° and 2 s, respectively. The measurements were performed over a range of 5 ° to 39 ° (2θ). To avoid the recrystallization of the drug because of processing steps, the extrudates were cut in 2 cm long pieces and arranged to cover the complete sample holder of the instrument.

3.2.2.3.2 Differential scanning calorimetry (DSC)

Further solid-state assessment of an amorphous form was based on thermal analysis by using a differential scanning calorimeter DSC 3 (Mettler Toledo, Greifensee, Switzerland). The measurements were conducted at a heating rate of 10 °C/min from -20 to 140 °C. The surrounding of the sample cell was purged with nitrogen at 200 mL/min. To evaluate the thermal history of the sample, the first heating was used. The samples were cut into small pieces and 5 - 9 mg was placed in an aluminum pan with a pierced lid. The thermal events were analyzed with the STARe Evaluation-Software Version 16 (Mettler Toledo, Greifensee, Switzerland).

3.2.2.3.3 Polarized light microscopy (PLM)

An assessment of crystallinity was based on polarized light imaging using a microscope Olympus BX60 (Volketswil, Switzerland) equipped with a polarization filter. Extrudates that were transparent were placed in the sample holder and analyzed by taking pictures with full polarized light to detect crystals

as birefringent spots. The images were compared with pictures in unpolarized light. All of these pictures were acquired with a digital camera XC30 from Olympus attached to the microscope. The magnification remained constant throughout the whole measurement (scale bars are displayed in every image).

3.2.2.3.4 Scanning electron microscopy (SEM) with energy dispersive X-ray spectroscopy (EDX)

Cross sections of the extrudates were analyzed with a SEM TM3030 Plus (Hitachi, Tokyo, Japan). Elemental constitution was evaluated using EDX with an acceleration voltage of 15 kV. The Quantax 70 system was employed, which consisted of an X Flash Min SVE signal processing unit, Megalink interface, a scan generator, and an X Flash silicon drift detector 410/30H (Bruker Nano GmbH, Berlin, Germany). Images were processed for detection of the halogen chloride to analyze the spatial distribution of FE on the sample.

3.2.2.3.5 Confocal laser scanning microscopy (CLSM)

The 3D CLSM (Keyence VK-X200) images were acquired on a Keyence VK-X200 confocal laser microscope with a wavelength of 408 nm to measure even larger areas of the samples. Image magnifications are shown in the pictures. Cross sections of the extrudates were evaluated after cutting the extrudates with a razor blade.

3.2.2.3.6 Atomic force microscopy (AFM)

Measurements were performed on a NanoWizard 4 from JPK (maximum XY scan range: 100 x 100 mm, Z-height maximum: 15 mm) at ambient conditions of 25 °C. The cantilever Tap190 was used in the so called tapping or AC (amplitude control) mode. In this mode, the probe is oscillated near its mechanical resonance frequency. During each cycle of the oscillation, the probe lightly taps the surface and the amplitude of oscillation is reduced due to damping or dissipation of energy already in close proximity of the interacting surface. The AFM system uses this change in amplitude to track the surface topography. If the phase imaging mode is carried out, the phase shift relative to the driving oscillator is monitored in addition to the amplitude. Typically, the phase signal is sensitive to variations in composition, adhesion, friction, viscoelasticity as well as other factors. Therefore, material differences manifest in brighter and darker regions in the phase images, comparable to the way topography changes are recorded in height images. The cantilever had a force constant of 48 N/m and a resonant frequency of 190 kHz. All pictures are given in 512 x 512 pixel and adjusted coloring for comparison. Samples were cut to investigate the cross sections and placed into the sample holder of the instrument.

3.2.2.3.7   **Dynamic flow properties**

A rotating drum system (Revolution®, Mercury Scientific Inc., USA) was employed to measure powder flow properties. The powder movement in the barrel with a diameter of 55 mm and a width of 35 mm was scanned by a camera (resolution of 648×488 pixel). The acquired pictures at 10 frames per second were analyzed by the Revolution® V3.00 software (Mercury Scientific Inc., USA). Prior to the measurement, the drum was filled with a constant sample volume of 14.5 mL, and the initial rotation time was set to 45 s. After that time, 150 avalanches were monitored at a rotation speed of 1 rpm. All measurements were performed in triplicates. The measured properties were avalanche angle [°] and absolute break energy [mJ/kg]. The avalanche angle was recorded as the angle between the center point of the powder edge and the highest position before the occurrence of an avalanche. The absolute break energy was defined to be the maximum energy in the powder sample before the beginning of an avalanche. This value is considered as the required energy for the start of an avalanche [174,175].

3.2.2.3.8   **Comparison of dissolution behavior**

Drug dissolution was studied for comparison of the extruded formulations and the physical mixture. Prior to dissolution, all samples including the physical mixture were milled in a vibrational mill for 1 min at a speed of 20/s. A USP II dissolution apparatus filled with phosphate buffer solution at pH 6.4, as described by PhEur. 2.9.3, in combination with 0.5 % sodium dodecyl sulfate was used. The paddle speed and temperature were set to 100 rpm and 37.0 °C, respectively. This experimental procedure was in accordance with quality control dissolution setups [94]. Upon withdrawal from the dissolution media, the samples were filtered through a 0.4 µm filter directly. The withdrawn media was replaced immediately with temperature-controlled dissolution media. Samples were analyzed by a high pressure liquid chromatography system from Agilent (Agilent Technologies, Santa Clara, USA) equipped with a UV detector, which was set to 287 nm. The flow rate was set to 0.25 mL/min with a run time of 10 min and an injection volume of 20 µL. As separation reverse phase column a ZORBAX Elipse Plus C18 (Agilent Technologies, Santa Clara, USA) was used.

3.3 Results and discussion

3.3.1   **Molecular considerations for polymer and co-former selection**

The polymer selection is critical for any solid dispersion and should particularly consider the type of intended release as well as miscibility with a given drug [176]. It has been attempted previously to choose polymers based on *ab initio* considerations of molecular drug interactions[177], which should not only help to achieve a good kinetic stability of the solid dispersion, but also facilitate sustained supersaturation upon formulation dispersion [118]. Further selection criteria are linked to the intended processing (i.e., HME), why the glass transition temperature (T_g), the melting point (T_m), degradation temperature (T_{deg}), as well as the resulting melt viscosity at extrusion temperature should be considered.

Optimal is of course when formulators could choose from a broad variety of alternative polymers to meet the technical needs of manufacturing; however, such a selection is rather limited with pharmaceutically acceptable polymers. To generate more potential variations and thereby options, the current work hypothesized that co-processing of a polymer with small molecular additive could provide a specifically modified polymer matrix with advantages for solid dispersions produced by HME. The model polymer EE was selected for this purpose, as the aminoalkyl group can interact with acidic small molecular additives in line with the scope of the current study. Moreover, the polymeric side chains of EE seem attractive regarding possible hydrophobic interactions with a drug [171,172,178]. Strong hydrogen bonding of a weak carboxylic acid with EE's tertiary amines have been reported, and direct drug-polymer interactions were shown not to lead to any salt-formation [121]. Unlike this previous study, such polymer interactions were in the current work harnessed by bicarboxylic additives. Those additives have proven to be beneficial for HME processing by Parikh and Serajuddin, although in their work, the interaction was formed between an API and the acid [179]. Compared to monocarboxylic acids, the additional carboxy group should reduce the risk to make the EE polymer matrix too hydrophobic upon aqueous dispersion in gastrointestinal fluids. Thus, promising bicarboxylic acid candidates included succinic acid, maleic acid, fumaric acid, tartaric acid, malonic acid, and MA, which were studied during initial extrusion trials with EE. For the assessment of amorphous stability, FE was chosen as a model drug due to its well-described amorphous instability [38]. Initial extrusion trials with bicarboxylic acids could not result in completely amorphous FE formulations as demonstrated by PXRD measurements or showed poor processing ability. Different mechanisms possibly contributed to less favorable extrusion results such as decomposition, differences in melt viscosity or melting point, or lack of miscibility. On the basis of the initial bicarboxylic acid screening, a focus was made on the most promising compound, MA as co-former for EE.

3.3.2 Modified polymeric matrix

3.3.2.1 Molecular interaction

In line with the targeted molecular assembly of EE and MA, a first objective of this work was to verify the molecular interaction as well as the potential benefits for the HME of EE and MA experimentally. Technical extrudability was indeed improved in the presence of MA. Compared to pure EE, the ease of resolidification and strand formation from the orifice of the extruder was improved in the modified matrix. The final product was a transparent and homogeneous extrudate. FTIR measured on the extrudate (Figure 3.1) showed the broadening of the O-H peak in the region of 3400 cm^{-1}, which led to a flatter, hardly detectable peak. This could be associated with MA, since it is the only molecule in the mixture with a free hydroxyl group [144]. It also has to be taken into account that the amorphous nature of the extrudate caused a rather general peak broadening. Moreover, a specifically broad peak holding

for an asymmetrical stretching vibration at 1580 cm^{-1} was identified, which can be associated with hydrogen bonding interaction of the carboxylic group of MA [146,180].
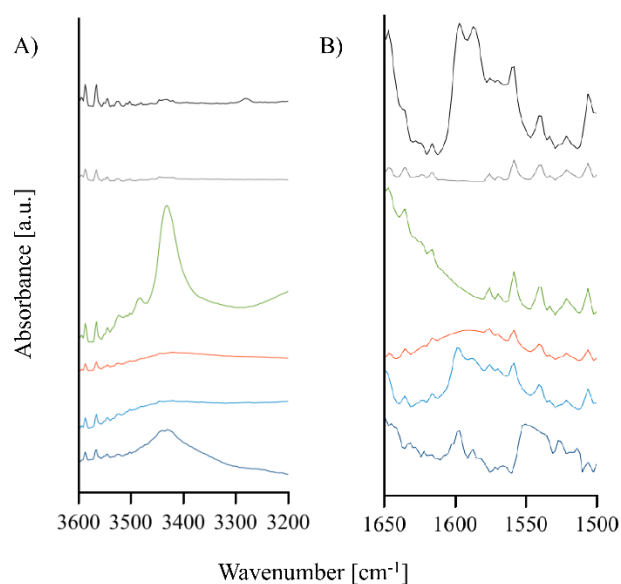

Figure 3.1. (A,B) FTIR spectra of the different formulations between 3200−3600 cm^{-1} and 1500 −1650 cm^{-1}, respectively. The curves represent powders of FE (black), EE (gray), MA (green), extrudates of MA /EE (red), FE/MA/EE (light blue), and the physical mixture of FE/MA/EE (dark blue).

The vibrational FTIR spectroscopy was complemented by NMR analysis. While in the ^{1}H-NMR, a differentiation between the different hydroxyl groups of MA and therefore their specific interaction with the polymer was hardly detectable, ^{13}C-NMR was applied for a more detailed analysis. An interesting region for the two carboxylic groups of MA was shown between 172 and 176 ppm, which in the ^{13}C spectrum corresponds to a shift of the two carbons in the two carboxylic groups (Figure 3.2). In comparison to the pure MA, the spectrum of the extruded polymeric matrix showed a peak shift, which was more intense for the carboxylic group with an alpha hydroxyl group (Figure 3.2). Therefore, this group is likely to show an interaction with the polymer, which was formed during the extrusion [178]. Neither FE nor EE showed interfering peaks in the investigated region, because the ester peak of FE could be clearly distinguished from the carboxylic peaks of MA.
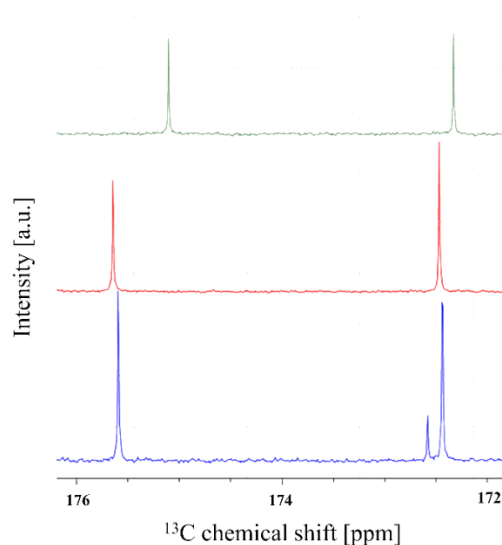
Figure 3.2. ^{13}C NMR spectra region between 176 and 172 ppm of MA (green), MA / EE (red), and FE /MA /EE (blue).

The observed shift was in line with a simulation of the spectrum as calculated by the ACD/C+H NMR Predictor. Moreover, the same shift could be observed in the formulation with FE (Figure 3.2). Consequently, the interaction was not interrupted by the addition of the model API, which showed a peak between the two carboxylic peaks of MA.

3.3.2.2 Amorphous form and phase behavior

An initial physical characterization of the modified matrix was based on DSC and PXRD analysis. The thermograms of the modified matrix displayed a single glass transition and no melting endotherm, which supported the transparent aspect of the extrudates and hence miscibility of polymer and co-former (Figure 3.3).
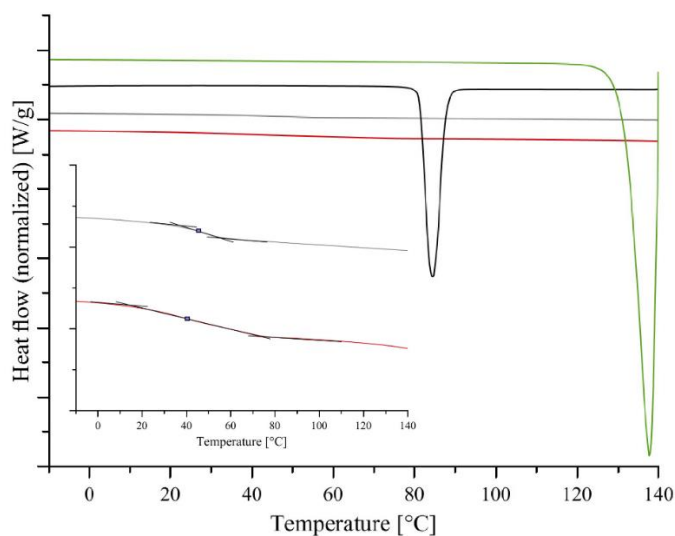
Figure 3.3. DSC thermograms of MA (green), FE (black), EE (gray), and MA/EE (red). Insert shows the T_g of EE and MA/EE

These findings were in accordance with the observations provided by the PXRD experiments, where the distinct peaks of crystallinity of MA were no longer visible in the modified matrix (Figure 3.4).
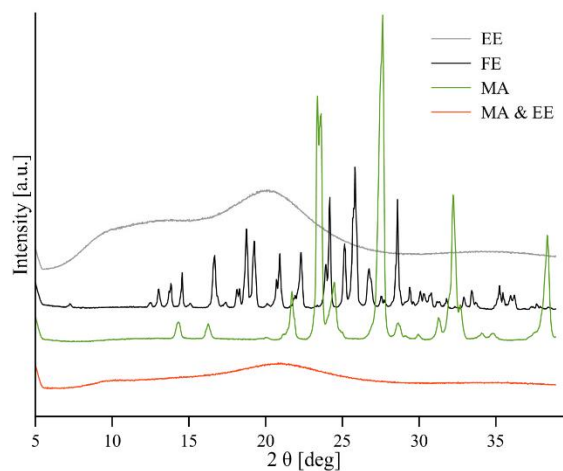
Figure 3.4. PXRD of MA (green), FE (black), EE (gray), and MA/EE (red)

The diffraction pattern and thermograms were complemented with imaging methods. The extrudates of the novel matrix exhibited a smooth surface and absence of noticeable features inside the matrix as evidenced by CLSM (data not shown). For a homogeneity analysis on a nanometer scale, extrudates were studied further by AFM phase analysis [181]. Figure 3.5 shows that only one phase was present in the cross section of the modified polymer matrix. Different sampling areas were scanned, and no signs of separating domains that could suggest the beginning of a phase separation were observed. Imaging by AFM is a meaningful complementary analysis to other previously mentioned bulk methods. Especially phase separations of non-crystalline components are not detected by a classical PXRD analysis, and it can be challenging for DSC, in which a single T_g is not always a reliable marker of homogeneity in a nanometer domain [182]. However, since the AFM imaging also suggested homogeneity across the analyzed length scales, the modified polymeric matrix was considered a glassy solution. The results therefore experimentally confirmed that a single-phase modified matrix could be obtained as hypothesized.
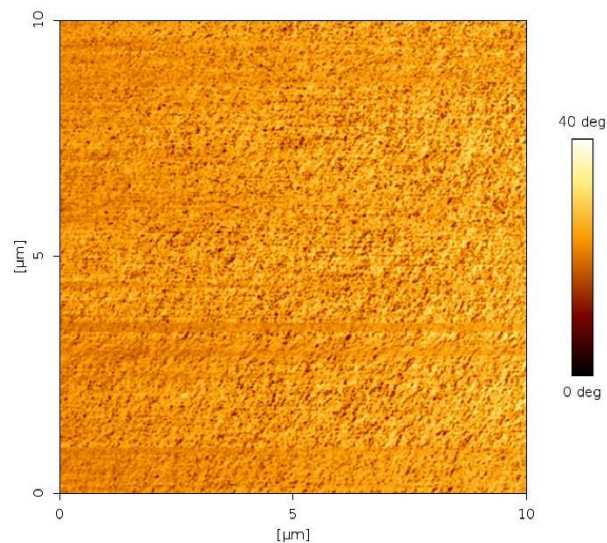
Figure 3.5. AFM phase images of the modified polymeric matrix (MA /EE)

3.3.3 Formulation of a model drug in the modified polymer matrix

An important study objective was to demonstrate the utility of the modified polymer matrix with a poorly water-soluble model drug. FE was used for this purpose, and it was hypothesized that mainly the hydrophobic side chains of EE would lead to interactions with the drug, while the tertiary amine of the polymer would mostly be interacting with MA. The assumption of hydrophobic side chain interactions was encouraged by recent studies that successfully used EE in combination with non-acidic drugs [171,183]. Based on such dispersive interactions with the lipophilic drug FE and the targeted molecular interactions with MA, Figure 3.6 shows an image of the assumed molecular architecture. The amine moieties of the polymer are in close proximity with carboxyl groups of the MA (shown in magenta), as it was also experimentally confirmed by the spectroscopic results of the previous section. This polymer and co-former matrix can host FE mostly between the acyl chain residues, which offers various hydrophobic interactions. The multitude of interaction options entails a favorable enthalpy of mixing with the polymer matrix, while at the same time various configurations of drug inclusion are also beneficial with respect to the entropic contribution when mixing with the drug. FE may further profit from the modified matrix because the polymeric amine is mostly masked by MA. Nitrogen-containing functional groups are known in the field of glycerides to often reduce drug solubilization of lipophilic drugs [184]. However, to verify these theoretical considerations experimentally, a proof-of-concept study was conducted. The modified matrix was first manufactured as a co-extruded material of EE and MA. The milled extrudate served as a novel polymeric matrix for HME together with FE. A comparison to this modified matrix approach was to directly compound EE, MA, and drug in a single HME step. Apart from such "direct extrusion" samples, there was also a comparison made with extruded drug with EE alone (i.e., without the co-former MA).
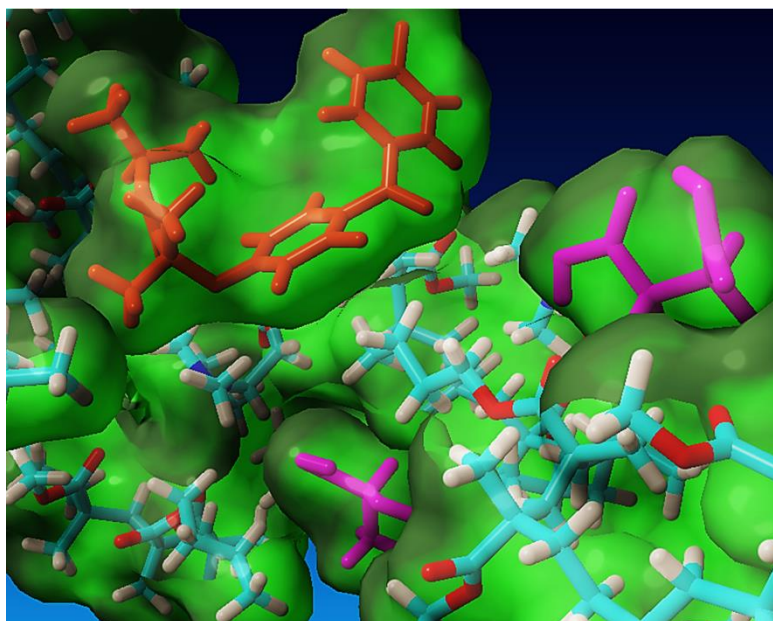
Figure 3.6. Visualization of the polymer matrix (EE displayed as tubes with standard color codes) together with FE (bronze tubes) and the co-former MA (magenta tubes). Only a part of the matrix is shown together with molecular surfaces for clarity of presentation. Graphic is based on YASARA version 16.12.6 using an AMBER14 force field.

3.3.3.1 Drug formulation processability, homogeneity and stability

A first advantage of the FE formulation with the modified matrix was observed during HME. The polymer EE was barely extruded in other studies with drugs like FE that exhibit a low melting point [185,186]. Thus, pure EE with FE produced soft strands with slow resolidification kinetics when exiting the extrusion orifice. This processing behavior was similar to what was obtained with polymer alone and in our experience; it could be barely improved by any optimization of process parameters. Moreover, even after longer cooling a certain stickiness remained. In contrast to these results, drug formulated with the modified matrix resulted in a fast resolidification upon extrusion, and the extrudates were comparatively harder and therefore more suitable for any down-stream processing. The drug formulation with MA appeared to have similar properties to the modified matrix alone and clearly different to polymer without MA, which exhibited marked particle aggregates after milling. These qualitative observations were compared with quantitative flow properties of the milled materials in the Revolution analyzer (Table 3.2) [187–189].

Table 3.2. Flowability and process assessment parameters for all formulations

	Absolut Break energy [mJ/kg]	Avalanche Angle [deg]	Feeding properties	Cleaning (i.e. lack of stickiness)[a]	Manufacturing
MA / EE	119.38 ± 0.27	44.33 ± 0.21	+	++	Extrusion, milling
FE / MA / EE (direct extrusion)	127.11 ± 0.12	43.67 ± 0.25	+	+	Extrusion, milling
FE / MA / EE (matrix extrusion)	124.31 ± 0.25	45.63 ± 0.12	+ +	+	Extrusion, milling, extrusion, milling
FE / EE	212.74 ± 5.14	87.4 ± 6.51	-	-	Extrusion, milling
EE powder	228.76 ± 2.19	74.80 ± 3.27	-	- -	n/a [b]

[a] For all formulations and the pure powder EE, processing parameters for feeding and cleaning are evaluated qualitatively in comparison to PVP VA 64, which is known to have good flowability properties.

[b] The pure EE was analyzed as received from the supplier.

The strong cohesion forces within the bulk of EE or FE / EE formulation resulted in an increased absolute break energy, which correlated with an increase of the avalanche angle. The comparison between pure EE and MA / EE revealed the improvement of particle flowability by the formation of the modified matrix, and such improvement was also observed when drug was included as in the direct extrusion and matrix extrusion.

The drug-containing formulation of the modified matrix as well as the reference manufactured by direct extrusion and pure drug with EE displayed no crystallinity of FE when investigated by DSC and PXRD immediately after the manufacturing. However, these classical analytical methods have limited sensitivity for small traces of initial crystallinity, and moreover, the beginning of an amorphous phase separation is often better detected by AFM.
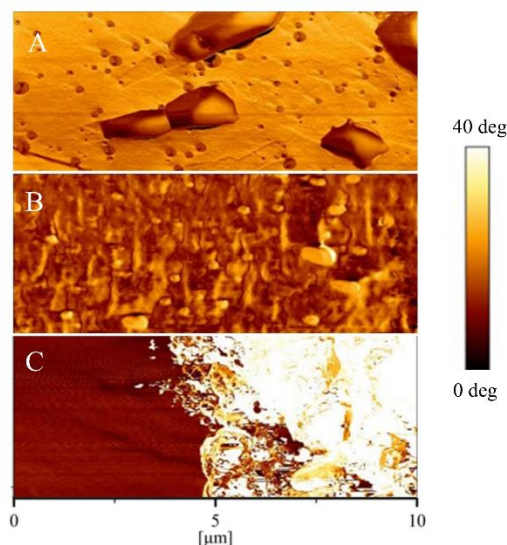
Figure 3.7. (A-C) AFM phasing images of samples from the modified polymeric systems with FE represented in the matrix extrusion (A) and direct extrusion (B), both in comparison to the FE /EE extrudate (C).

Figure 3.7 depicts AFM images of the different extrudate products with drug. Extrudates with MA displayed some micro pores (Figure 3.7A and 3.7B) but the submicron structure was very homogeneous in the case of matrix extrusion (Figure 3.7A) and slightly less homogeneous for direct extrusion (Figure 3.7B) because of the formation of small domains that were only visible at a high magnification [93]. However, there was no clear indication of a phase separation in both formulations containing MA. On the other side the FE / EE extrudate (Figure 3.7C) showed a spreading phase separation, which is often accompanied by drug crystallization [190].
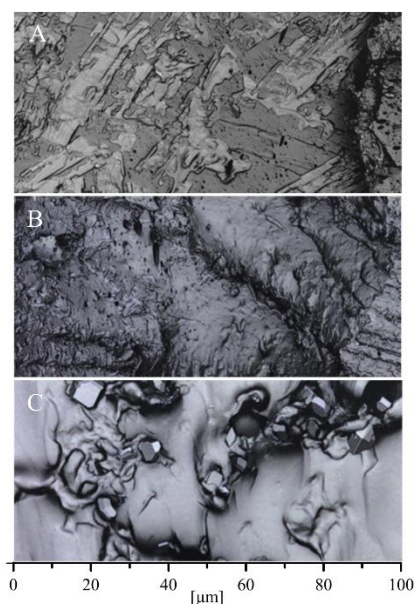
Figure 3.8. (A-C) CLSM images of the samples of drug products as modified matrix extrusion (A), direct extrusion (B), and FE /EE (C).

When a larger length scale was considered in images of CLSM, there was some crystalline material observed (Figure 3.8C), probably as a result of the previously described phase separation in the FE / EE formulation (Figure 3.7C). By contrast, in the products with MA no crystals were observed (Figure 3.8A and 8B), where only some surface effects were seen because of the sample preparation. In summary, the physical imaging methods performed pointed towards the observation of a phase separation (Figure 3.7C) and some drug crystallinity (Figure 3.8C) of FE / EE extrudate, which made a clear difference to the formulations with MA.
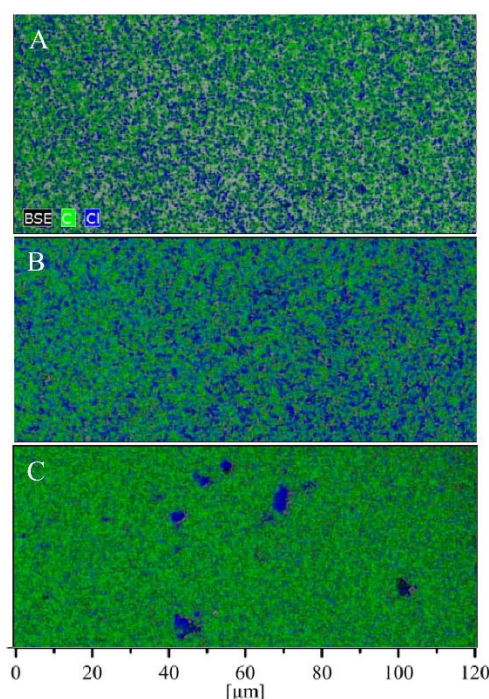
Figure 3.9. (A-C) SEM EDX images of the matrix extrusion (A), direct extrusion (B), and control (C). The green area represents the distribution of carbon, whereas the blue areas are correlated with the distribution of chlorine atoms

In addition to the physical imaging techniques, the extrudates were further investigated by the chemical imaging of SEM EDX to identify domains of FE, as detected by the distribution of chloride that is given as blue clusters in Figure 3.9. For the FE / EE formulation, an accumulation of mesoscopic drug clusters was evidenced. This was in agreement with findings of the inhomogeneous drug distribution in the polymer alone. As expected, there were no pronounced large drug clusters evidenced in the matrix extrusion and direct extrusion (Figure 3.9A and 3.9B). It may be that the matrix extrusion was most homogeneous with respect to drug distribution but a clear differentiation to direct extrusion was hard to make by a qualitative comparison.

Finally, polarized light microscopy (PLM) was used to compare the different samples. This imaging technique is different from AFM, CLSM, or SEM-EDX as a lower spatial resolution is given in this

optical microscopy. However, once nuclei grow to relatively bigger crystals; PLM has the advantage that the crystals are well detected as shining birefringent structures (data not shown). This was only detected in samples of FE with EE after two weeks storage at room temperature, whereas the samples of melt extrusion and direct extrusion did not show any crystals in line with the aforementioned results from AFM, CLSM and SEM-EDX.

3.3.3.2 Amorphous dissolution benefits

Dissolution of the formulations was conducted, using the method described for quality control [94], to identify any potential difference in the formulations with respect to their dissolution behavior. The scope was to reveal potential differences, which should be differentiated from the rationale to mimic *in vivo* conditions, since this would otherwise require biorelevant dissolution testing [94,95,191].

For a comparison, all samples were milled in a vibration mill for 1 minute. Although all samples were treated equally, the FE / EE formulation showed very poor milling processability, which resulted in agglomeration under different milling conditions. This was likely a consequence of the earlier described technical issues of FE / EE with especially the pronounced cohesion of the material. Probably as a result of this difference, the comparison between the two extruded formulations and the physical mixture showed a clear improvement in drug release for the extruded formulations. Since the FE / EE formulation did not result in a comparable processed formulation, which was also visible in the dissolution behavior, it can be concluded that the direct extrusion and the matrix extrusion were a clear advancement in terms of drug release compared to the physical mixture (Figure 3.10). In accordance with the previous analytical results, which showed phase separation and recrystallization of FE / EE, repeated dissolution experiments over time may further reveal differences in dissolution performance during storage.
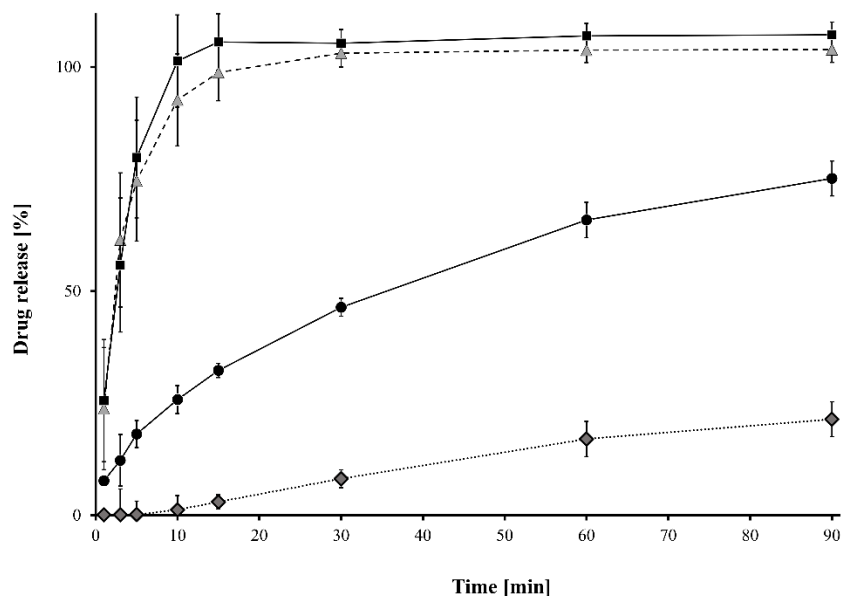
Figure 3.10. Dissolution curves of the matrix extrusion (black squares), direct extrusion (gray triangles), FE /EE extrudate (black dots), and physical mixture FE /EE /MA (gray diamonds).

3.4 Conclusions

Various aspects in HME processing of amorphous solid dispersions limit the selection of pharmaceutical polymers for a given drug. This work started from a molecular rationale to modify a polymer matrix of EE physically by co-extruding it with a bivalent acid. The molecular rationale differs greatly from classic formulation approaches, where plasticizer or antiplasticizer are screened empirically without a clear molecular rationale. Therefore, the described approach offers new opportunities based on molecular pharmaceutics to modify a polymeric matrix by means of selected small molecular additives. Such a theoretically designed modified matrix was experimentally verified as a glassy solution that was homogenous at the different length scales studied. Moreover, spectroscopic methods confirmed the assumed molecular interactions. An explicit objective was to show benefits of the new polymeric matrix with a model drug FE. This drug was selected to interact primarily with the acyl side chains of the polymer via hydrophobic interactions, while the masked tertiary amine of EE would primarily interact with the co-former MA. Benefits of the modified matrix compared to amorphous dispersions of FE in EE without co-former were demonstrated for technical feasibility but also with respect to drug distribution and lack of crystalline material. Moreover, drug dissolution was enhanced for the direct extrusion and matrix extrusion formulations, when compared to the reference formulations of pure drug and polymer.

Interesting findings were the slight differences in technical feasibility as well as drug distribution between direct extrusion and matrix extrusion with the additive MA. This could be used potentially by excipient suppliers, which would be able to offer directly a modified matrix to the pharmaceutical industry to widen the selection of suitable polymeric vehicles for HME. This approach to modify the polymeric matrix based on a molecular rationale is highly interesting and more research could target specific solubility parameters that are currently not available with existing pharmaceutical polymers for HME. The idea to modify polymers non-chemically can be harnessed in the future to target a specific increase or decrease of the glass transition or, for example, to tailor polymer swelling in water for a desired drug release. Finally, research in the future could emphasize the effects of modified matrices on long-term physical stability of amorphous solid dispersions.

Chapter 4

Polyelectrolytes in Hot Melt Extrusion: A Combined Solvent-Based and Interacting Additive Technique for Solid Dispersions

Summary

Solid dispersions are important supersaturating formulations to orally deliver poorly water-soluble drugs. A most important process technique is hot melt extrusion but process requirements limit the choice of suitable polymers. One way around this limitation is to synthesize new polymers. However, their disadvantage is that they require toxicological qualification and present regulatory hurdles for their market authorization. Therefore, this study follows an alternative approach, where new polymeric matrices are created by combining a known polymer, small molecular additives, and an initial solvent-based process step. The polyelectrolyte, carboxymethylcellulose sodium (NaCMC), was tested in combination with different additives such as amino acids, meglumine, trometamol, and urea. It was possible to obtain a new polyelectrolyte matrix that was viable for manufacturing by hot melt extrusion. The amount of additives had to be carefully tuned to obtain an amorphous polymer matrix. This was achieved by probing the matrix using several analytical techniques, such as Fourier transform infrared spectroscopy, differential scanning calorimetry, hot stage microscopy, and X-ray powder diffraction. Next, the obtained matrices had to be examined to ensure the homogeneous distribution of the components and the possible residual crystallinity. As this analysis requires probing a sample on several points and relies on high quality data, X-ray diffraction and starring techniques at a synchrotron source had to be used. Particularly promising with NaCMC was the addition of lysine as well as meglumine. Further research is needed to harness the novel matrix with drugs in amorphous formulations.

4.1 Introduction

The rising number of poorly water-soluble drugs in the development pipelines as well as on the market encouraged the pharmaceutical industry to develop new formulation techniques. One strategy is the formulation of a drug in an amorphous form as a solid dispersion, which normally leads to drug supersaturation upon oral administration to promote absorption [45,55,165–167]. Among the different process techniques for the manufacturing of amorphous solid dispersions, hot melt extrusion (HME) and spray drying are the most common methods [41,45]. These two process techniques mostly use a combination of drug and polymeric compound. However, HME formulations currently available on the market utilize only about six of the pharmaceutically accepted polymers or a combination of these [41]. Contemporary research is primarily focused on finding new combinations of well-established polymers with plasticizers and surfactants [192], or even on designing new monomers for novel synthetic polymers that come with the aforementioned multiple development hurdles to reach the pharmaceutical market [107]. Another approach is the fine tuning of the extrusion process by changing screw configuration, temperature profiles or by employing different downstream processing steps [106,193]. Recently, we introduced the approach to molecularly modify a polymeric matrix by interacting excipients [122]. The difference to a classical mixture approach with excipients is that molecular interactions are specifically targeted by design and cannot be facilitated in an extrusion of the physical mixture. In line with this idea, the current study explores the possibility to use selected additives that can interact ionically or via hydrogen bonding to enable HME of a matrix based on the polyelectrolyte carboxymethylcellulose sodium (NaCMC) for the first time.

NaCMC was recently extruded with polydimethylsiloxane as a polymeric mixture to form material for 3D printing [194] or it is occasionally used in spray drying [195]. The polymer shows good water solubility and extensive swelling behavior, which are both interesting properties for a new modified matrix produced by HME.

The concept of formulating ionic substances to produce a semi-solid or even liquid with a lower melting point is a well-known technique of "ionic liquids" and an important pharmaceutical application in the field of lipid-based formulations [196,197]. Recent publications highlighted the positive implications of salt formation on HME [120,179], but primarily for keeping the drug in amorphous form through the formation of ionic interactions [91,146]. Such an approach is of particular interest, since the direct extrusion of neat unprocessed NaCMC is not applicable, because it decomposes at 252 °C instead of having a melting point [198].

Therefore, this paper studies polymeric films of NaCMC in combination with six interacting small molecular additives that were first transformed into a solid excipient dispersion through solvent evaporation. In a second processing step, HME was performed. The solvent evaporation step (involving a medium with a high dielectric constant) enabled targeted ionic interactions between polyelectrolyte

NaCMC and the ionizable additive [91]. The main reason, why a solvent evaporation step was conducted prior to extrusion was that the compounds used would not be feasible for extrusion as otherwise neat powders because of their high melting points.

As the first group of co-formers to be studied with NaCMC, the basic amino acids, histidine, lysine, and arginine, were chosen, as they have been proven to interact with acidic groups of mostly drugs in various studies and consequently improved formulation properties such as amorphous stability, miscibility and plasticizing effects [124,140,145,147,153,158,173,199,200]. The second group of substances consisted of water-soluble inactive substances, which were also hypothesized to likely form an interaction with NaCMC after solvent evaporation and extrusion. The chosen co-formers were urea, meglumine and trometamol (TRIS).

Powder X-ray diffraction (PXRD) was applied to determine the maximum amount of additive that is still feasible for successful miscibility and an extrusion process to form an amorphous product. Two limiting factors had to be considered during the described processing: on the one hand, the unfavorable extrusion properties of NaCMC, which required a high amount of additive to enable the extrusion and on the other hand, the crystalline structure of the additives, which would lead to a crystalline product in high concentrations because of insufficient miscibility. While the preliminary measurements could be carried out using the laboratory diffractometer, conclusive results could only be obtained by using the data collected at a synchrotron source. Namely, to ensure the amorphous formulation, it was necessary to collect high quality PXRD data that is sensitive to extremely low amounts of crystalline phases in the sample. Secondly, to examine the distribution of the additive in the sample, the sample had to be probed on several points, which again required a specific sample stage at a synchrotron source.

Further assessment included thermal analysis by differential scanning calorimetry, which was complemented by hot stage microscopy and hot stage attenuated total reflectance Fourier transform infrared spectroscopy (ATR-FTIR) to show crystallinity and form changes upon heating [91]. The hot stage microscopy images were used as a complimentary analysis of the thermal miscibility and melting behavior of the evaporates during the extrusion [193,201].

This paper highlights the capability of different small molecular additives to enable the formulation of a polymeric compound, which would otherwise not be suitable for extrusion. Such a combination resulted in the development of a new modified excipient matrix for HME that formulators will find helpful to cope with challenging pharmaceutical compounds.

4.2 Materials and Methods

4.2.1 Materials

Carboxymethylcellulose sodium salt (low viscosity), urea, meglumine, TRIS, L-lysine, L-aspartic acid, and L-histidine were bought from Sigma Aldrich (St. Louis, MO, USA). Purified water, which was used for the solvent evaporation, was taken from a MilliQ Millipore filter system (Millipore Co., Bedford, MA, USA).

4.2.2 Methods

4.2.2.1 Preparation of Hot Melt Extrudates

Binary mixtures of NaCMC and the additive (according to the composition given in Section 3.1.1 and Section 3.2.1) were mixed in a mortar and dissolved in MilliQ water in a round bottom flask. Afterwards, the water was removed by a rotary evaporator (Rotavapor Büchi, Flawil, Switzerland), which resulted in a transparent film. This film was cut into smaller pieces and extruded on co-rotating screws with a 9-mm diameter and 180 mm in length in a ZE9 ECO twin-screw extruder by ThreeTec (Birren, Switzerland). A screw speed of 80 rpm was applied at a temperature of 130 °C through all three heating zones. The final extrudates were cooled to room temperature and stored in falcon tubes.

4.2.2.2 Laboratory Powder X-Ray Diffraction (PXRD)

Mixtures were studied for their potential amorphous form by PXRD on a D2 Phaser diffractometer (Bruker AXS GmbH, Karlsruhe, Germany) with a 1-D Lynxeye detector. The instrument was equipped with a Ge-monochromator (Cu Kα radiation) providing X-ray radiation at a wavelength of 1.541 Å. During the measurements, a voltage of 30 kV and a current of 10 mA were used. The increment and time per step were set to 0.020 ° and 1 s, respectively. The measurements were scanning a range of 5° to 40° (2θ).

4.2.2.3 Differential Scanning Calorimetry (DSC)

Samples were further assessed by a differential scanning calorimeter on a DSC 3 (Mettler Toledo, Greifensee, Switzerland). The samples were cut in small pieces and 5 to 9 mg was placed in a 40 μL aluminum pan with a pierced lid. A heating rate of 10 °C/min from −10 °C to 140 °C was applied, while the surrounding sample cell was purged with nitrogen 200 mL/min. Moreover, the combination of heating, cooling and heating cycles was used to fully evaluate the samples. For the assessment of the initial form, the first heating was used. The thermograms and glass transition temperatures (T_gs) were analyzed with the STARe Evaluation-Software Version 16 (Mettler Toledo, Greifensee, Switzerland). All thermograms show exothermic events as upward peaks.

4.2.2.4 Hot Stage Attenuated Total Reflectance Fourier Transform Infrared Spectroscopy (ATR-FTIR)

A Cary 680 Series FTIR spectrometer (Agilent Technologies, Santa Clara, CA, USA) was used, which was equipped with a heatable attenuated total reflectance accessory (Specac Limited, Orprington, UK) and the control panel 6100+ by WEST (West Control Solutions, Gurnee, IL, USA). The scanning range of 4000–600 cm^{-1} was selected with 1500 scans over a period of 30 min and a resolution of 4 cm^{-1}. The heating rate was set to 5 °C/min going from 30 °C to 130 °C. For the evaluation, a spectrum was extracted and evaluated by the software ACD/Spectrus Processor 2016.1.1 (Advanced Chemistry Development, Canada) every minute (i.e., every 5 °C). Every spectrum shows a 5 °C temperature increase going from the front to the back of the figures. The increase of peaks towards higher temperatures in the area of 2000 cm^{-1} is related to the heat implications on the ATR crystal. For the hot stage FTIR analysis, the solvent evaporated films were used, whereas the FTIR spectra at room temperature were recorded from the physical mixture, solvent evaporates, and extrudates.

4.2.2.5 Synchrotron Powder X-ray Diffraction

X-ray powder diffraction data were recorded at the ID22 beamline at the European Synchrotron Radiation Facility (ESRF, France) using a two-dimensional detector (PerkinElmer XRD 1611CP3) and an incident X-ray energy of 60 keV ($\lambda = 0.20678$ Å, $Q_{max} = 24$ Å^{-1}). A beam size of about 0.5 mm x 0.5 mm was used. Reference samples were packed in 0.7-mm diameter borosilicate capillaries. Extrudate samples were mounted directly on capillary supports and measured as is. In order to minimize any possible radiation damage, samples were cooled down to 100 K using an Oxford Cryosystem Cryostream. To improve the overall statistics, 200 two-dimensional images were recorded (2 s per frame) and averaged. The one-dimensional diffraction patterns were retrieved after integration using the PyFAI software [202]. Five diffraction patterns on five different locations were recorded on each extrudate sample in order to check for heterogeneity.

4.2.2.6 Hot Stage Microscopy (HSM)

The HSM analysis employed a Leica DMRM at magnifications of 100×, which is also displayed as a scale bar in the images. The microscope was equipped with a temperature-controlled microscope stage from Linkram. This analysis was used for the evaluation of the behavior of the formulation upon heating in the extruder and to complement the DSC analysis [106,129,179]. For a close relation to the extrusion process, the temperature ramp was set from room temperature (RT) to 130 °C. During this ramp, the temperature was kept steady and images were taken at RT, 90 °C, and 130 °C. The obtained images were converted into black and white to highlight the melting process.

4.3 Results and Discussion

4.3.1 Amino Acids as Additives

4.3.1.1 Characterization of the Formulations

Formulations containing the additives arginine and lysine were found to be amorphous after evaporation as well as extrusion. In contrary, it was not possible to convert histidine to an amorphous form neither with evaporation nor with extrusion. Table 4.1 highlights the different aspects, which were essential during processing of the formulation such as a qualitative evaluation of technical feasibility during HME. The extrusion was evaluated compared to a standard extrusion of the polymer, PVPVA 64, which is considered arbitrarily as ideal for extrusion. Such extrusion behavior is influenced by melt viscosity, thermoplasticity, and degradation [193].

Table 4.1. Properties of amino acid / polyelectrolyte matrices

Additive	Maximum Amorphous Amount	Molar Fraction (Monomeric) *	T_g After Evaporation	T_g After Extrusion	Extrudability **
Amino Acid + NaCMC					
Lysine	50% (w/w)	0.64	30.27 °C	30.62 °C	++
Arginine	33% (w/w)	0.43	35.36 °C	33.15 °C	+
Histidine	20% (w/w)	0.30	36.59 °C	-	- -

* For the calculation, the molar weight of the NaCMC monomer was used.

** Technical feasibility was qualitatively assessed and details are given in the text.

The optimal amounts of additives necessary to produce an amorphous polymer matrix are presented in Table 4.1, expressed as loadings in weight/weight as well as the calculated molar fractions of the formulation components. Lysine resulted in the highest amount of additive, which was formulated in an amorphous form in combination with NaCMC, whereas histidine being less feasible for the evaporation and the later extrusion could only be incorporated in the lowest molar ratio used in this study. This is also reflected by very poor extrusion behavior as well as the disappearance of the T_g in the DSC measurements of the corresponding extrudates, which may be explained by recrystallization from amorphous state as crystallinity was found in the extruded histidine formulation (Figure 4.1). For the above-mentioned table, it has to be mentioned that lower amounts of additive during a previous formulation development were leading to worse extrusion performances, which underlines the insufficient extrusion performance of neat NaCMC.
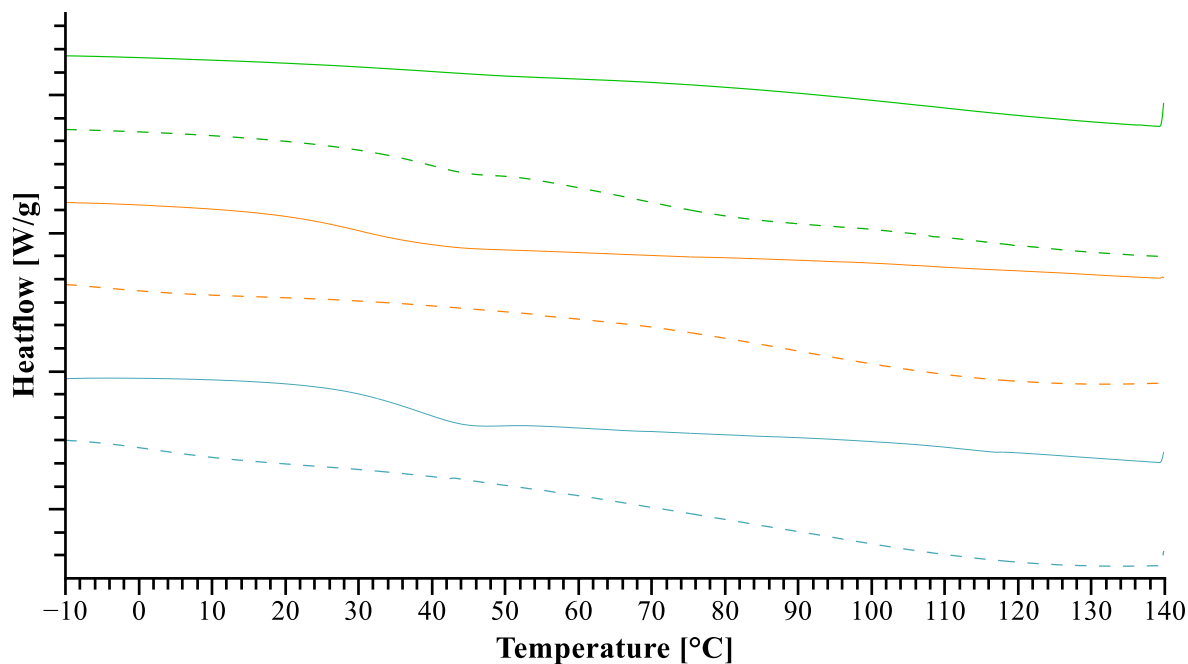
Figure 4.1. The solid lines represent the differential scanning calorimetry (DSC) thermograms of the extrudates and the dotted lines represent the evaporates which were used for the later extrusion. The amino acids added to sodium carboxymethylcellulose (NaCMC) are arginine (cyan), lysine (orange), and histidine (green).

In detail, the dotted lines in Figure 4.1, representing the solvent evaporates, show only slight indications of a T_g in all samples. Whereas only the thermograms of extrudates containing lysine and arginine show the presence of a clear T_g in the extrudates (see Table 4.1). This can be associated with an amorphous form of the additive in the formulation [203] and gives a first indication of formed molecular interactions [153,199]. These two additives also formed more prominent T_gs during the extrusion, which entails a higher amount of amorphous additive in the formulation. Consequently, such a processing was beneficial for the formation of an amorphous modified matrix of NaCMC. However, this still needed further measurements for confirmation.

As mentioned before, the T_g in the histidine extrudates disappeared after extrusion, which suggested that the amorphous form changed during extrusion, leading to a crystalline fraction as indicated by the diffraction peaks in the corresponding PXRD analysis (Figure 4.S3). Although a T_g was detectable for lysine and arginine after the extrusion in the DSC, it has to be kept in mind that the substances used show rather high individual melting points, which would have led to degradation during the thermal measurement.

Therefore, to obtain high quality data that is sensitive to extremely low amounts of crystalline phase in the sample, it was necessary to perform the diffraction and scattering experiments at a synchrotron source.

Thus, synchrotron X-ray diffraction offered a more thorough assessment of the amorphous form to complement the DSC and benchtop PXRD data, which indicated that the raw substances were crystalline except for the polyelectrolyte NaCMC (Figure 4.S1). PXRD data collected at the synchrotron source

featured Bragg peaks that could be related directly to the crystallinity of the respective additive. Pronounced crystallinity evidenced in the histidine evaporate was in accordance with the initial X-ray and DSC assessment and was still detectable after extrusion, which is pointed out by the peaks at $1.07 A^{-1}$, $1.71 A^{-1}$, $2.11 A^{-1}$, $2.60 A^{-1}$, $2.81 A^{-1}$, $3.06 A^{-1}$, $3.61 A^{-1}$ (Figure 4.2). Moreover, the measurement at five different locations throughout the extrudate showed the inhomogeneous distribution of the crystalline additive in the extrudate (Figure 4.2), which can potentially lead to more recrystallization. The diffraction pattern of the arginine extrudate indicated a more homogeneous distribution of the additive compared to histidine, although peaks at $3.05 A^{-1}$ still underline some partial crystallinity of the extrudate, which was detectable neither in the initial benchtop PXRD assessment nor by DSC.
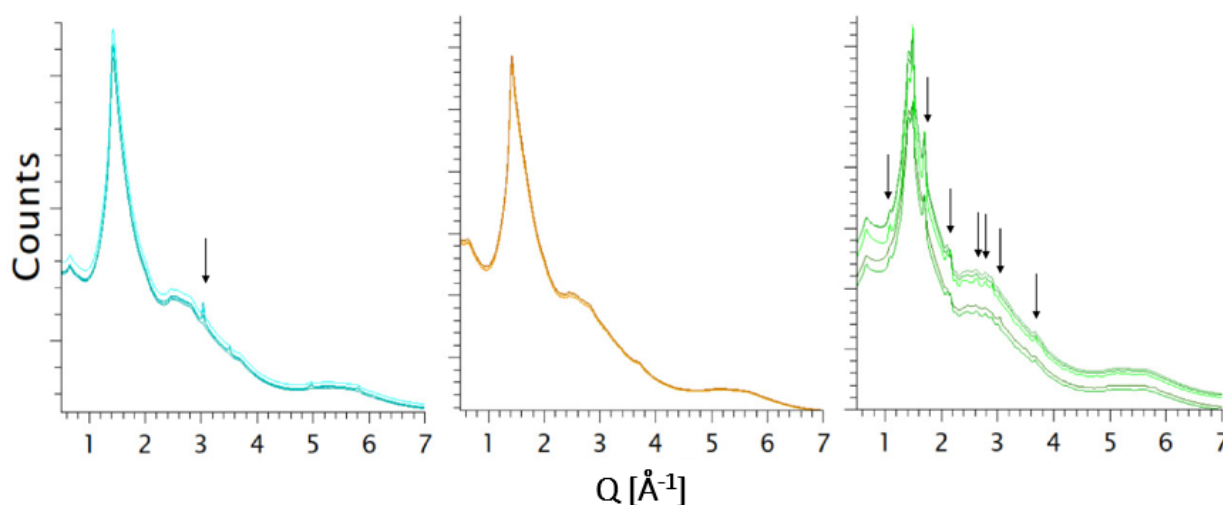
Figure 4.2. X-ray synchrotron results (i.e., arbitrary counts versus Q vector, $Q = 4\pi\sin(\theta)/\lambda$) are displayed from the extrudates with amino acid co-formers. The amino acids added to NaCMC are from left to right: arginine (cyan), lysine (orange), and histidine (green). Each diffraction pattern corresponds to a measured area in the extrudate.

The FTIR spectra of arginine/NaCMC in Figure 4.3B exhibit reduced guanidyl vibrations of arginine at $1675 cm^{-1}$ and $1614 cm^{-1}$, which can be associated with the interaction between the ionized arginine side chain and the negatively charged NaCMC [199].

For the co-former lysine, only smaller shifts in the FTIR spectrum are present in the evaporate and the extrudate including the shoulder of the COO^- bond at $1607 cm^{-1}$, which is less pronounced in the extrudate than in the physical mixture [194,204]. In addition, a slight shift and a pronounced broadening of the peaks at $1570 cm^{-1}$ and $1540 cm^{-1}$ [205] both highlight the interaction of the carboxylic group of NaCMC (Figure 4.3C). The analysis of histidine/NaCMC in Figure 4.3A shows pronounced similarities of the physical mixture and extrudate. This supported the previous findings of the extrusion leading to a change in the solvent evaporate with recrystallization of histidine [158].

As mentioned in the previous section, the NaCMC was completely amorphous prior to processing. Therefore, the observed peak broadening and shifts are related to the amorphization of the additive.
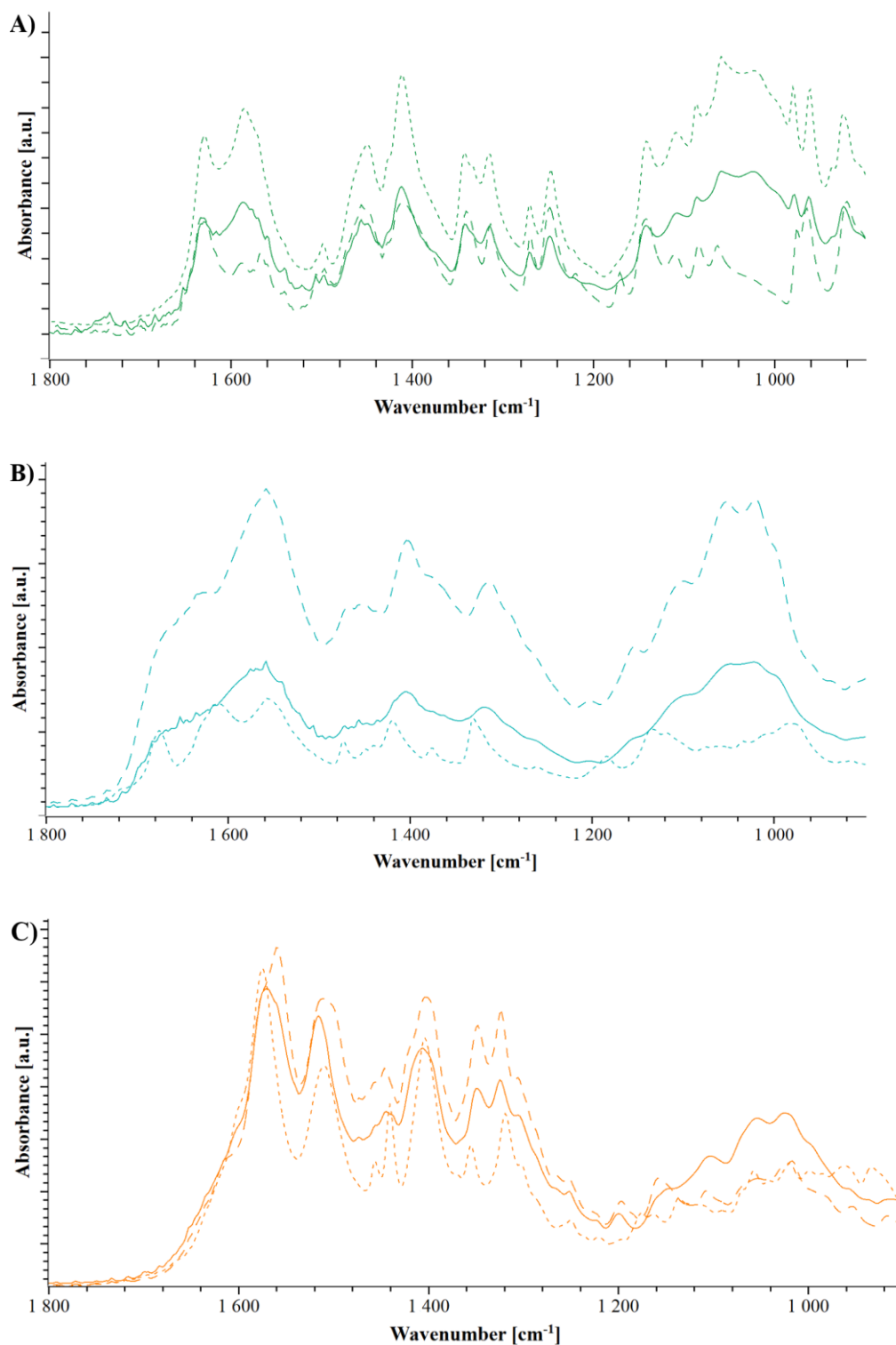
Figure 4.3. Fourier transform infrared spectroscopy (FTIR) spectrograms of NaCMC and histidine (**A**, green), arginine (**B**, cyan) and lysine (**C**, orange). Dotted lines represent the physical mixture, dashed lines represent the solvent evaporates and the extrudates are shown in solid lines.

4.3.1.2 Heat Assisted Characterization

The hot stage microscopy was applied to better understand the processes occurring during the extrusion of the evaporated films and to complement the results of extrusion performance using the different additives. It should be noted that bright structures in the HSM images are not necessarily related to crystallinity as they can also highlight an increase in capillarity of the samples.

Thus, Figure 4.4 top shows an increasing number of capillaries building up in the polyelectrolyte film containing arginine, which can be directly associated with the positive extrusion performance. In this case, even though the HSM suggests a successful extrusion, as highlighted in the previous section, the arginine extrudate still contained crystallinity. This could be explained by the insufficient mixing behavior of the two excipients, which is underlined by the minimal changes visible in the heat-resolved FTIR. In Figure 4.4 bottom, only minor changes in the FTIR are visible during the heating.
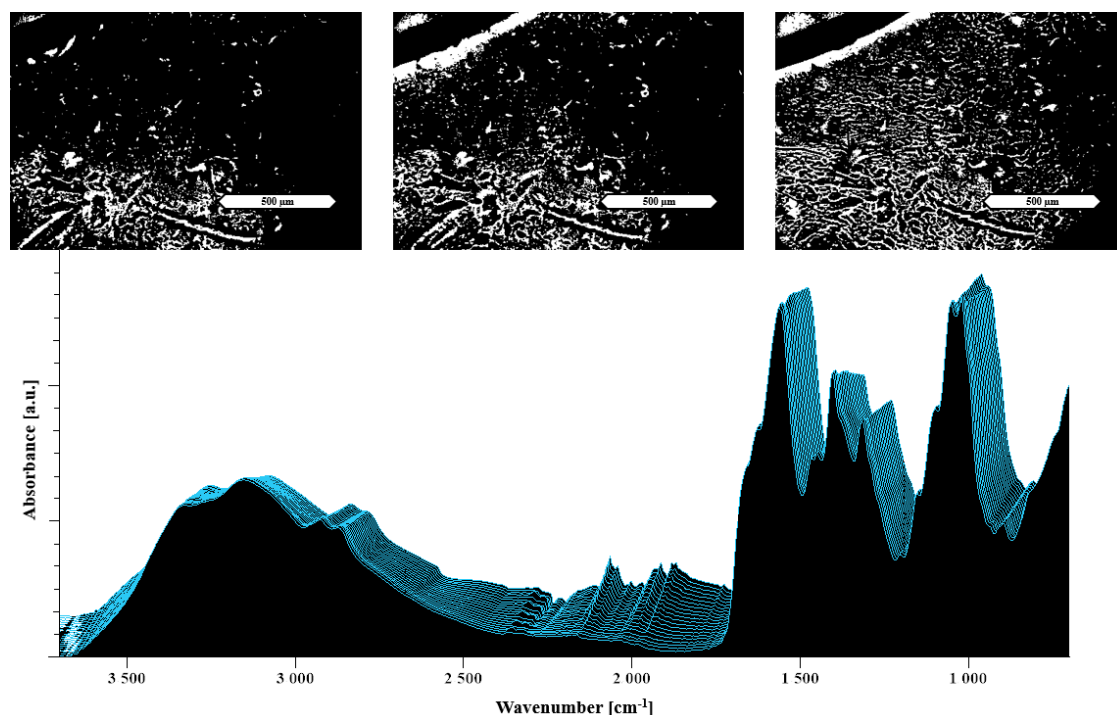
Figure 4.4. Hot stage microscopy (HSM) images at the top and temperature-resolved FTIR of 33% arginine in NaCMC at the bottom. The images show HSM images taken at RT, 90 °C and 130 °C (from left to right). The displayed scale bar refers to 500 μm. Each spectrum was measured at temperatures from 30 °C (measured first in the front) to 130 °C (in the back) by increasing steps of 5 °C.

The evaporated film containing lysine showed no crystals in the microscopic images and small indications of melting in the images taken at 130 °C in comparison to RT (Figure 4.S4). Even in case of minor melting events, the torque in the extruder facilitates the plasticizing and melting of the evaporate during the extrusion. Therefore, the analysis of films represents a kind of "worst case scenario" regarding shear forces. It is still possible to successfully obtain an extrudable amorphous formulation as in the given case of lysine. The heat-resolved FTIR spectra in Figure 4.S4 at the bottom show an increase

in the peak at 1560 cm^{-1} and 1516 cm^{-1}, which are related to the carboxylic groups of NaCMC [205]. Such an observation can be interpreted as an increase of the interaction between NaCMC and lysine. The HSM images of the histidine evaporate at RT showed pronounced crystallinity, which was in accordance with the PXRD diffraction patterns (Figure 4.S2). Moreover, the images taken at the operating temperature of the extruder (130 °C) did not show any reduction in crystallinity or a phase transition, which could be associated with a glass transition. This is supported by the measurable crystallinity and immiscibility in the extrudate (Figure 4.5 in green) [91].
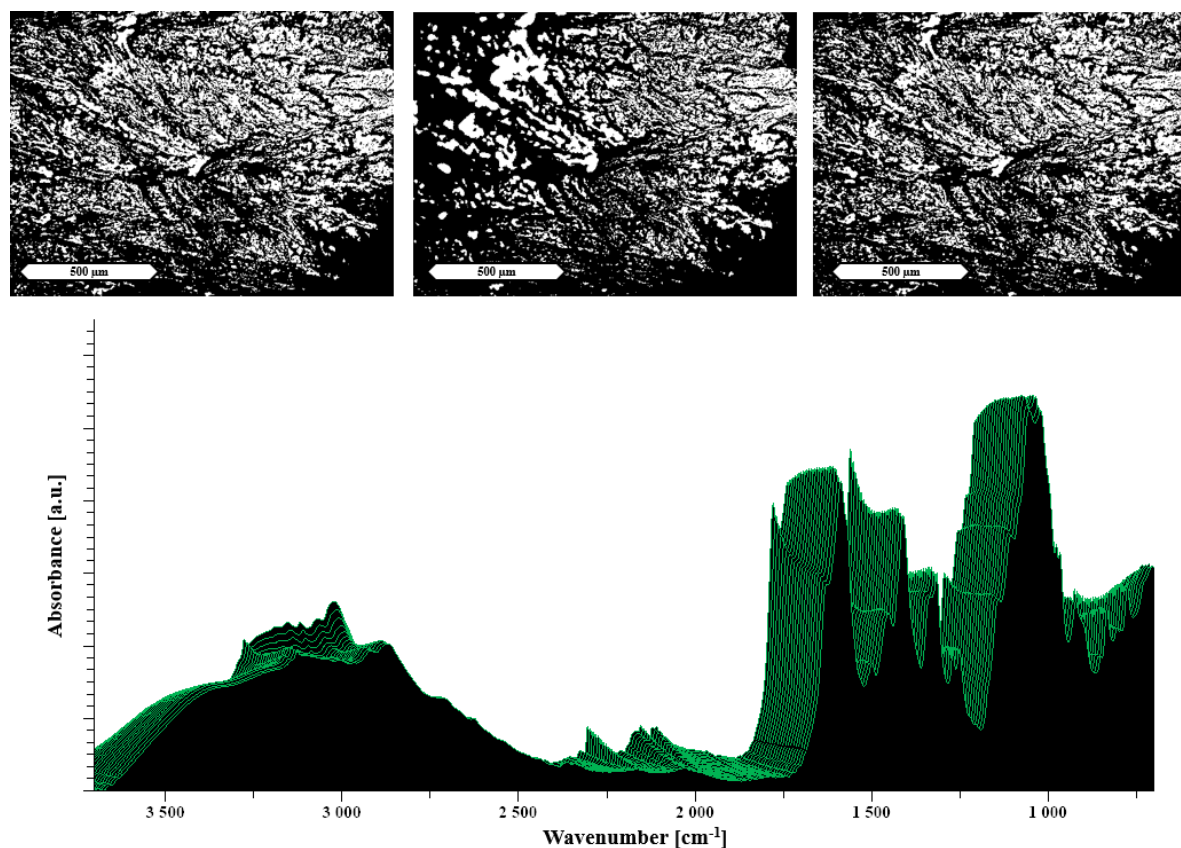
Figure 4.5. The images at the top show HSM images of histidine/NaCMC evaporated films taken at RT, 90 °C and 130 °C (from left to right). At the bottom, a temperature-resolved FTIR spectrum is shown. The displayed scale bar refers to 500 μm. Each spectrum was measured at temperatures from 30 °C (measured first in the front) to 130 °C (in the back) by increasing steps of 5 °C.

The thermal evaluation of the evaporated films aligned the prior solid-state characterization as well as the actual behavior in the extruder, meaning the formulations containing arginine and lysine, which were successfully incorporated in a concentration of 33% and 50%, respectively, performed well in the extruder and could only be differentiated by a synchrotron X-ray measurement showing slight crystallinity in the arginine formulation. By contrast, the histidine formulations demonstrated poor melting behavior as well as pronounced crystallinity after extrusion. Moreover, the distribution of

histidine was insufficient throughout the extrudate, which leads to differences in the diffraction pattern evidenced by the synchrotron X-ray measurement.

4.3.2 Additives other than Amino Acids

4.3.2.1 Characterization of the Formulations

Analogous to previous results, it was necessary to combine solvent evaporation and HME in the mixtures of NaCMC and the further tested co-formers. This was suggested by the X-ray diffraction patterns of the formulations following solvent evaporation. The X-ray diffraction pattern of the TRIS/NaCMC solvent evaporates showed Bragg peaks that indicated the presence of TRIS in a crystalline form (Figure 4.S2). However, TRIS was completely transferred into an amorphous form following a subsequent HME step (Figure 4.S3). The urea and meglumine formulations were amorphous after the solvent evaporation and did not recrystallize to a detectable extent based on the benchtop PXRD results (Figure 4.S3).

Table 4.2 presents a comparison of the maximal amount of additives for which the polymer matrix was kept in an amorphous state. The differences in molar weight have to be taken into account for such an evaluation, leading to a comparable molar fraction of meglumine and urea and a lower loading as well as molar fraction of TRIS (Table 4.2). This observation was a first indicator of the different technical feasibility of the various additives to obtain suitable modified matrices of NaCMC. A higher loading of TRIS led to crystallinity after evaporation as well as extrusion. Therefore, a lower loading had to be chosen, which resulted in non-ideal extrusion performance as described in the introduction. The additives meglumine and urea could be incorporated at much higher molar ratios and positively influenced the extrusion process.

Table 4.2. Properties of the other additive polyelectrolyte matrices.

Additive	Maximum Amorphous Amount	Molar Fraction (Monomeric) *	T_g After Evaporation	T_g After Extrusion	Extrudability **
Other Additive + NaCMC					
Meglumine	50% (w/w)	0.57	5.58 °C	9.18 °C	+
Urea	20% (w/w)	0.52	37.99 °C	40.36 °C	0
TRIS	25% (w/w)	0.42	-	39.18 °C	-

* For the calculation, the molar weight of the NaCMC monomer was used. ** Technical feasibility was qualitatively assessed and details are given in the text.

The thermograms in Figure 4.6 indicate the presence of remaining water after the solvent evaporation, given as a broad peak around 100 °C. The T_g of urea can be hardly detected because of small difference in heat capacity at the glass transition and for the TRIS formulation, no T_g could be detected. On the other hand, the extrudate of meglumine shows a rather pronounced T_g and also a shift towards a lower temperature in comparison to all other extrudates, which can be associated with the good miscibility of meglumine and NaCMC [206,207].
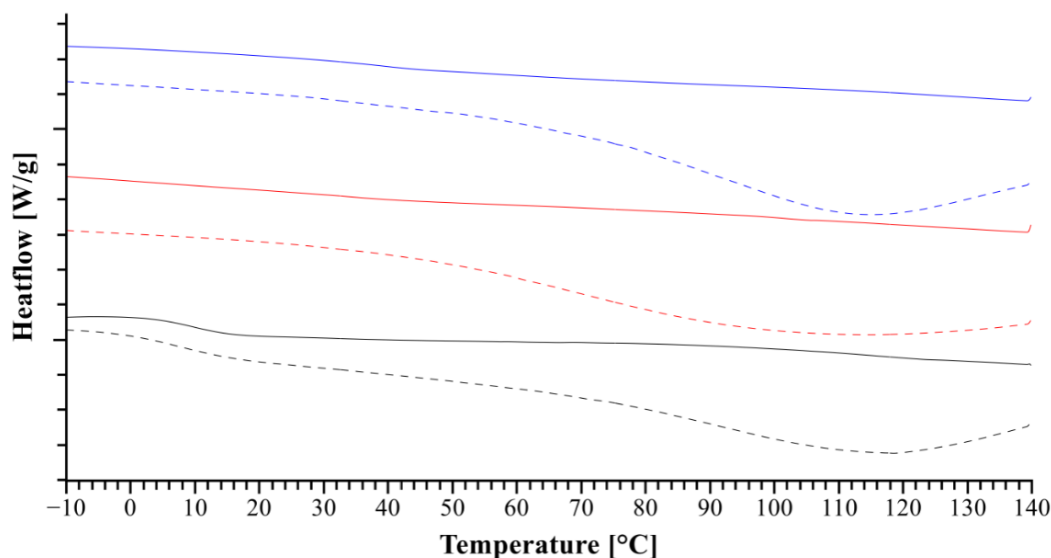
Figure 4.6. The solid lines represent the thermograms of the extrudate and the dotted lines represent the evaporates, which were used for the later extrusion. The additives used in addition to NaCMC are meglumine (black), TRIS (red) and urea (blue).

All samples were measured at five different areas. However, differences in the patterns can be seen only for the case where TRIS was used as the additive, particularly for differences in scattered intensity and the emergence of Bragg peaks at Q values of 3.03 A^{-1}, 3.50 A^{-1}, 4.95 A^{-1} and 5.81 A^{-1}. By contrast, the patterns of the extrudates containing meglumine and urea present no observable differences in their X-ray synchrotron results (Figure 4.7). The absence of Bragg peaks in the patterns collected on samples containing meglumine and urea prove that the obtained polymer matrices were fully amorphous at the molar fractions of 0.57 and 0.52, respectively. The PXRD patterns, collected on the sample containing TRIS at the synchrotron source, showed indications of crystallinity, which were not detectable in the patterns of the laboratory diffractometer. Such crystallinity could be a sign of recrystallization after the extrusion as well as residual crystallinity. Both sources of crystallinity are related to the instability of an amorphous form [208].
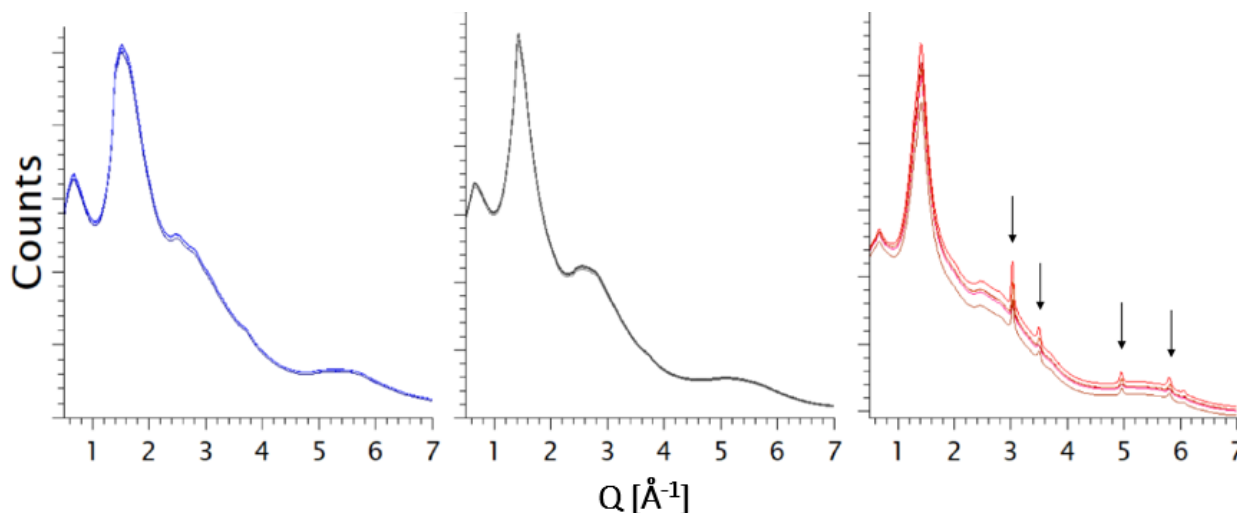
Figure 4.7. X-ray synchrotron results (i.e., arbitrary counts versus Q vector) of co-formers other than amino acids. The additives in addition to NaCMC are: urea (blue), meglumine (black), and TRIS (red). Each diffraction pattern corresponds to a measured area in the extrudate.

In the FTIR spectra, the combination of NaCMC and meglumine shows the previously discussed broadening due to the amorphization [209,210]. It can be seen how following solvent evaporation, distinct peaks are observed, which are broadened in one peak at 1000 cm^{-1} and 1400 cm^{-1}. Moreover, the previous discussed carboxylic peak at 1570 cm^{-1} of NaCMC is more pronounced and broader, which indicates a change in the intermolecular binding of the polyelectrolyte [204,205].

The FTIR spectrum of urea in line with the spectrum of NaCMC/meglumine shows an increase of the peak at 1580 cm^{-1}, which indicates the same interaction with the carboxylic group as meglumine [205]. The spectrum of TRIS showed specific peak broadening as a result of the amorphous formulation (Figure 4.8). However, this broadening is overlapping a lot with the peaks formed because of a potential interaction. The increase of broader peak between 1400 cm^{-1} and 1600 cm^{-1} can be interpreted as an indication of an interaction [120,194,211]. However, a further, more sensitive analysis is required for a precise statement about the interaction.
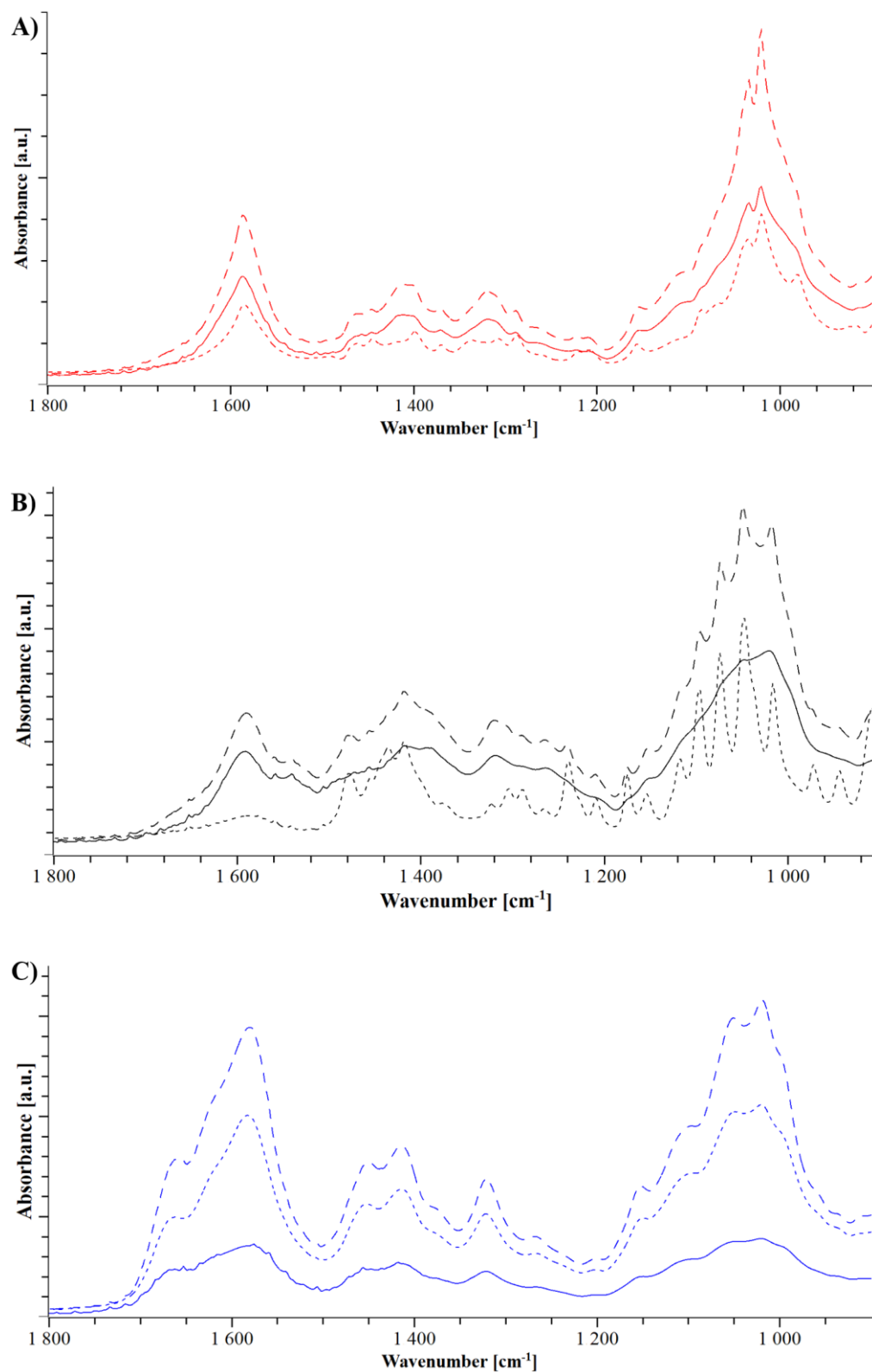
Figure 4.8. FTIR spectrograms of NaCMC and TRIS (**A**, red), meglumine (**B**, black), and urea (**C**, blue). Dotted lines represent the physical mixture, dashed lines represent the solvent evaporates and the extrudates are shown in solid lines.

Interestingly, the observed changes in the FTIR spectra indicate a likely change in the hydrogen bonding structure because of the processing rather than the formation of a distinct salt.

4.3.2.2 Heat Assisted Characterization

The microscopic images at the top of Figure 4.9 present the melting process of the meglumine formulation, which can be connected to the thermoplastic behavior in the extruder. The prominent peak broadening around 90 °C in the area above 3000 cm^{-1} is an indicator of a successful amorphization because of differences in the molecular arrangement as well as the near range order [199,210]. This finding is in line with the start of a melting process in the HSM image at 90 °C. Moreover, these findings are in accordance with the performance observed during extrusion of the meglumine formulation.
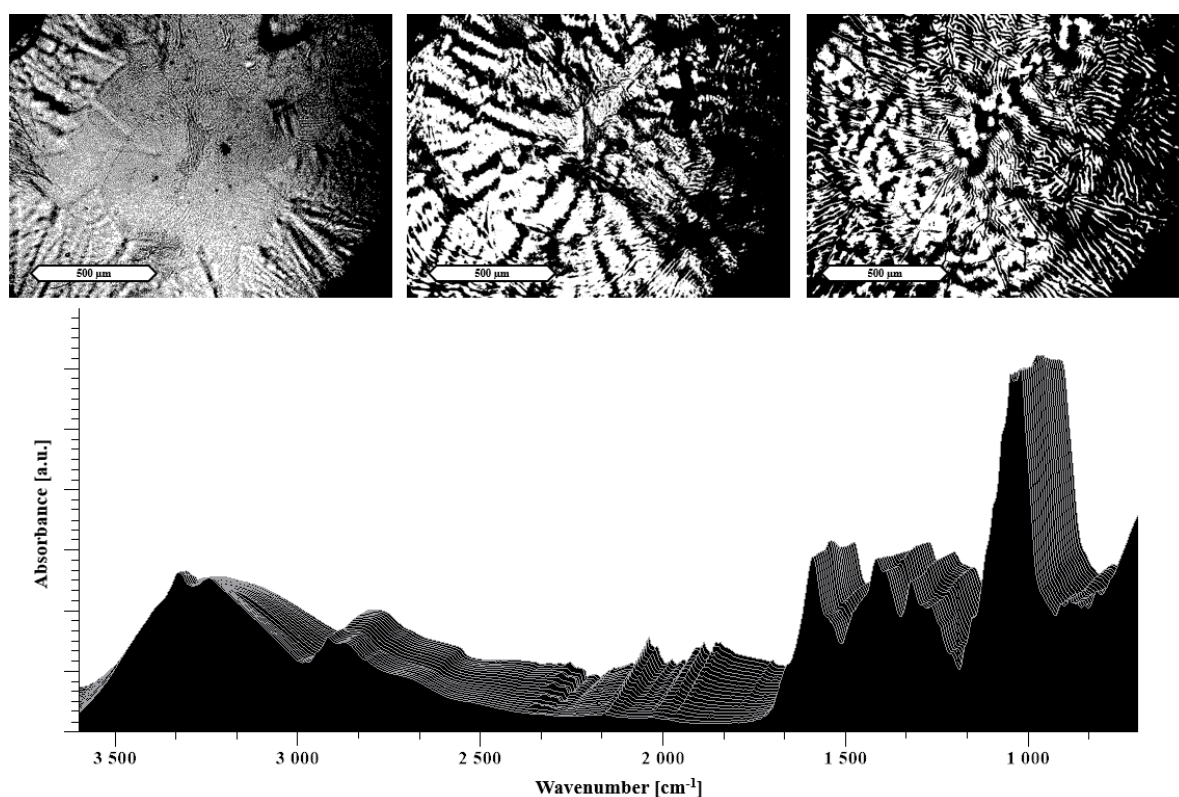
Figure 4.9. The images at the top show HSM images of 50% meglumine/NaCMC solvent evaporates taken at RT, 90 °C and 130 °C (from left to right). At the bottom, a temperature-resolved FTIR spectrum is shown. The displayed scale bar refers to 500 μm. Each spectrum was measured at temperatures from 30 °C (measured first in the front) to 130 °C (in the back) by increasing steps of 5 °C.

HSM images of the TRIS formulation show only minor changes. Although, an indication of minor "bubble-shaped" features was recorded that may be associated with small melting events taken place in the formulation (Figure 4.10). The FTIR spectrum supports the observation of a change with higher temperatures. The broadening of the peaks above 3000 cm^{-1} can not only be associated with the successful amorphization in the TRIS sample [210], as discussed before (Table 4.1), it furthermore

shows the decrease of hydrogen bonding throughout the heating process [205,212], leading to a lack of intramolecular interaction in the NaCMC, thereby resulting in more available interaction sites for TRIS.
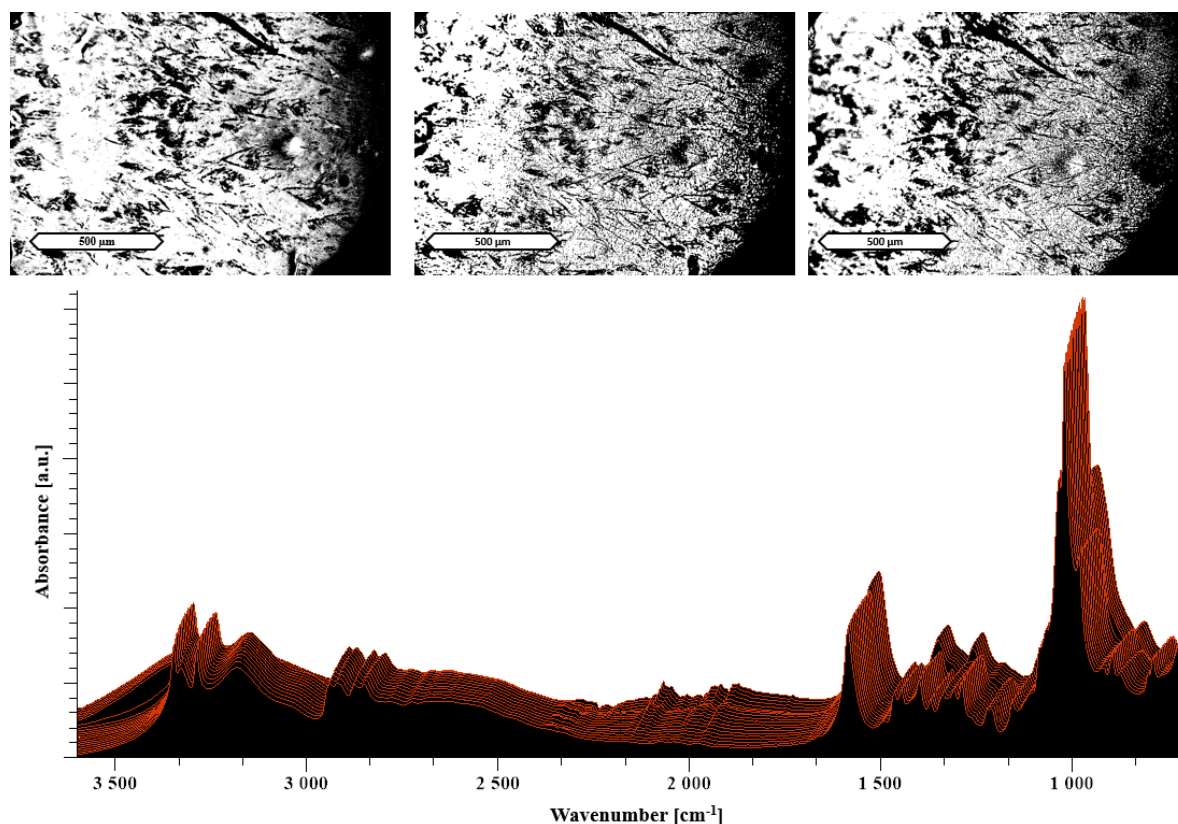

Figure 4.10. The images at the top show HSM images of 25% TRIS/NaCMC evaporated films taken at RT, 90 °C and 130 °C (from left to right). At the bottom, a temperature-resolved FTIR spectrum is shown. The displayed scale bar refers to 500 μm. Each spectrum was measured at temperatures from 30 °C (measured first in the front) to 130 °C (in the back) by increasing steps of 5 °C.

As described before, the urea formulation formed an amorphous stable formulation after evaporation and extrusion (Figure 4.S5). The HSM images show a melting process over the temperature range recorded. However, in the heat-resolved FTIR, only minor changes in peak intensity can be observed. In line with Figure 4.9, this suggests that urea has a plasticizing effect without showing a pronounced interaction with NaCMC. A possible reason for that is the lack of ionizable groups in the urea molecule.

4.4 Conclusion

The application of additives and targeted molecular interactions together with an initial solvent step enabled the extrusion of the polyelectrolyte, NaCMC. Differences in melting behavior and loading highlighted the suitability of the investigated additives to form as a fully amorphous polyelectrolyte matrix after extrusion. The additives, lysine and meglumine, in a concentration of 50% (w/w), have proven to be beneficial for extrusion and formation of a fully amorphous polymer matrix. Moreover, the

application of synchrotron X-ray diffraction helped to further differentiate between the formulations by examining the distribution of the additive throughout the matrix and residual crystallinity in the sample. PXRD data collected at the synchrotron source proved the amorphous state of the lysine, meglumine, and urea formulations compared to arginine and TRIS, for which crystallinity was not detectable by means of benchtop PXRD or DSC.

While recent work has shown that the formulation of an amorphous ionic interaction is possible by hot melt extrusion [179], the current concept presented a not extrudable polymer, which was altered by interacting additives in a modified matrix feasible for HME. We refrained from naming the obtained systems as ionic liquids because this would suggest exclusively ionic co-former interactions with the polymer. Moreover, ionic liquids have an arbitrary defined melting characteristic of <100 °C, which is not required for pharmaceutical application as solid dispersions. However, it is expected that the modified matrices share much of the molecular attractiveness of ionic liquids. Further studies may harness the potential benefits of the solvent evaporates for pharmaceutical HME, reaching from new systems for amorphous drug stabilization over the generation of drug supersaturation to the precipitation inhibition of poorly water-soluble compounds.

4.5 Supporting information

4.5.1   Powder X-ray diffraction patterns

The following graphs were used for the final formulation evaluation of the polyelectrolyte matrices. The following powder X-ray diffraction (PXRD) analyses were based on the benchtop X-ray diffractometer that is described in the methods section.
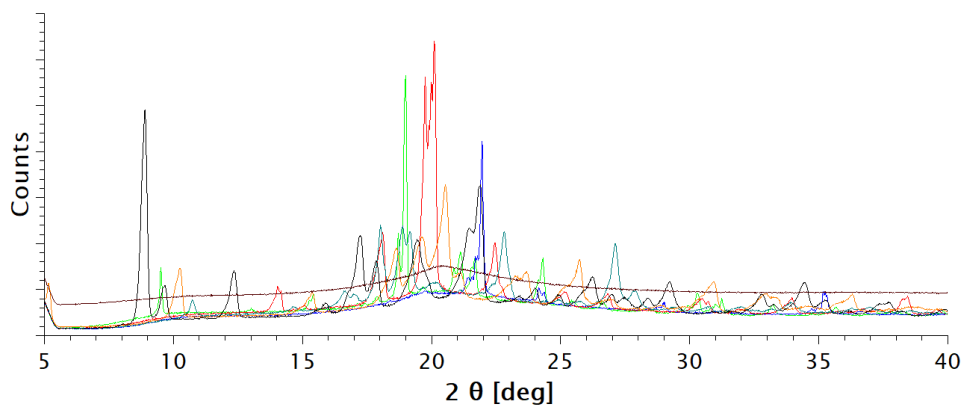

Figure 4.S1. PXRD patterns of the physical mixtures. Colors and labels are in line with Figure 4.2 and 4.8, which can be inferred from the main article. The diffraction pattern of pure NaCMC in shown in bordeaux with an offset.
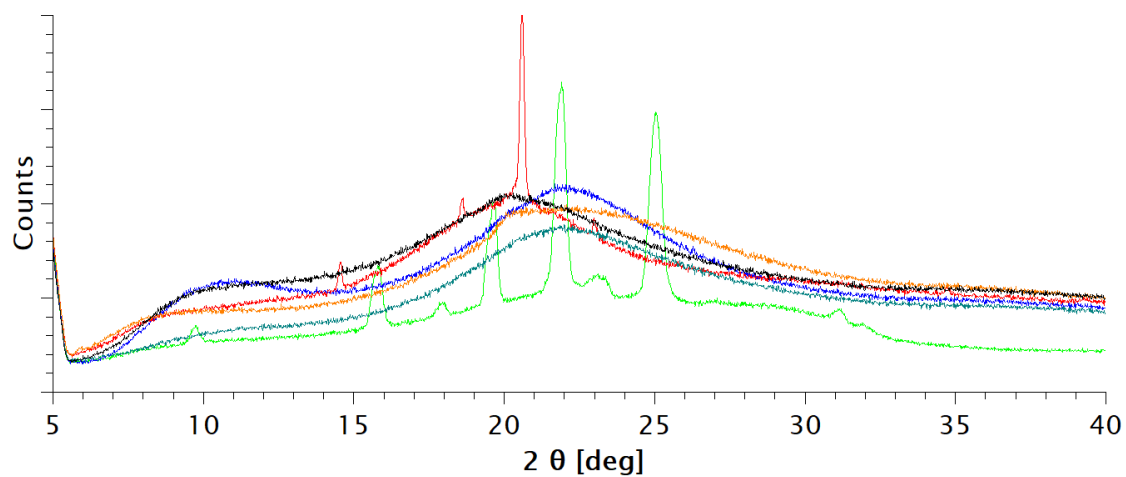
Figure 4.S2. PXRD diffraction patterns of the solvent evaporates. Colors and labels are in line with Figure 4.2 and 4.8, which can be inferred from the main article.
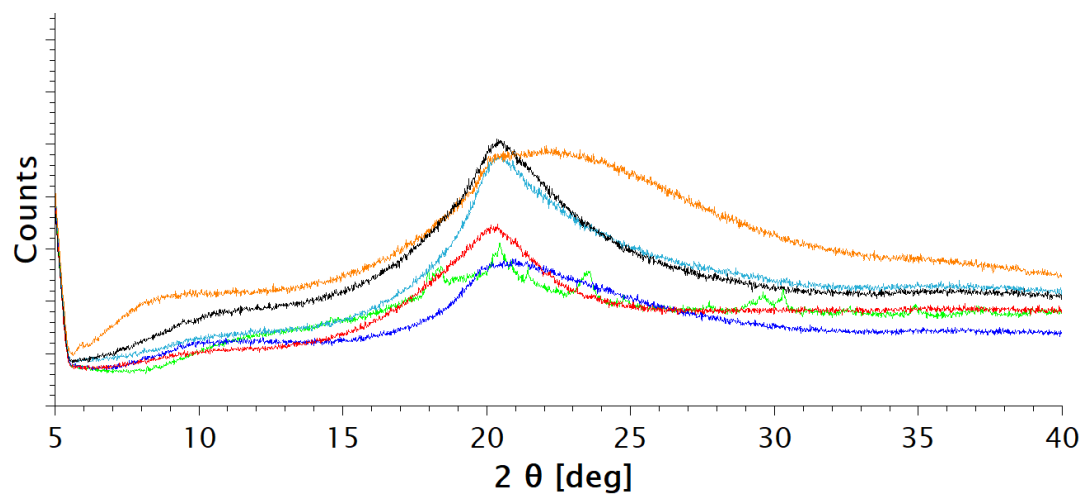

Figure 4.S3. PXRD patterns of the extrudates. Colors and labels are in line with Figure 4.2 and 4.8, which can be inferred from the main article.
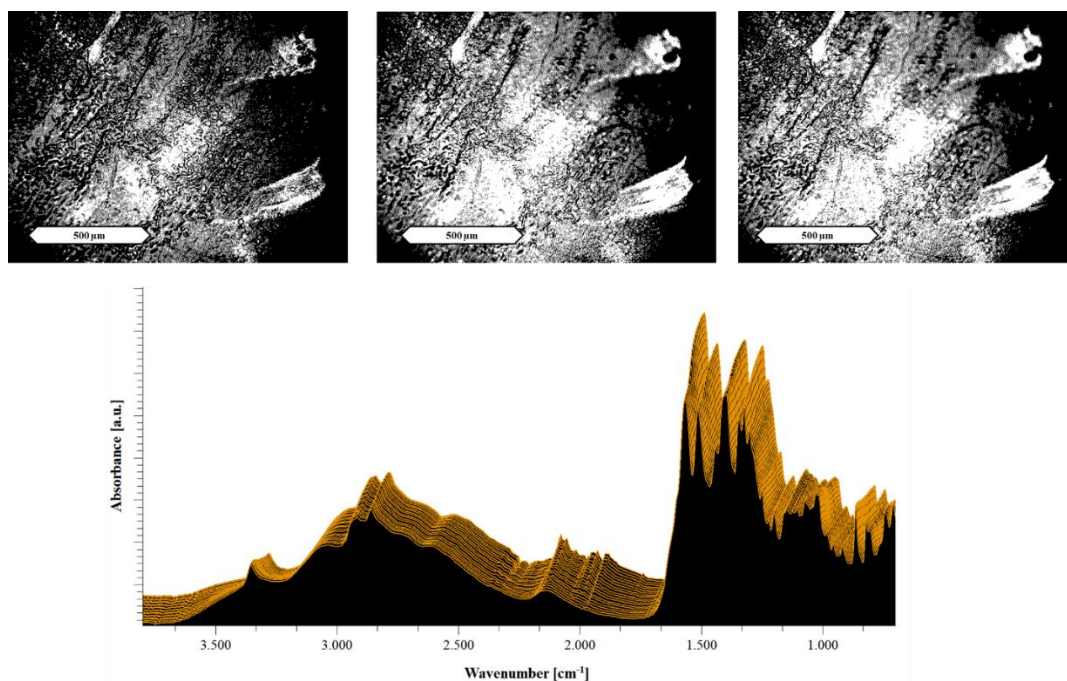
4.5.2 Hot stage microscopy and hot state FTIR

Figure 4.S4. Heat resolved FTIR and HSM images of 50 % lysine / NaCMC solvent evaporates. The images at the top show HSM images taken at RT, 90 °C and 130 °C (from left to right). Each spectrum was measured at temperatures from 30°C (measured first in the front) to 130°C (in the back) by increasing steps of 5°C.
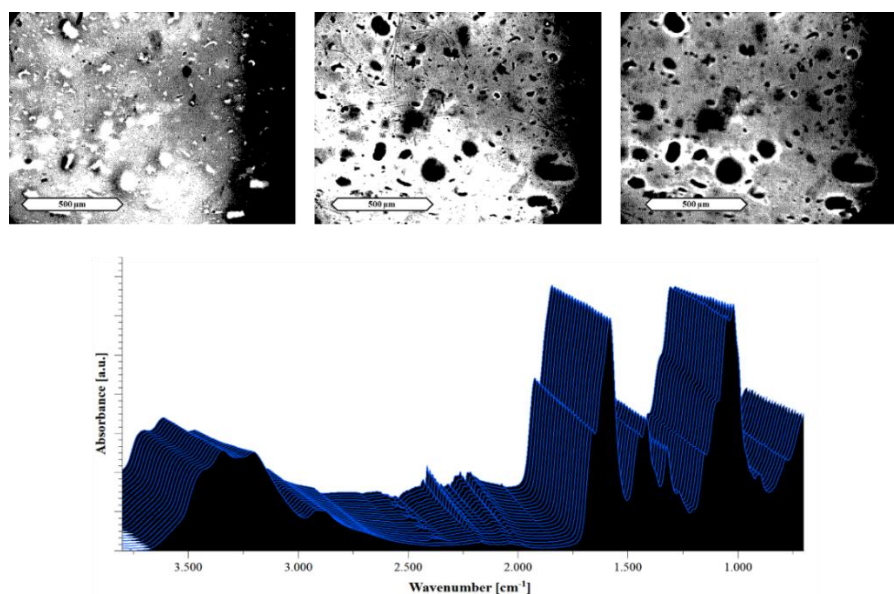

Figure 4.S5. The images at the top show HSM images of 20 % urea / NaCMC solvent evaporated films taken at RT, 90 °C and 130 °C (from left to right). At the bottom, a temperature resolved FTIR spectrum is shown. Each spectrum was measured at temperatures from 30 °C (measured first in the front) to 130°C (in the back) by increasing steps of 5 °C.

Chapter 5

Opportunities for successful stabilization of poor glass-forming drugs: A stability-based comparison of mesoporous silica versus hot melt extrusion technologies

Summary

Amorphous formulation technologies to improve oral absorption of poorly soluble active pharmaceutical ingredients (APIs) have become increasingly prevalent. Currently, polymer-based amorphous formulations manufactured by spray drying, hot melt extrusion (HME) or co-precipitation are most common. However, these technologies have challenges in terms of successful stabilization of poor glass former compounds in the amorphous form. An alternative approach is mesoporous silica, which stabilizes APIs in non-crystalline form via molecular adsorption to inside nano-scale pores. In line with these considerations, two poor glass formers, haloperidol and carbamazepine, were formulated as polymer-based solid dispersion via HME and with mesoporous silica, and their stability was compared under accelerated conditions. Changes were monitored over three months with respect to solid-state form and dissolution. The results were supported by solid-state nuclear magnetic resonance spectroscopy (SS-NMR) and scanning electron microscopy (SEM). It was demonstrated that mesoporous silica was more successful than HME in the stabilization of the selected poor glass formers. While both drugs remained non-crystalline during the study using mesoporous silica, polymer-based HME formulations showed recrystallization after one week. Thus, mesoporous silica represents an attractive technology to extend the formulation toolbox to poorly soluble poor glass formers.

5.1 Introduction

The increasing prevalence of poorly water-soluble drugs has driven the field of pharmaceutical technology to develop modern approaches for formulation development. A well-established technique is to formulate the drug in an amorphous form, which results in an increase in apparent solubility, dissolution performance, and subsequent oral bioavailability [45,55]. However, such an approach comes with difficulties related to thermodynamic instability of the amorphous state, which can lead to recrystallization and thus negation of the aforementioned formulation advantages [213].

To give guidance on the recrystallization tendency of drugs, Baird et al. developed a classification system based on a molecule's "glass forming ability" (GFA). The GFA is related to recrystallization behavior from super cooled melts [36–38]. Three classes of substances were defined: class one (GFA-I) drugs recrystallizing upon cooling from the molten state; class two (GFA-II) drugs recrystallizing after a heating-cooling-heating procedure, and class three (GFA-III) drugs that remain amorphous throughout the entire experiment. Although the classification was developed for undercooled melts, which can be directly related to hot melt extrusion (HME), it has proven to be accurate for solvent evaporation processes as well [214]. This is a particularly relevant consideration for mesoporous silica systems, given that drug loading is driven by solvent penetration into pores and subsequent evaporation [35].

GFA-I compounds, poor glass formers, are particularly prone to recrystallization in amorphous formulations [39]. One strategy to tackle this instability is to combine the drug with a polymer in an amorphous solid dispersion. A very common technique to manufacture amorphous solid dispersions is HME [41,79]. In this process, polymer and API are mixed in the molten state to form an extrusion strand, which is further processed into a solid dosage form, e.g. tablet or a capsule.

Another approach is to formulate GFA-I drugs with mesoporous silica. This is of particular interest due to the high stability of the amorphous API once it has been loaded into the porous network of the silica. This enhanced stability is related to nano-confinement in the meso-scale pores, which by definition range from 2-50 nm [215,216]. Stability is further improved with complementary pore-API interactions that lower the free energy of the system [217]. Muller and co-workers demonstrated amorphous stability at ambient and accelerated conditions for 30 different mesoporous silica formulations [218]. One key consideration for mesoporous silica formulations is the location of the API within the sample. For GFA-I compounds, it is essential that the loading process is carried out carefully, avoiding oversaturation of the silica, to ensure the drug is loaded within the pores and not on the outer surface. GFA-I compounds adsorbed on the outer surface are prone to rapid crystallization, which can be observed with techniques such as differential scanning calorimetry (DSC) and powder X-ray diffraction (PXRD). However, upon successful loading of the drug in the internal porous network, silica formulations can provide a viable

alternative for drugs that fail to form a stable amorphous formulation in classical solid dispersions [219–221]. Although amorphous stability in mesoporous silica has been well described, there has been no comparison on stability of poor glass formers in HME and mesoporous silica technology published to date.

Certainly, solid-state stability is not the only important formulation consideration for poorly soluble drugs that are also poor glass formers. It is also essential to consider stability of the supersaturation generated upon dissolution. Indeed, recent work has demonstrated that, due to their high propensity for recrystallization, poor glass formers may also have issues with rapid onset of precipitation upon release, thus limiting their therapeutic potential [222]. This is in line with the well-established "Spring and Parachute" model [98], which identifies the need for additional excipients to sustain supersaturation of APIs in solution [116]. For polymer-based solid dispersions, the polymer may be able to meet both requirements: suspending the drug in an amorphous form, and inhibiting precipitation from the supersaturated state. An example of such a polymer is polyvinyl alcohol that is interesting due to its low hygroscopicity and for which a special grade has been introduced recently for HME [223]. Unlike polymer-based solid dispersions, the ability of mesoporous silica to inhibit precipitation of the supersaturated API is limited. Therefore it is often necessary to incorporate precipitation inhibitors into mesoporous silica formulations [224].

In this study, the amorphous stability of two model poor glass formers, haloperidol and carbamazepine, formulated as HME and with mesoporous silica, was investigated in line with ICH Q1 [225] accelerated stability conditions over three months. The stability was monitored by means of PXRD and underscored with DSC measurements of the samples before and at the end of the study. To the best of our knowledge, such a comparative study has not been reported previously. This stability comparison was complemented by non-sink release testing in biorelevant media [191,226] to monitor potential supersaturation and recrystallization during drug release [224,227]. Non-sink dissolution was not used as a direct comparison between the two formulations, as the mesoporous formulations do not inhibit precipitation upon release. Rather, the release curves are demonstrative of the decrease in dissolution performance that can be observed upon solid-state transformation. Finally, solid-state nuclear magnetic resonance (SS-NMR) spectroscopy was applied to investigate any qualitative changes drug-polymer spectra in HME formulations over the duration of the stability study [228].

From a practical perspective, both drugs have no thermal instability, which avoids the risk of heat-induced degradation during the HME process [229,230]. The drug load selected for the technology comparison was the highest amount that enabled initial amorphous loading for both HME and mesoporous silica formulations, so that a direct comparison between techniques could be attained.

It was hypothesized that mesoporous silica formulations of haloperidol and carbamazepine would show enhanced solid-state stability over time compared to solid dispersion obtained from HME.

5.2 Materials and Methods

5.2.1 Materials

Haloperidol, carbamazepine, HPLC grade acetonitrile and HPLC grade methanol were purchased from MilliporeSigma (Darmstadt, Germany). Parteck MXP® and Parteck SLC® were kindly provided by Merck KGaA (Darmstadt, Germany). FaSSGF/FaSSIF/FeSSIF powder to make biorelevant dissolution medium, Fasted Simulated Intestinal Fluid (FaSSIF), was obtained from Biorelevant.com (London, UK).

5.2.2 Methods

5.2.2.1 Thermodynamic Solubility Determination

FaSSIF was prepared by weighing 45 mg of FaSSGF/FaSSIF/FeSSIF powder into 45 mL of phosphate buffer (pH 6.5) [95]. API (2-3mg) was accurately weighed into a Uniprep® syringeless filter (5mL; 0.45µm). 2 mL of FaSSIF was added and the samples were agitated at 450 rpm for 24 hours at 37 °C. The pH was checked at 7 hours and adjusted with 0.1 N NaOH or 0.1 N HCl, if a deviation greater than +/- 0.05 pH units was observed. The final pH was also recorded after 24 hours.

Samples were filtered into the inner chamber of the Uniprep through the built-in PTFE 0.45 µm Whatman filter after 24 hours. Filtrates were immediately diluted with acetonitrile and water (1:4 V:V) to avoid precipitation from the saturated solution. Samples were analyzed with UHPLC (Thermo Dionex Ultimate 3000, Thermo Fisher, MA, USA) to determine the API concentration. API concentration was determined based on a standard calibration curve of nine standard concentrations (50, 30, 10, 5, 3, 1, 0.5, 0.3, 0.1 µg/mL). Three control samples of known concentrations (30, 3, 0.3 µg/mL) were prepared and used to check the robustness of the calibration curve. The determination was carried out in duplicate.

5.2.2.2 Ultra-High Performance Liquid Chromatography (UHPLC)

UHPLC analysis was performed using a Thermo Dionex Ultimate 3000 (Thermo Fisher, MA, USA) equipped with a diode array detector at 282 nm for carbamazepine and 247 nm for haloperidol (Thermo Fisher, MA, USA). The separation was achieved on an Acquity UPLC BEH column C8 (2.1 x 50 mm, 1.7 µm, Waters, MA, USA). The mobile phases A and B consisted of water: formic acid 999:1 (V:V) and acetonitrile : formic acid 999:1 (V:V), respectively. Gradient and flow rate is shown in Table 5.1. System management, data acquisition and processing were based on the Chromeleon™ software package, version 7.2 (Thermo Fisher, MA, USA).

Table 5.1. UHPLC gradient and flow rates

Time (min)	Flow rate (mL/min)	% (V:V) Mobile phase A	% (V:V) Mobile phase B
0.00	0.83	90	10
0.83	0.83	10	90
1.20	1.50	90	10
2.00	1.50	90	10
2.01	0.83	90	10

5.2.2.3 Preparation of Hot Melt Extrudates

PVA was selected as an optimal polymer for hot-melt extrusion. This was based on three factors: 1) grade of PVA is specifically designed for optimal hot melt extrusion due to particle size distribution and viscosity 2) partial solubility parameters 3) low hygroscopicity of PVA reduces water uptake in the extrudates.

Binary mixtures of polyvinyl alcohol (PVA, Parteck MXP®) and drug at various drug loadings were mixed in a mortar and extruded on a ZE9 ECO twin-screw extruder by ThreeTec (Birren, Switzerland) with 9 mm diameter and 180 mm length co-rotating screws. A screw speed of 80 rpm was applied at a temperature of 190 °C through all three heating zones, which is in accordance with recommendation by the polymer manufacturer [231]. After extrusion, the extrudates were ground in a mortar, and the fraction retained between mesh sizes 150 and 425 µm was retained for use in the study. The final extruded mixtures were cooled to room temperature and stored in falcon tubes. Mixing feasibility of the selected polymer for both drugs was verified by the Hansen solubility parameters [124,129], which were calculated using the quantitative structure property relationship (QSPR) method of the COSMOquick software (COSMOlogic, Germany, Version 1.6) [127,232]. For the investigation of the formulations, a 7.5 % (w/w) drug loading of haloperidol and 20 % (w/w) was used for carbamazepine. This was selected on the basis of the highest drug load that was initially successful for both formulation technologies, and was the result of a formulation screening.

5.2.2.4 Preparation of API-Loaded Silica Formulations

Mesoporous silica formulations were prepared using the incipient wetness method [216]. API (3 g) was dissolved in acetone (300 mL; 10 mg/mL), which was added drop-wise at a rate of 0.5 mL/minute to Parteck SLC® mesoporous silica (7 g), under constant stirring and heating at 60 °C. After complete addition of the concentrated API solution, the samples were dried overnight in a vacuum oven at 60 °C to ensure complete removal of the solvent. For the investigation of both formulations a drug loading of 7.5 % for haloperidol and 20 % for carbamazepine was used.

5.2.2.5 Storage of Samples for Stability Studies

For storage of the samples in the stability study, each of the formulations was placed in a separate glass jar with a secure lid. A separate beaker containing saturated sodium chloride solution, also placed in the beaker, ensured a constant relative humidity of 75% in the surrounding environment [233]. This enclosed system was then placed in a stability cabinet set to 40 °C to obtain storage conditions in accordance with ICH Q1.

5.2.2.6 Powder X-Ray Diffraction

Samples were prepared between X-ray amorphous films and measured in transmission mode using Cu-Kα1-radiation and a Stoe StadiP 611 KL diffractometer (STOE & Cie GmbH, Darmstadt, Germany) in transmission mode equipped with Dectris Mythen1K PSD (DECTRIS Ltd., Baden-Daettwil, Switzerland). The measurements were evaluated with the software WinXPow 3.03 by Stoe (STOE & Cie GmbH, Darmstadt, Germany), the ICDD PDF-4+ 2014 Database (ICDD, PA, USA), and Igor Pro Version 6.34 (Wavemetrics Inc., OR, USA) Angular range: 1-65 °2θ; PSD-step width: 2 ° 2 θ; angular resolution: 0.015 °2 θ measurement time: 15 s/step, 0.25 h overall.

5.2.2.7 Non-Sink Mini-dissolution in FaSSIF

The equivalent of 5 mg API of extrudate or API-loaded silica was weighed into a glass vial. 5 mL of FaSSIF was added. The vials were agitated at 37 °C and 450 rpm in a shaker (IKA -Werke GmbH & CO. KG, Staufen, Germany) for 2 hours. Samples of 0.3 mL were taken at 2, 15, 60, 90 and 120 minutes, filtered (0.45 PTFE Whatman filters), diluted with acetonitrile and water, and analyzed by UHPLC. The mini-dissolution trials were conducted in duplicate for all samples.

5.2.2.8 Scanning Electron Microscopy

Samples were prepared on carbon tape and imaged using a TM3000 Tabletop Scanning Electron Microscope (Hitachi, Tokyo, Japan), tungsten source, using low vacuum and accelerating voltage of 5 kV and 15 kV. A 4-Quadrant BSE detector was used, and imaging was at a magnification between 15x – 30,000x.

5.2.2.9 Differential Scanning Calorimetry

Samples were assessed by differential scanning calorimetry on a DSC 3 (Mettler Toledo, Greifensee, Switzerland). An amount of 5 to 9 mg sample was placed in a 40 μL aluminum pan with a pierced lid. A heating rate of 10 °C/min from 20 °C to 200 °C was applied under nitrogen purging at 200 mL/min. The thermograms were analyzed with the STARe Evaluation-Software Version 16 (Mettler Toledo, Greifensee, Switzerland).

5.2.2.10   Solid-State Nuclear Magentic Resonance (SS-NMR) Spectroscopy

SS-NMR experiments were conducted with magic-angle-sample (MAS) spinning using a Bruker 4 mm MAS HXY probe in double resonance mode with a Bruker Avance I 600 MHz wide bore NMR spectrometer (Bruker, Rheinstetten, Germany) with a 4 mm rotor. The readout on the probe thermocouple was set to 290 K. The sample spinning frequency was set to 10 kHz. All spectra were recorded with ^{1}H-^{13}C-cross polarization (CP) using a contact time of 1 ms. 100 kHz high power proton decoupling following the SPINAL64 scheme was applied during acquisition. The recycle delay was 3 s. The spectra were indirectly referenced to 4,4-dimethyl-4-silapentane-1-sulfonic acid (DSS) via the CH_2 signal of Adamantane at 40.49 ppm.

5.3 Results

5.3.1   Macro- and Microscopic Changes

Qualitative macroscopic differences were observed between the fresh and one-week stressed samples of the hot-melt extrudates (Figure 5.1). Extrudates of carbamazepine and haloperidol were transparent immediately after manufacturing. This indicates the presence of molecularly dispersed API throughout the polymer in the amorphous form [79]. However, after only 7 days exposure to 40 °C and 75% RH, both extrudates became opaque, indicating phase separation in the formulations [107]. This was in contrast to mesoporous silica formulations, in which no macroscopic differences were observed between the fresh and one-week stressed samples. Indeed, the appearance of mesoporous silica formulations remained consistent over the duration of the 3-month study.
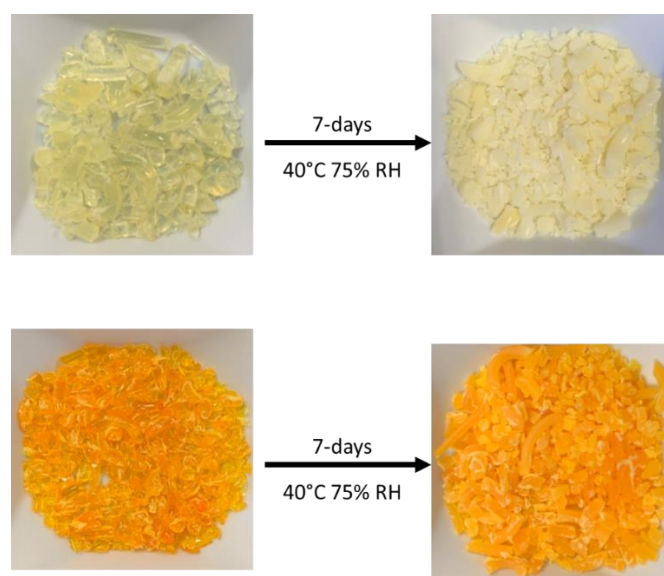

Figure 5.1. Haloperidol (top) and carbamazepine (bottom) HME before (left) and after (right) 7 days accelerated stability conditions as specified in the materials and methods section.

Changes in the extrudate samples over time were also observed on a microscopic level in the SEM images. In freshly prepared formulations, the extrudates showed no heterogeneity but at the end of the stability study, after 90 days, phase separation and recrystallization were observed. API-loaded silica formulations, however, did not exhibit qualitative changes under either visual inspection or by SEM (Figure 5.2 and 5.3).
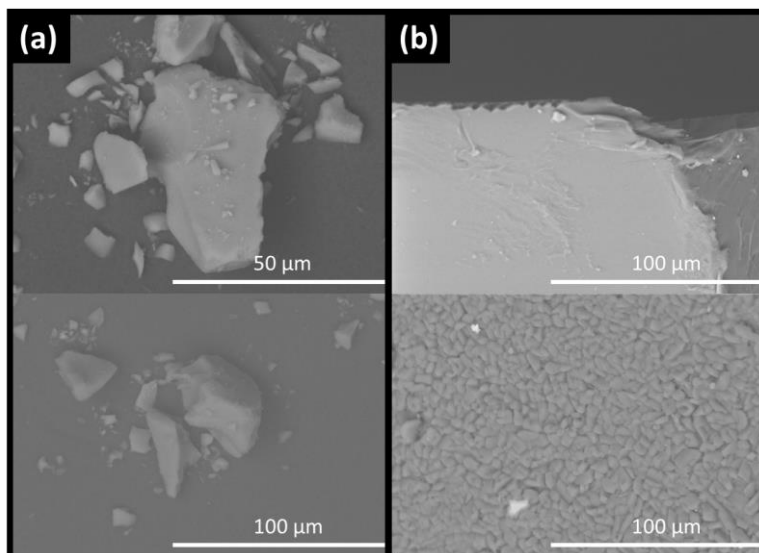

Figure 5.2. SEM images for carbamazepine loaded silica (a) and HME (b) showing particle size and morphology at 0 days (top) and 90 days stability (bottom) as specified in the materials and methods section.
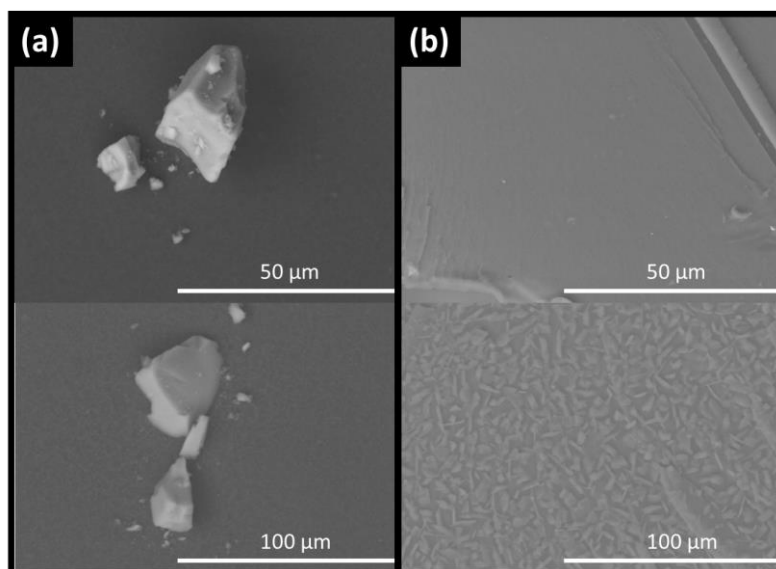
Figure 5.3. SEM images for haloperidol loaded silica (a) and HME (b) showing particle size and morphology at 0 days (top) and 90 days stability (bottom) as specified in the materials and methods section.

5.3.2 Solid-State Stability of the Amorphous Form

Both haloperidol and carbamazepine were crystalline before formulation with either HME or mesoporous silica. The outcome of the empirical loading approach is shown in Table 5.2. For mesoporous silica, both APIs were successfully stabilized in the amorphous form at an initial concentration of 30% (w/w). However, HME was only successful in stabilizing amorphous API for carbamazepine at 20% (w/w) and haloperidol at 7.5% (w/w) (data not shown). At higher concentrations, the extrudates were crystalline upon cooling. Therefore, for the comparative accelerated stability study of the formulations a drug load of 20% (w/w) carbamazepine and 7.5% (w/w) haloperidol was selected for both the mesoporous silica and HME based solid dispersions. PXRD indicated that the initial form in both formulations was amorphous (Figure 5.4 and 5.5).

Table 5.2. Loading capacities for both formulation techniques

Formulation	Loading Content (%, w/w)			
	30	20	15	7.5
Haloperidol HME	*Crystalline*	*Crystalline*	*Crystalline*	*Amorphous*
Haloperidol loaded silica	*Amorphous*	*Amorphous*	*Amorphous*	*Amorphous*
Carbamazepine HME	*Crystalline*	*Amorphous*	*Amorphous*	*Amorphous*
Carbamazepine loaded silica	*Amorphous*	*Amorphous*	*Amorphous*	*Amorphous*

Differences between silica-based formulations and PVA extrudates were apparent after one month of storage at elevated temperatures, with both HME formulations showing development of crystallinity. The crystalline percentage increased month by month over the duration of the study (Figure 5.4 and 5.5). Conversely, both API-loaded mesoporous silica formulations remained amorphous for the duration of the three-month stability study, with no evidence of crystallinity in the PXRD patterns (Figure 5.4 and 5.5).

These findings were underscored by the absence of melting endotherms in the DSC thermograms of the silica-based formulations after 90 days [234]. By contrast, melting peaks were observed in both samples of the extruded formulations after 90 days, indicating the presence of drug crystallinity (data not shown).
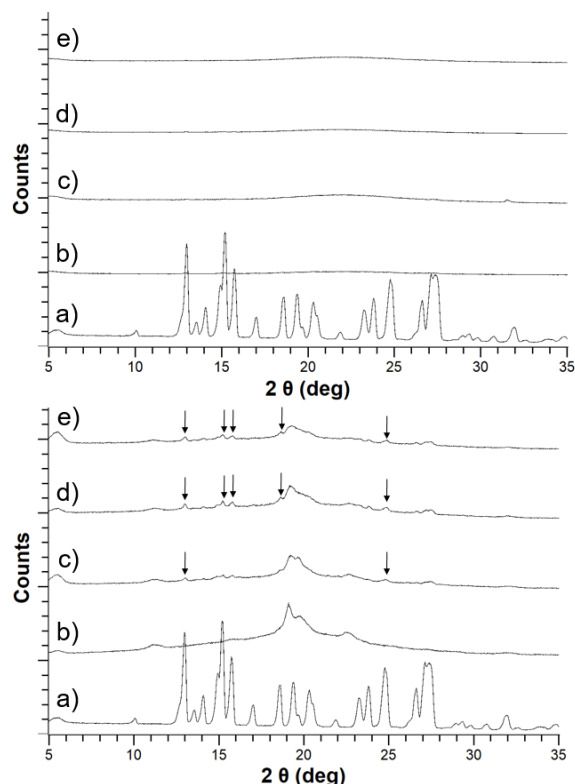
Figure 5.4. PXRD patterns for carbamazepine loaded silica (top) and carbamazepine HME (bottom) showing crystalline carbamazepine (a), unstressed carbamazepine formulation (b) and stressed carbamazepine formulations at 30 (c), 60 (d) and 90 (e) days. The arrows indicate crystalline peaks in the diffractograms.

Although drug-polymer interactions were not detectable in the SS-NMR spectroscopy for carbamazepine and haloperidol HME, it was possible to observe qualitative differences before and after storage of the samples at 45 °C/70% RH. Specifically, the freshly prepared samples had broad peaks in the spectra, related to the amorphous state of the sample. By contrast, an increased fine structure observed in the NMR-spectra at the end of the study indicated an increase in crystallinity. This was especially pronounced for haloperidol, with the stressed sample exhibiting peaks corresponding to the crystalline pure drug at 118 ppm, 153 ppm and 200 ppm in Figure 5.6 top correspond to peaks of the crystalline drug (Figure 5.6 bottom).
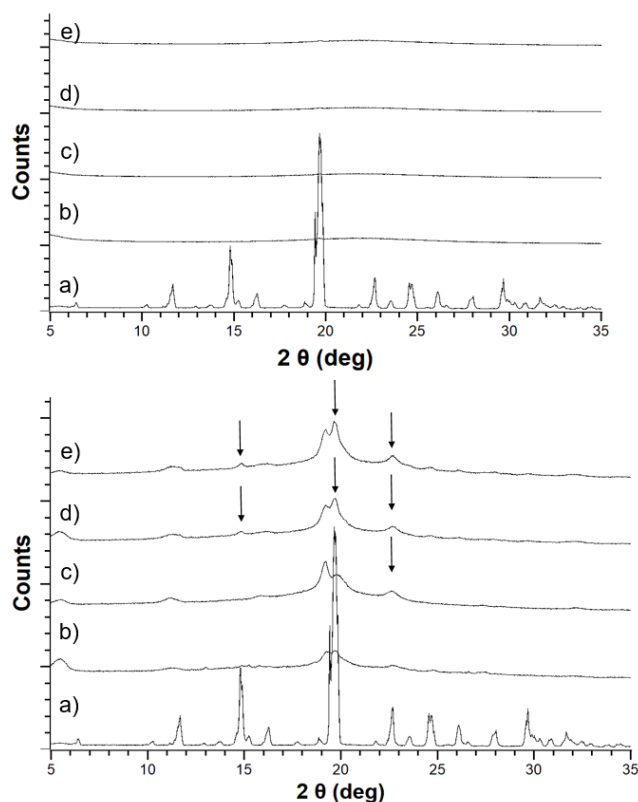
Figure 5.5. PXRD patterns for haloperidol loaded silica (top) and haloperidol HME (bottom) showing crystalline haloperidol (a), unstressed haloperidol formulation (b) and stressed haloperidol formulations at 30 (c), 60 (d) and 90 (e) days. The arrows indicate crystalline peaks in the diffractograms.

For carbamazepine, the change was more subtle, because of overlapping peaks. However, it was obvious that the stressed sample exhibited crystalline peaks that were not observed in the freshly prepared samples e.g. at 131 ppm, as shown in Figure 5.7. The presence of sharper peaks in the stressed samples underscores the recrystallization in the formulations suggested by the X-ray diffraction data.
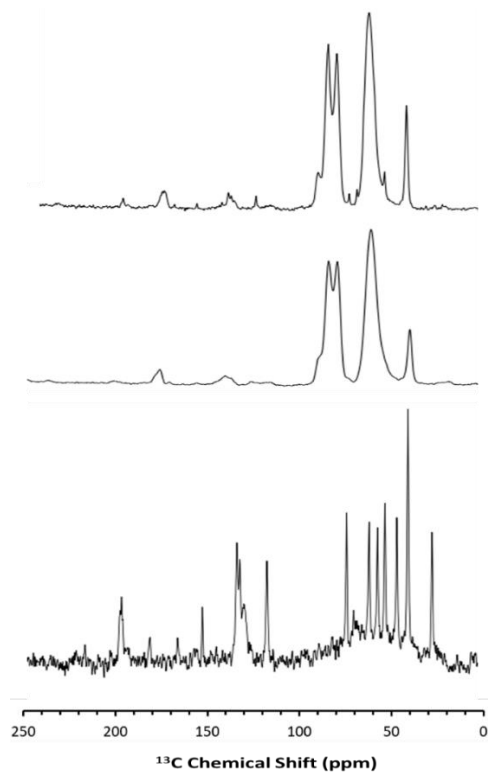
Figure 5.6. ^{13}C SS-NMR spectra for crystalline haloperidol (bottom), HME formulation at 0 days (middle) 90 days (top).
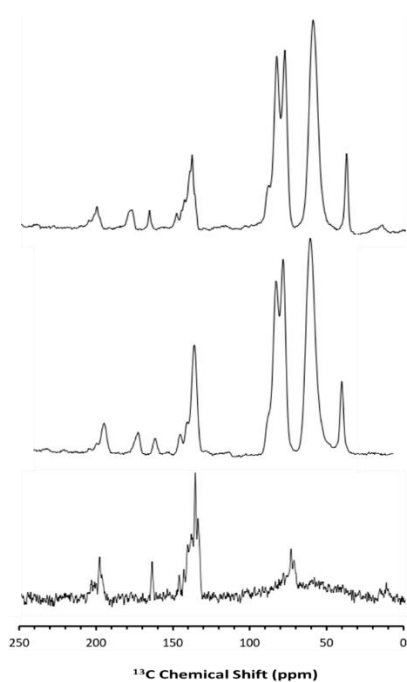

Figure 5.7. ^{13}C SS-NMR spectra for crystalline carbamazepine (bottom) and carbamazepine HME formulation at 0 days (middle) 90 days (top).

5.3.3 Stability of the Supersaturated State in FaSSIF

The thermodynamic solubility of haloperidol and carbamazepine in FaSSIF was measured to be 259 ($\pm$ 1) µg/mL and 203 ($\pm$ 2) µg/mL. Accordingly, the crystalline APIs showed a dissolution profile approaching these values over the course of the FaSSIF dissolution experiment.

Although both drugs have some solubility in FaSSIF, the dissolution was enhanced by both the mesoporous silica and HME formulations. For carbamazepine, a maximum supersaturation of 1.8 and 1.5-fold was generated for the silica and HME formulations, respectively. For haloperidol, a maximum supersaturation of about 2.0-fold was generated for both silica and HME.

The PVA in the HME formulation was able to sustain supersaturated concentrations for both APIs by inhibiting precipitation from aqueous medium. Mesoporous silica, on the other hand, was barely able to inhibit drug precipitation from the supersaturated state and therefore, precipitation was observed for both APIs, with concentrations returning to the thermodynamic solubility.

For mesoporous silica formulations, further development of the formulation would include a screening and a selection of a precipitation inhibitor to include in the formulation. The precipitation inhibitor would prevent the precipitation of the supersaturated API and could subsequently enhance oral absorption. However, although important, the precipitation inhibitor in a mesoporous silica formulation is not expected to impact on the solid-state stabilization of the API in the amorphous form. This is due to the fact that precipitation inhibitors are simply blended with the drug-loaded silica when the drug is already loaded onto the porous silica and stabilized in the solid state. Therefore, as the focus of this study was on the innate stabilization potential of mesoporous silica using poor glass formers, incorporation of a precipitation inhibitor was out of scope.

For both APIs, the dissolution profiles from mesoporous silica formulations were comparable throughout the duration of the entire accelerated stability study. Particularly notable was that the degree of supersaturation, or 'spring', remained consistent over the whole stability study (Figure 5.9). For HME formulations, the curves showed a decrease in supersaturation in each successive month of the stability study. After 30 days, the HME formulation containing carbamazepine was still able to generate supersaturation, but the profile was no longer stable: the carbamazepine concentration returned to the thermodynamic solubility within 60 minutes. This difference between fresh and 30-day carbamazepine samples was indicative of the presence of seed crystals in the formulations. Such seeds foster crystallization in the formulation as well as in solution to most likely override the inhibition of precipitation by the polymer [235]. Furthermore, the release performance of carbamazepine HME declined even further at 60 days and 90 days. By 90 days, no supersaturation was observed at any measured time point during the experiment, and the dissolution curve resembled that of crystalline carbamazepine more closely (Figure 5.8).
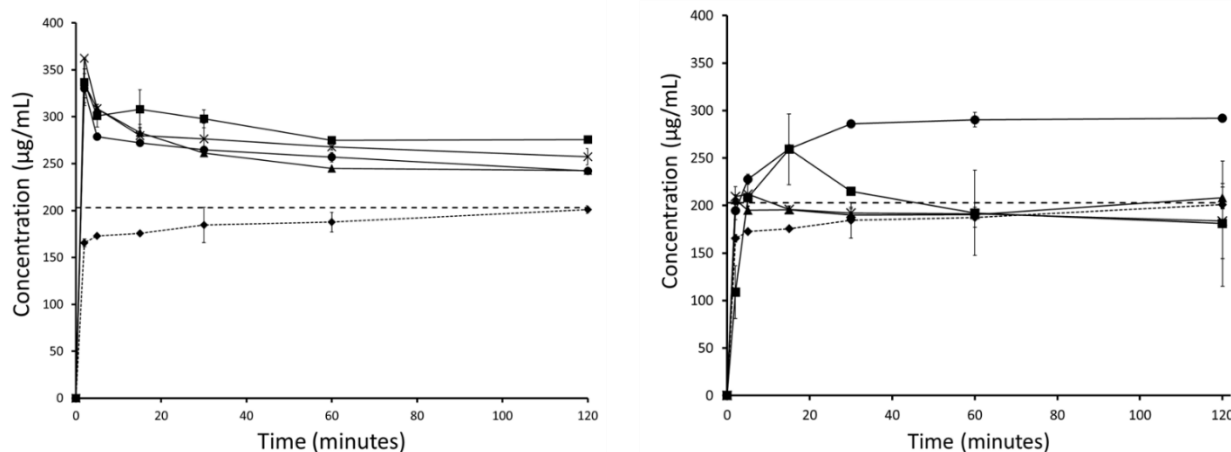
Figure 5.8. FaSSIF mini-dissolution curves for carbamazepine loaded silica (left) and carbamazepine HME formulation (right) showing crystalline carbamazepine (♦), unstressed carbamazepine formulation (●) and stressed carbamazepine formulations at 30 (·), 60 (X) and 90 (▲) days.

Similar reductions in dissolution performance with storage were observed for the HME formulation of haloperidol. Although the dissolution performance of the haloperidol HME did not decline as quickly as that of the carbamazepine HME, its dissolution profile also resembled that of the crystalline API after 90 days (Figure 5.9).
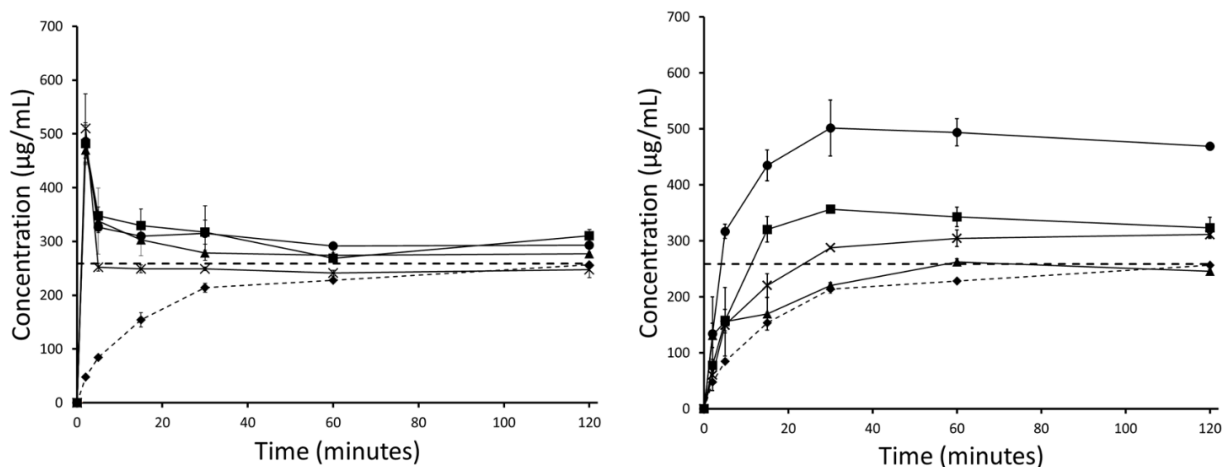

Figure 5.9. FaSSIF mini-dissolution curves for haloperidol loaded silica (left) and haloperidol HME formulation (right) showing crystalline haloperidol (♦), unstressed haloperidol formulation (●) and stressed haloperidol formulations at 30 (·), 60 (X) and 90 (▲) days.

5.4 Discussion

Development of amorphous solid dispersions requires a thorough understanding of the factors that influence stability in the amorphous form. One such factor is the GFA. According to the classification system proposed by Baird et al [36], GFA-I drugs are especially challenging when developing

amorphous formulations, due to the high propensity for re-crystallization of such compounds. It is essential to demonstrate good physical stability in amorphous formulations to ensure that recrystallization does not occur over time, as this would reduce the shelf-life of the product [236]. As crystallization is based on the stochastic nucleation process, a lack of physical stability could lead to variable product quality among batches. Any initial crystallization in the batch, or differences in the rate of crystallization, could lead to out-of-specification results based on insufficient drug product performance, for example in dissolution testing. Variability among batches would thus be problematic in terms of meeting regulatory and commercial requirements. Herein, it has been demonstrated that mesoporous silica can be used to successfully stabilize compounds of poor amorphous stability that are unsuitable for formulation in standard polymer-based amorphous solid dispersions.

Initial formulation development demonstrated the potential impact that such a poor amorphous stability could have on the viability of a formulation. For both HME formulations, significantly lower percentage drug loads were attainable in the initial formulation development. This is a crucial topic for the development of amorphous formulations. Taking the example of haloperidol, it was only possible to stabilize 7.5% (w/w) of the API in the amorphous form in the HME. Assuming a theoretical dose of 200 mg, one would require a tablet of approximately 2.6 g in weight to incorporate the entire dose in a single dosage form. Furthermore, this represents a very conservative estimation, as the actual API content would likely be reduced further to 3.25% when one considers that 50% of the tablet may consist of fillers, binders, glidants and disintegrants. Ultimately, a low drug loading would be a substantial risk to the viability of the formulation, and could result in failure of the project. Mesoporous silica, however, was successful in stabilizing more reasonable drug loads in non-crystalline form.

Furthermore, the successful low drug loading HME formulations developed for carbamazepine and haloperidol were observed to be unstable during the ICH Q1 stability study (Figure 5.4 and 5.5). Instability in polymeric amorphous solid dispersions can be linked with increasing temperature and humidity. As temperature or water content in amorphous formulations increases, mobility of the drug within the polymer dispersion increases. Mehta and co-workers demonstrated this effect on model amorphous solid dispersions (ASDs). In their study, an increase in molecular mobility of all APIs in the polymer ASDs led to a decrease in recrystallization time [65,236]. As both studies by Mehta and colleagues investigated the physical stability of good to moderate glass formers (GFA-II/III), it is likely that the effect of moisture and temperature on increasing molecular mobility and subsequent physical instability would be even greater for GFA-I compounds.

The observed instability of these poor glass formers is even more remarkable when one considers that, of the available polymers for hot melt extrusion, PVA has an extremely low hygroscopicity [231]. This low hygroscopicity would have a stabilizing effect on the formulation due to a reduction in the uptake

of water in the stressed conditions. However, this effect is not enough to prevent the poor glass formers from re-crystallizing in the extrudates.

For mesoporous silica, however, molecular mobility is greatly reduced regardless of moisture or temperature. Brás and colleagues demonstrated that adsorption and nano-confinement of ibuprofen onto mesoporous silica resulted in a significant reduction of all known types of molecular mobility [64]. Most interestingly, the Johari-Goldstein β relaxation, a type of molecular mobility associated with re-crystallization, was reduced. This was a crucial observation, as it has been shown that increased Johari-Goldstein relaxation is related to physical instability of the amorphous form [64,65]. Similar to the work by Mehta and colleagues, Bras et al. focused on good glass formers (GFA-III). Additional work demonstrated that a reduction in molecular mobility leads to successful stabilization of the very poor glass former menthol (GFA-I), which has a glass transition temperature of -54.3 °C [237]. In a further study, Cordeiro and colleagues successfully stabilized amorphous menthol due to nano-confinement within mesoporous silica. This stabilization was related to a decrease in molecular mobility of both α (free transitional mobility in space) and the aforementioned Johari-Goldstein β relaxations. Furthermore, a new type of molecular mobility, the S-type, was observed. S-type refers to mobility of a hindered molecule that is nano-confined within a single pore, and is much slower than standard molecular mobility events [237]. Based on these findings as well as those of our study (Figure 5.4 and 5.5), mesoporous silica may be a suitable way forward to stabilizing GFA-I glass formers under accelerated conditions.

There are only a handful of known GFA-I compounds that are also BCS II compounds and which would thus benefit from the apparent solubility increase of the amorphous form. In a recent review, Kawakami provided an overview of pharmaceutical compounds according to GFA classes [60]. Of the GFA-I compounds in the database only 29% were determined to be BCS II/IV, which is far lower than the commonly reported percentage of commercial compounds that fall into the poor solubility category (60%) [35]. Hence, there appears to be a disconnect between the prevalence of compounds with poor solubility and the occurrence of poor glass formers on the market. This could be related to the difficulty in formulating such compounds, and the reduction in formulation performance related to physical instability.

For the two model BCS II drugs selected in this study, clear differences were observed in the non-sink release profiles of loaded silica and HME formulations. As expected from the literature, silica alone was not able to sustain supersaturated concentrations of API in solution resulting in precipitation [224]. Conversely, in the HME formulations, the API is sustained in solution by the polymer itself, which can function not only as a matrix polymer but also as a precipitation inhibitor during drug release. However,

it was observed that dissolution of API loaded silica formulations remained consistent throughout the 3-month study (Figure 5.8 and 5.9), whereas the kinetic release of HME formulations tended towards crystalline drug solubility (Figure 5.8 and 5.9). Here, we see the effect of phase separation and recrystallization on the dissolution performance of amorphous solid dispersions, with the presence of a crystalline phase reducing the achievable supersaturation and decreasing the dissolution performance of the compound [60]. Interestingly, both HME formulations retained some supersaturation after the first month of the stability study, indicating that full conversion from amorphous to crystalline had not yet occurred (Figure 5.8 and 5.9). However, the supersaturated solutions generated by the carbamazepine HME were less stable than those generated by the haloperidol HME and precipitation occurred (Figure 5.8). This was related to the presence of seed crystals in the formulation, which sped up the rate of nucleation and reduced the ability of the polymer to prevent precipitation. Patel and co-workers demonstrated that a small amount of crystalline indomethacin significantly increased its recrystallization from the supersaturated state, even in the presence of precipitation inhibitors [235]. The present results support the view that GFA-I compounds may not be good candidates for formulation in polymeric amorphous solid dispersions, such as hot-melt extrudates, which have been investigated here. However, this is also expected by other formulations based on polymeric amorphous dispersions, e.g. spray dried dispersions or co-precipitates. Mesoporous silica, on the other hand, is an attractive formulation option for poorly soluble glass formers, generating consistent and supersaturated dissolution profiles.

5.5 Conclusion

The increasing prevalence of poorly soluble BCS II drug candidates in pharmaceutical development remains a challenging issue. Although polymer-based stabilization of the API in an amorphous form has been a common approach to their formulation for several decades. Such an approach may not be suitable for poorly soluble compounds that also show poor GFA. These compounds, which demonstrate both poor solubility and poor amorphous stability, are challenging for formulation with typical polymer-based technologies due to possible phase separation and recrystallization. Ultimately, these compounds may have an increased risk of failure during pharmaceutical development, as they constitute a risk from both a bioavailability and amorphous stability perspective. In this study we demonstrated that poor glass forming (GFA-I) APIs have increased risk of recrystallization in polymer-based amorphous solid dispersions. By contrast, mesoporous silica was shown to provide optimal stabilization for such APIs. Therefore, mesoporous silica could be an attractive formulation technology to expand the formulation toolbox for APIs that are poor glass formers. More research in the future will clarify whether mesoporous silica should become a method of choice for oral delivery of poorly soluble GFA-I compounds.

Chapter 6

In vivo performance of innovative polyelectrolyte matrices for hot melt extrusion of amorphous drug systems

Summary

Hot melt extrusion of amorphous systems has become a pivotal technology to cope with challenges of poorly water-soluble drugs. Previous research showed that small-molecular additives with targeted molecular interactions enabled introduction of a polyelectrolyte matrix to hot melt extrusion that would be otherwise not possible to process due to the unfavorable melting properties of the pure polymer. Carboxymethyl cellulose (NaCMC) with lysine or alternatively meglumine was leading to modified polymeric matrices that showed adequate processability by hot melt extrusion and yielded stable amorphous formations. The investigated formulations, including fenofibrate as a model drug, were characterized by attenuated total reflectance Fourier transform infrared spectroscopy, differential scanning calorimetry, as well as viscosity measurements after aqueous dispersion. Further biopharmaceutical assessment started with biorelevant non-sink dissolution testing followed by a pharmacokinetic in vivo study in rats. The in vitro assessment showed superiority of the lysine containing formulation in the extent of in vitro supersaturation and overall drug release. In accordance with this, the in vivo study also demonstrated increased exposure of the amorphous formulations and in particular for the system containing lysine. In summary, the combination of polyelectrolytes with interacting additives presents a promising opportunity for the formulation of poorly water-soluble drugs.

6.1. Introduction

The challenge of improving the bioavailability of poorly water-soluble drugs is a crucial aspect that pharmaceutical experts have to cope with throughout modern pharmaceutical development. An approach, which has gained popularity in the recent decade, is the formulation of drug in an amorphous form. Such a formulation approach typically leads to an apparent solubility increase and hence drug supersaturation upon dispersion after oral administration [54]. A high level of stabilized supersaturation in the small intestine results in enhanced bioavailability of orally delivered drugs [96,238]. Especially enabling formulations like amorphous systems processed by hot melt extrusion (HME) are capable of enhancing the supersaturation of BCS (i.e. biopharmaceutics classification system) class II drugs like fenofibrate (FE) to an extent that the absorption upon oral administration can become comparable to that of a BCS class I drug [239]. The assessment of such drug supersaturation is ideally performed under non-sink conditions using biorelevant media [95,191,226]. Since the supersaturation potential is dependent on the amorphous stability of the drug in the solid state [55,60], a combination of this assay with a stability-based comparison of supersaturation capabilities is applied in the so-called screening of polymers for amorphous drug stabilization (SPADS) approach, which is a screening method applied in the pharmaceutical industry for polymer selection during the development of amorphous solid dispersions (ASDs) [118].

Polymers with high molecular weight often affect drug precipitation following dispersion by a decrease of molecular mobility [116]. Such polymers can inhibit nucleation and/or growth as it was for example shown for the active pharmaceutical ingredient (API) indomethacin [235] and a variety of commonly used pharmaceutical polymers [240]. The functionality of polymers to act as precipitation inhibitors in solution is crucial in a supersaturating formulation [116,224,241]. An example of such a stabilizing polymer is the polyelectrolyte sodium carboxymethyl cellulose (NaCMC). Polyelectrolytes are commonly used as superdisintegrants in conventional solid dosage forms or they can find application as ionic liquids, where the combination of ionically interacting substances may lead to benefits in a pharmaceutical dosage form [197]. For the latter application, the intense swelling of superdisintegrants leads to faster disintegration of the solid dosage form, which would also be beneficial in a polymeric ASD but should be balanced with a risk of precipitation because of a too fast drug release [116,242].

In particular, NaCMC showed attractive stabilization of supersaturated drug [243] and an increase in overall oral bioavailability [48]. One factor might be the viscosity increase as stabilization of a supersaturated drug [117,244]. Even before drug gets entirely into solution, a polymer such as NaCMC could exert stabilizing effects in contact with aqueous media. Most recently, Edueng and colleagues identified the need for understanding the influence of the viscous interface between amorphous material and water on nucleation kinetics [13].

Unfortunately, the polyelectrolyte NaCMC is not applicable for HME in the neat form due to its high melting point and thermal degradation at the required processing temperature [198]. Therefore, the

principle of molecularly interacting conformers [91] was investigated with a new focus of changing polymer properties rather than targeting direct drug-additive interactions [122,148]. In case of polyelectrolyte NaCMC, it was possible to obtain an extrudable polymeric matrix of the polyelectrolyte and a stable glass formation was demonstrated by means of synchrotron powder X-ray diffraction [148]. Although this recent work identified meglumine (Meg) and lysine (Lys) as most suitable co-formers in the applied dataset, a biopharmaceutical assessment with an *in vivo* study have not yet been conducted to support the potential of the new approach. The present study therefore used the identified polyelectrolyte matrices to incorporate FE as a poorly water-soluble model drug, because it is known to precipitate rapidly from supersaturated solution and its stabilization by excipients was found to be difficult [245].

In this study, the solid dispersions were developed with regards to a drug load that provided completely amorphous formulations. The amorphous form of FE in both formulations was evaluated by differential scanning calorimetry (DSC) and powder X-ray diffraction (PXRD). Regarding drug release testing, the two formulations were compared with their corresponding physical mixtures in a non-sink Level II [246] fasted simulated intestinal fluid (FaSSIF) dissolution experiment [191,226]. To gain further insights in the stabilization properties of NaCMC, viscosity measurements were performed. For a better correlation with the performed dissolution experiments, the viscosity was measured in Level II FaSSIF after the duration of the dissolution experiments. Moreover, the formulations and their physical mixtures were investigated in a pharmacokinetic (PK) study in rats to investigate the viability of the approach using NaCMC amorphous formulations produced by HME and FE as a model compound.

6.2 Materials and Methods

6.2.1 Materials

FE, NaCMC (low viscosity), Lys and Meg were bought from Sigma-Aldrich (Bruchs, Switzerland). FaSSGF/FaSSIF/FeSSIF powder media was bought from biorelevant.com (Biorelevant.com Ltd, London, UK). Purified water for the viscosity measurements as well as the dissolution media was taken from a MilliQ Millipore filter system (Millipore Co., Bedford, MA, USA). All solvents for the UPLC analysis were of LC-MS quality and bought from Sigma Aldrich (Bruchs, Switzerland). Filters and other consumables were bought from Sigma-Aldrich (Bruchs, Switzerland).

6.2.2 Methods

6.2.2.1 Preparation of hot melt extrudates

Binary mixtures of NaCMC and Meg or Lys in a ratio of 50/50 % (w/w) were mixed in a mortar and dissolved in MilliQ water in a round bottom flask. Afterwards, the water was removed by a rotary evaporator (Rotavapor Büchi, Flawil, Switzerland). The resulting film was cut into smaller pieces and ground in a mortar. This powder was mixed with FE in a ratio of 92.5/7.5 % (w/w) and extruded on a ZE9 ECO twin-screw extruder (co-rotating screws with a 9-mm diameter and 180 mm in length) by ThreeTec (Birren, Switzerland). A screw speed of 80 rpm was applied at a temperature of 130 °C through all three heating zones. The final extrudates were cooled to room temperature and stored in falcon tubes. This experimental procedure is in line with the previous work in which the polyelectrolyte matrices were developed [148].

6.2.2.2 Powder X-ray diffraction

The extrudates were analysed by PXRD on a D2 Phaser diffractometer (Bruker AXS GmbH, Karlsruhe, Germany) with a 1-D Lynxeye detector. The instrument was equipped with a Ge-monochromator (Cu Kα radiation) providing X-ray radiation at a wavelength of 1.541 Å. During the measurements, a voltage of 30 kV and a current of 10 mA were used. The increment and time per step were set to 0.020 ° and 1 s, respectively. The measurement 2θ angles were stretching over a range of 5° to 40°.

6.2.2.3 Differential scanning calorimetry

Samples were further assessed by a differential scanning calorimeter on a DSC 3 (Mettler Toledo, Greifensee, Switzerland). The samples were cut in small pieces and 5 to 9 mg were placed in a 40 μL aluminum pan with a pierced lid. A heating rate of 10 °C/min from −10 °C to 140 °C was applied, while the surrounding sample cell was purged with nitrogen at 200 mL/min. Moreover, a combination of heating, cooling and heating cycles was used to fully evaluate the samples. For the assessment of the initial form, the first heating was used. The thermograms and glass transition temperatures (T_gs) were analyzed with the STARe Evaluation-Software Version 16 (Mettler Toledo, Greifensee, Switzerland). All thermograms show exothermic events as upward peaks.

6.2.2.4 Determination of thermodynamic solubility

Level II FaSSIF was prepared according to the instructions of biorelevant.com by weighing 45 mg of FaSSGF/FaSSIF/FeSSIF powder into 45 mL of phosphate buffer (pH 6.5) [95]. Fenofibrate (2-3mg) was transferred into a glass vial, 2 mL of FaSSIF were added and the samples were agitated at 450 rpm for 24 hours at 37 °C. The pH was checked at 7 h and adjusted with 0.1 N NaOH or 0.1 N HCl.

Samples were filtered into a quartz glass cuvette through a 0.45 μm PTFE Whatman filter after 24 hours. Filtrates were immediately diluted with acetonitrile and water (1:4, v/v) to avoid precipitation from the

saturated solution. Samples were analyzed by a UV/VIS spectrometer (Jasco, Easton, MD, USA) at 287 nm. The experiment was carried out in triplicates.

6.2.2.5 Non-sink dissolution

The equivalent of 10 mg API of extrudate was transferred into a glass vial. After adding 10 mL FaSSIF, the vials were agitated at 37 °C and 450 rpm in a shaker for 2 hours [224]. Samples were taken at 2, 5, 10, 15, 30, 60, 90 and 120 minutes, filtered (0.45 µm PTFE Whatman filters), diluted, and analyzed by a UV/VIS spectrometer (Jasco, Easton, MD, USA) at 287 nm. The mini-dissolution trials were conducted in duplicate for all samples.

6.2.2.6 *In vivo* bioavailability study

For the in vivo pharmacokinetic study a protocol was used, which was approved by the institutional animal ethics committee in accordance with Belgian law regulating experiments on animals and in compliance with EC directive 2010/63/EU and the NIH guidelines on animal welfare. Male Sprague-Dawley rats (6 for each formulation) weighing 280–320 g on the day of the experiments were purchased from Charles River Laboratories Deutschland (Sulzfeld, Germany). The animals were acclimated for a minimum of 5 days. The animals had free access to a standard rodent diet and water ad libitum during the study. The animals were fasted 16-20 hours before the administration and throughout the study with free access to water. The extrudates were each delivered as ground powders for their corresponding study arm. Prior to administration, the powders were suspended in Level II FaSSIF and delivered to the animal by oral gavage at a volume of 6.25 mL/kg with a FE dose of 20 mg/kg. By individual tail vein puncture, 100 µL blood samples were collected into tubes containing dipotassium EDTA, plasma was harvested by centrifugation for 10 min at $1000\times g$, followed by separation into polypropylene tubes and immediate freezing and storage at -20 °C. Samples were taken at 0.5 h, 1 h, 2 h, 3 h, 4 h, 6 h, 8 h, 10 h, 24 h, and 28 h following oral dosing. The animals were euthanized after the experiment.

6.2.2.7 Bioanalytical Procedure

The analysis of the plasma samples was performed according to a validated method proposed and applied by Berthelsen et al. [247] In short, 50 µL of the plasma were precipitated with acetonitrile 1:4 (v/v) in an Eppendorf® tube and the mixture was placed in an ultra-sonic bath for 10 min. Subsequently, the samples were transferred and frozen for 10 min at -20 °C, followed by centrifugation at 5 °C and 17,500 rpm for 16 min. The resulting clear supernatant was transferred into a UPLC vials for further analysis.

6.2.2.8 Ultra-High Performance Liquid Chromatography (UHPLC)

UPLC analysis was performed using a Waters ACQUITY UPLC System (Waters Corporation, MA, USA) equipped with a photodiode array detector. The separation was achieved on an Acquity UPLC BEH column C18 (2.1 x 50 mm, 1.7 µm, Waters, MA, USA) and a guard column ACQUITY UPLC BEH column C18 VanGuard Pre-column (2.1 mm x 5 mm 130 Å, 1.7 µm) with an injection volume of 4 µL. The column oven temperature was maintained at 55 °C. The mobile phases A and B consisted of water: trifluoroacetic acid 999:1 (v/v) and acetonitrile, respectively. The gradient method employed began by an isocratic elution at 80:20 A:B for 0.8 min, followed by a linear increase to 0:100 A:B until 3.1 min and return to 80:20 A:B at 3.2 minutes and equilibration over a runtime of 4 min at a constant flow rate of 0.6 mL/min. Chromatograms were extracted at 287 nm for FE determination. System management, data acquisition and processing were based on the Empower software package, version 7.2 (Waters, MA, USA).

6.2.2.9 Viscosity measurement of the dissolution samples

Prior to the measurement, the samples were filtered through a 0.8 µm mixed cellulose ester filter to eliminate all non-dissolved particles. The measurement setup was reported in previous work [248].

In brief, the micro-electro-mechanical system capillary rheometer, m-VROC™ (RheoSence, San Ramon, CA), was employed to measure the viscosity of the dissolution samples. This instrument is a microfluidic slit rheometer, which enables viscosity measurements of various sample amounts. It measures the viscosity from the pressure drop of a sample as it flows through the rectangular slit. The glass syringe (Hamilton 81260 SYR 1000 mL) was loaded with sample and placed inside of the thermal block (37 °C ± 0.2) of the instrument. After the stabilization of the measurement temperature, the sample was pumped through the flow channel of the chip at shear rate 4000 s^{-1}. The pressure drop was detected by a sensor (cell VROC-mA10; 10K Pa full scale, 100-µm flow channel). On the basis of these measurements the viscosity was calculated using m-VROC Control Software (RheoSence, San Ramon, CA). The measurements were performed in triplicates.

6.2.2.10 Attenuated total reflectance Fourier transform infrared spectroscopy

The FTIR spectrometer Cary 680 (Agilent Technologies, Santa Clara, CA, USA) was used for the determination of interactions. The scanning range of $4000 - 600 \ cm^{-1}$ was selected at a resolution of $4 \ cm^{-1}$. For the evaluation, a spectrum was extracted and evaluated by the software ACD/Spectrus Processor 2016.1.1 (Advanced Chemistry Development, Canada).

6.2.2.11 Molecular modeling and statistical analysis

Graphical representation of molecular interactions was based on a molecular dynamics simulation in vacuum using the tube model in the program suite YASARA v. 18.11.10 (YASARA Biosciences GmbH,

Vienna Austria). An AMBER14 force field was employed and each molecule was first energy minimized. Sodium carboxymethylcellulose was represented as oligomer (n=10) and was in contact with one FE molecule to roughly approximate average relative amounts in line with the investigated formulations. Moreover, 10 molecules of either Lys or Meg were added and the simulation was running for about 1 ns at 300 K.

Data from the *in vivo* study in rats were analyzed using non-compartmental PK analysis. Maximum drug plasma concentration (C_{max}) values after oral dosing were extracted directly from the observed data, while area under the plasma concentration-time curve (AUC) value were calculated using the linear trapezoidal rule using Excel 2013 (Microsoft). The software StatGraphics Version 16 (Statgraphics Technologies Inc., The Plains, VA, USA) was used for all statistical calculations. For each formulation, an Analysis of the Variance (ANOVA) with a Fisher LSD post hoc test at a 95 % confidence interval was performed. A value of $p < 0.05$ comparing the formulations with the corresponding physical mixtures with respect to the previously mentioned pharmacokinetic responses was considered statistically significant.

6.3 Results

6.3.1 Molecular dynamics simulation

Before preparation of the formulations, the different systems were simulated on an atomistic level for visualization and to gain some qualitative structural insights. Assuming a simplified local composition, a small-scale molecular dynamics simulation was run for 1 ns (300 K) using an AMBER14 force field. The Figures 6.1 and 6.2 show a possible configuration of how the model drug FE may qualitatively interact with the modified matrix. Figure 6.1 suggests that the drug is embedded in a pocket-like structure for the formulation containing Lys. Pronounced hydrogen bonding of lysine side chains with fenofibrate is possible while meglumine is expected to mostly interact with polar interactions and possible weaker hydrogen bonds of hydroxyl groups that are present in the polymer. Consequently, the situation of FE appeared to be different with the system including Meg as co-former in which the drug appears to be rather attached to the surface of the modeled polymeric matrix (Figure 6.2). Moreover, interaction of fenofibrate with the lysine side chain are expected in the dry state as well as upon aqueous dispersion, which makes a difference to the before mentioned hydroxyl interactions by meglumine.
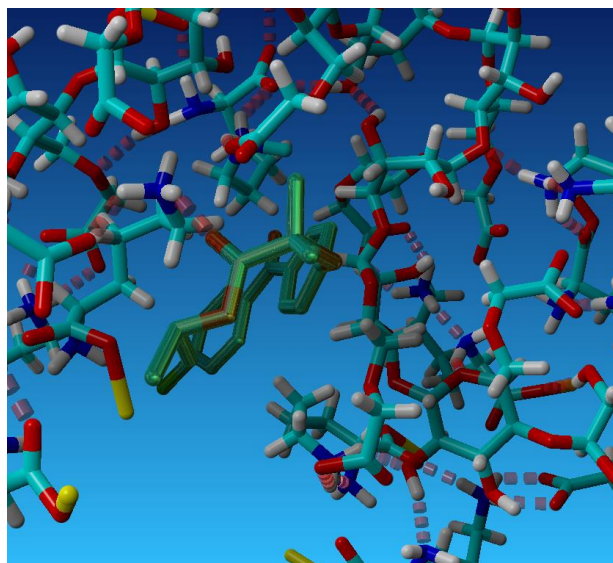
Figure 6.1. Visualization of a simplified molecular structure of the formulation Lys/NaCMC/FE based on an AMBER14 force field and 1 ns molecular dynamics simulation at 300 K (using the software YASARA [249]). Fenofibrate is in green, sodium ions are shown as yellow (tube model) and hydrogens are represented by dashed red lines.
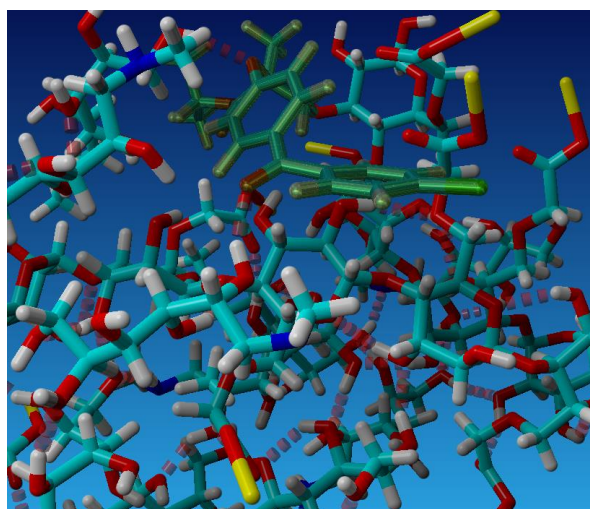

Figure 6.2. Visualization of a simplified molecular structure of the formulation Meg/NaCMC/FE based on an AMBER14 force field and 1 ns molecular dynamics simulation at 300 K (using the software YASARA [249]). Fenofibrate is in green, sodium ions are shown as yellow (tube model) and hydrogens are represented by dashed red lines.

6.3.2 Solid-state analytics

The successful amorphization of the model drug was investigated by PXRD (Figure 6.3) as well as DSC (Figure 6.4.). An amorphous halo diffraction pattern was indeed obtained for the two developed formulations in comparison with the crystalline reference drug that displayed distinct Bragg peaks of the API [86].
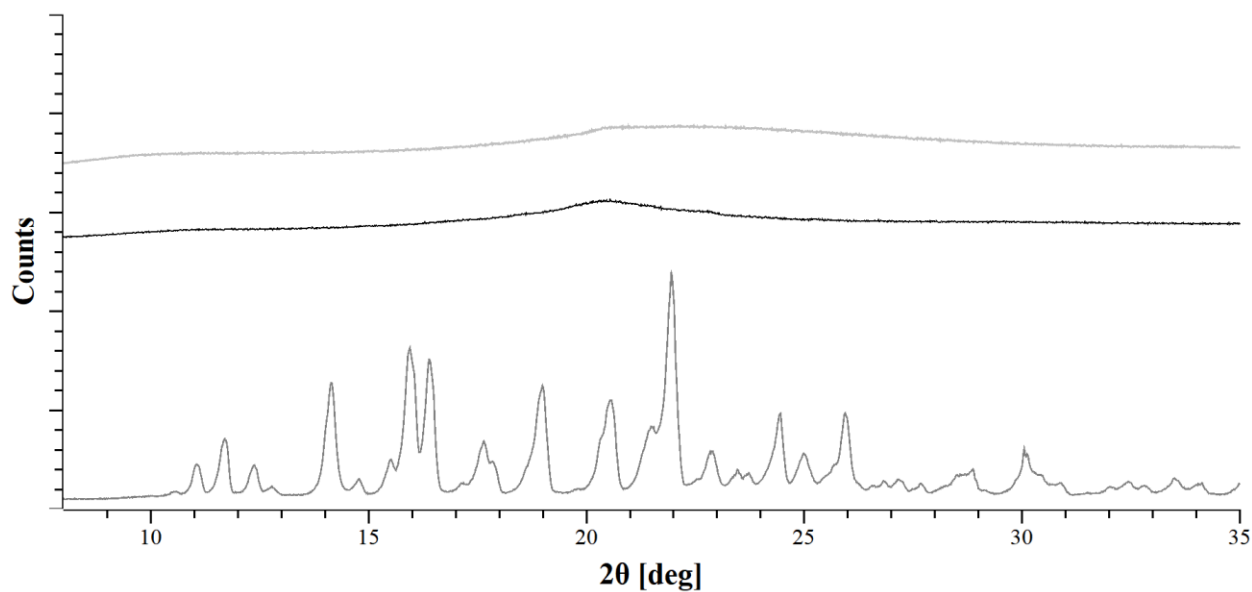
Figure 6.3. PXRD patterns of pure FE (gray, bottom), Lys/NaCMC/FE (light gray, top), Meg/NaCMC/FE (black, middle)
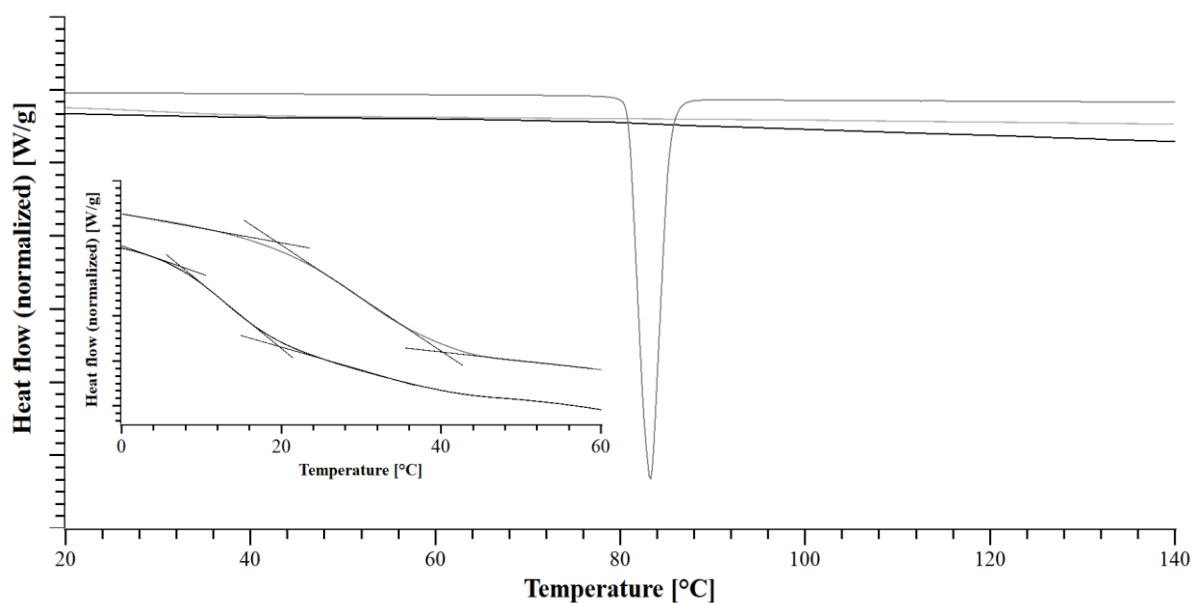
Figure 6.4. Thermograms of Lys/NaCMC/Fe (light gray,middle), Meg/NaCMC/Fe (black,bottom) and pure FE (gray,top). Insert shows T_g of Lys/NaCMC/Fe (light gray,top), Meg/NaCMC/Fe (black,bottom) in the area between 0 and 60 °C.

In the DSC thermograms, no melting peak could be detected in the formulations (Figure 6.4 black and light gray) in contrast to the pure model drug, which had a clear melting peak. The detected glass transitions at 29.70 (± 0.20) °C for the Lys formulation and 10.02 (± 0.82) °C for the Meg formulation

(Figure 6.4 insert) were in line with previously performed measurements the polyelectrolyte matrices [148].
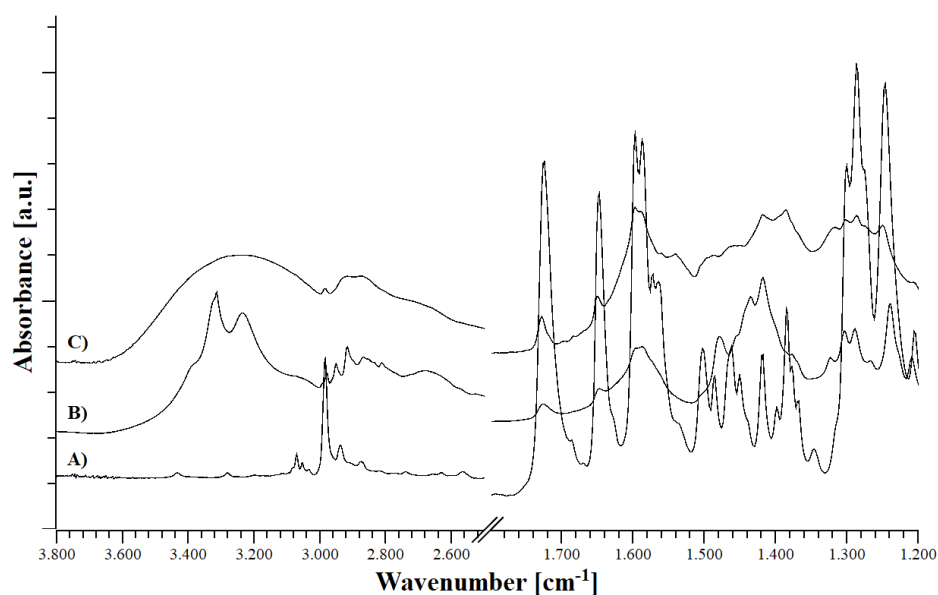
Figure 6.5. FTIR Spectrum of FE (**A**), Meg/NaCMC/FE physical mixture (**B**), Meg/NaCMC/FE extrudate (**C**)

The comparison of the spectra corresponding to the physical mixture, the formulation and the pure API (Figure 6.5) showed a significant peak broadening between the physical mixture and the formulation because of the amorphization, which is also visible in Figure 6.3 and 6.4. This broadening is even more pronounced around 3400 cm^{-1} in the area of the O-H and N-H stretching vibration of the Meg formulation.
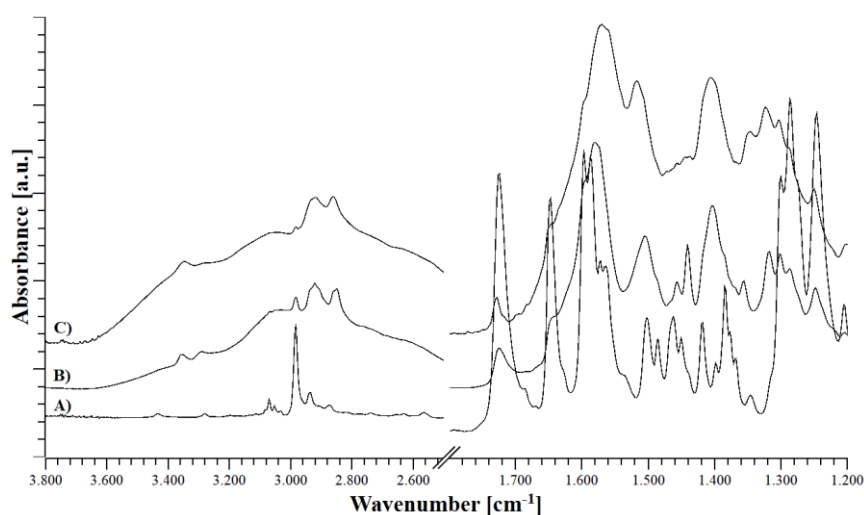
Figure 6.6. FTIR Spectrum of FE (**A**), Lys/NaCMC/FE physical mixture (**B**), Lys/NaCMC/FE extrudate (**C**)

In the formulation of Lys/NaCMC/FE, the amide bands at 1572 and 1509 cm^{-1} were significantly broadened, which almost led to the formation of a combined peak (Figure 6.6). Moreover, the extrusion

resulted in a broadening of the amine-stretching band at 3340 cm^{-1}. In general, the peaks of FE were less visible in the extruded formulation.

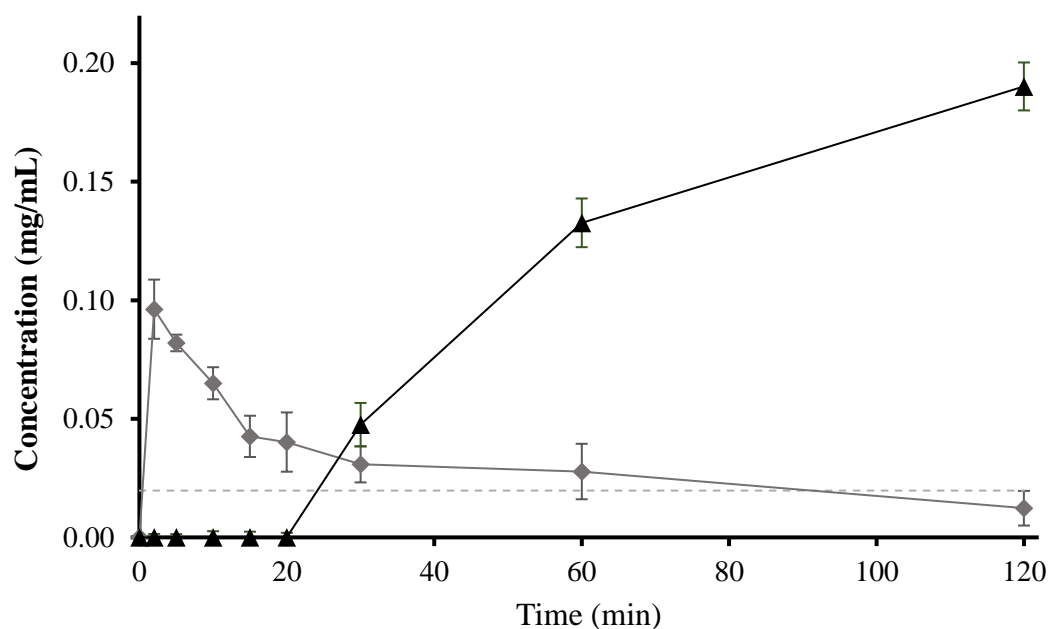### 6.3.3 Biorelevant *in vitro* dissolution study

Figure 6.7. Non-sink dissolution profiles of Lys/NaCMC/FE: physical mixture (gray diamonds), extruded formulation (black triangles). The dotted line represents the solubility of FE.

The measured solubility of FE in Level II FaSSIF was 0.0154 (± 0.0005) mg/mL in agreement with current literature (Figure 6.7) [250,251]. For the physical mixture a short concentration increase can be observed at the beginning of the dissolution experiment, which was followed by a rapid decline to the thermodynamic solubility. The formulation containing Lys had a dissolution profile with a delayed release. After 30 min, the profile showed supersaturated concentrations, which were stable and increasing until 120 min. A rough estimation of the supersaturation shows about 12-fold increase, which is in line with other studies on extruded FE formulations in Level II FaSSIF [252].
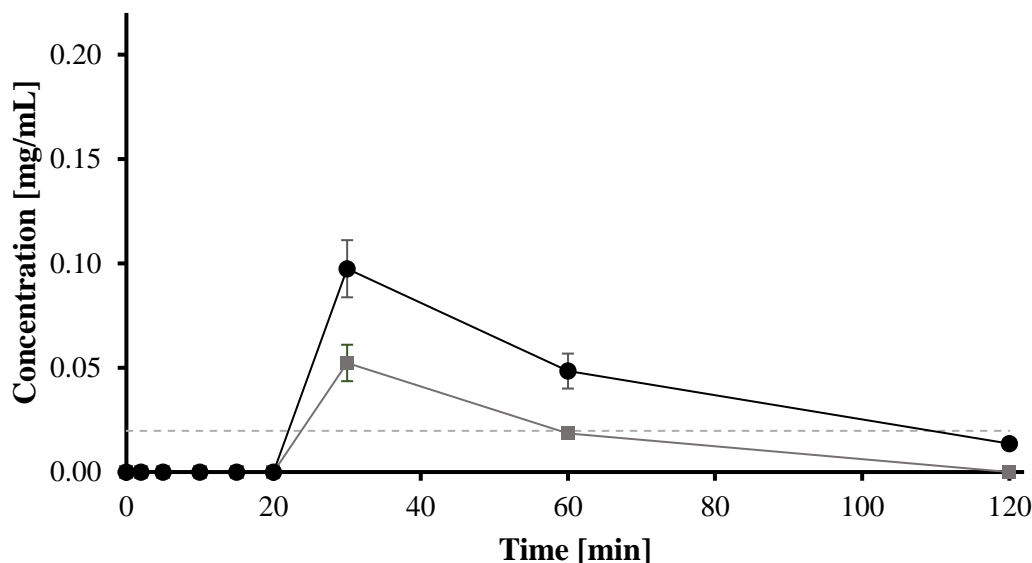
Figure 6.8. Non-sink dissolution profiles of Meg/NaCMC/FE: physical mixture (gray squares), extruded formulation (black spheres). The dotted line represents the solubility of FE.

The release profile of the Meg/NaCMC/FE formulation showed the identical delay in release as with the Lys formulation. Release profiles of both formulations indicated polymer swelling causing a delayed release. In contrast to the dissolution profile of Lys/NaCMC/FE, the supersaturation of Meg/NaCMC/FE is less pronounced. The overall dissolution performance was still improved in comparison to the physical mixture.

Although, the Lys/CMC/FE extrudate presented the slowest release it was the formulation, showing the highest supersaturation and was able stabilize this state over the time of the experiment.

Table 6.1. Viscosity of the formulations and physical mixtures in Level II FaSSIF

Composition		Viscosity $_{2h}$ (mPa s)
Lys, NaCMC, and FE	Formulation	3.08 ± 0.01
	Physical mixture	3.25 ± 0.07
Meg, NaCMC, and FE	Formulation	3.18 ± 0.01
	Physical mixture	2.81 ± 0.03

The dissolution study was complemented by viscosity measurements in Level II FaSSIF at the end of the experiments. These measurements showed an increase of viscosity in all formulations and physical mixtures at the end of the study compared to the pure Leve II FaSSIF with a viscosity of $1.11 \, (\pm 0.04)$ mPa s (Table 6.1). The values among the samples did not vary greatly and highest differences were noted between the physical mixtures of the different systems.

6.3.4 *In vivo* rat study

Drug dissolution and subsequent absorption in the gastrointestinal tract of the rat resulted in high plasma levels for both formulations. The amorphous formulations generally showed faster absorption and higher concentrations than the physical mixtures. A comparison between these reference physical mixtures showed a tendency of the Lys system to provide higher exposure though not statistical significant. There was a pronounced difference between the physical mixture containing Meg and the corresponding amorphous formulation, whereas the comparison between the Lys amorphous formulation and the physical mixture was less distinct (Figure 6.9).
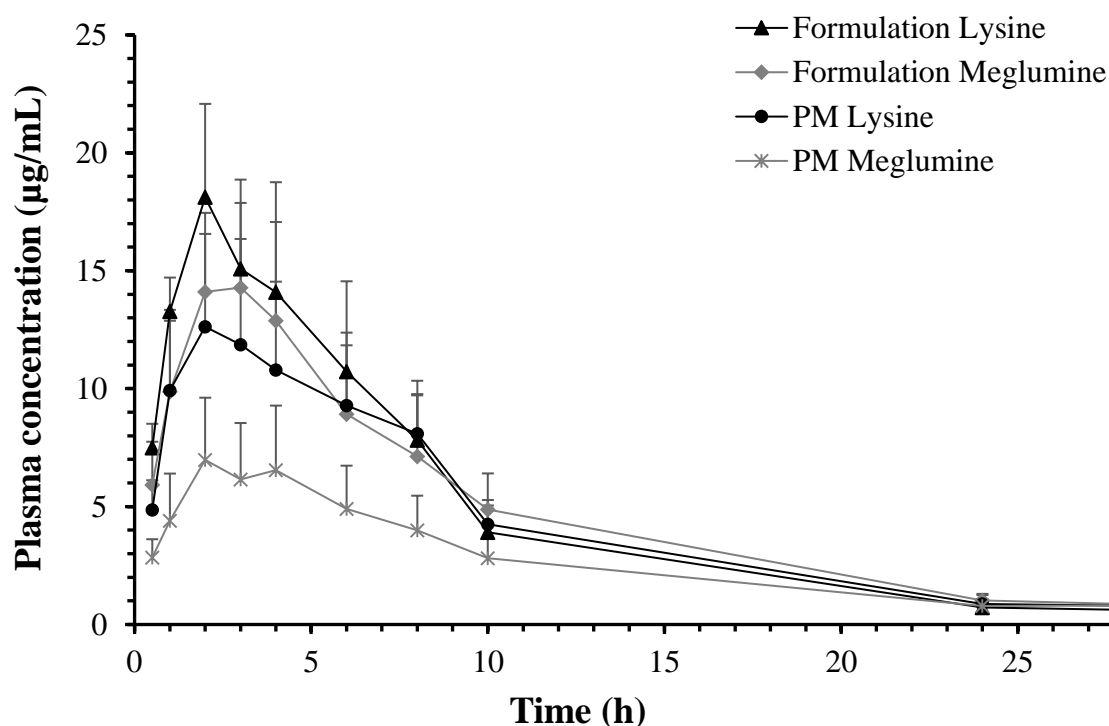

Figure 6.9. Plasma concentration (fenofibric acid) – time profile after oral administration of Lys/NaCMC/FE: physical mixture (black spheres), extruded formulation (black triangles) and Meg/NaCMC/FE: physical mixture (gray crosses), extruded formulation (gray diamonds).

For both formulations, the C_{max} values showed a statistical significant difference between the formulation and the corresponding physical mixture. Even though the AUC_{0-28h} tended to differ, only the Meg formulation showed a significant difference between the formulation and the physical mixture.

Table 6.2. Pharmacokinetic parameters of the rat study for physical mixtures and formulations of FE at 20mg/kg.

Composition		C_{max} (µg/mL)[a]	AUC_{0-28h} (µg*h/mL)[a]
Lys, NaCMC, and FE	Formulation	18.24 ± 3.4 [b]	144.09 ± 36
	Physical mixture	13.25 ± 3.9	129.91 ± 28
Meg, NaCMC, and FE	Formulation [b]	16.30 ± 2.3	140.09 ± 38[b]
	Physical mixture	7.09 ± 2.5	76.61 ± 13

[a] Concentrations as fenofibric acid

[b] Statistically different ($p < 0.05$) compared to the corresponding physical mixture

6.4 Discussion

The polymer selection in the development of a solid dispersion is a key factor for amorphous stability and beneficial drug supersaturation kinetics upon release. Such multiple functionality of an ideal polymer would call for selecting from a broad range of pharmaceutical polymers but there is unfortunately only a limited amount polymers available that are orally acceptable. Consequently, the development of new polymer matrices is needed but as new chemical entities, it would mean substantial work effort with regard to toxicological qualification and regulatory approval [168]. An interesting alternative approach is to target specific molecular interactions of small molecular additives that are already regulatory approved for the administration route with pharmaceutical polymers to obtain modified polymeric matrices [122]. Such an approach bears the potential to customize polymeric matrices, for example regarding stability, a manufacturing process or a release profile.

A recently published article from our research group highlighted the beneficial properties of the two additives, Meg and Lys, on the processability of the polyelectrolyte NaCMC. These additives enabled HME processing of the otherwise high melting/degrading polyelectrolyte, NaCMC, resulting in a homogenous glass [148]. The present research used the drug FE as a model compound to investigate these polyelectrolyte matrices *in vitro* as well as *in vivo* to assess their biopharmaceutical performance.

FE could be incorporated at a concentration of 7.5 % (w/w), which was determined as the stable amorphous drug load in the formulation. At such low drug loadings, the polymer plays an important role in the release in a way that liquid-liquid phase separation and drug enrichment on the polymeric surface would have a low relevance, which otherwise may have a negative impact on the dissolution performance [44]. Therefore, the effects of the modified matrix with its hydration kinetics and molecular interaction with drug were expected to dominate biopharmaceutical performance.

The dissolution curves in the current study highlighted, how different polymeric matrices impact the release and supersaturation behavior of FE. The delayed release in the dissolution curve of the Lys as well as the Meg extrudate may be explained by an increase in viscosity by NaCMC as expected for this polyelectrolyte [252].

Moreover, Lys as a highly water-soluble amino acid with protonated amines in water can form both ionic interactions with NaCMC as well as exhibit a likely pronounced hydrogen bonding with the drug. Meg as co-former would interact via hydrogen bonding with NaCMC and although there is no charge upon aqueous dispersion, there is still the possibility to exhibit some weak hydrogen bonding with FE.

The highly soluble amino acid as co-former led to a modified polyelectrolyte matrix that greatly enhanced the maximum drug supersaturation and could sustain it over a sufficiently long time to alter the effective drug absorption. While the present research had a focus on modification of the polymer matrix, the use of highly soluble amino acids has been suggested before in other co-amorphous systems where the primarily goal was the interaction of drug and co-former to target increased amorphous stability [146].

The existence of different relevant molecular interactions was in agreement with FTIR spectroscopic results of both systems. In particular, the O-H and N-H stretching vibration of Meg were broadened in the extrudate, which could be interpreted as a less defined structure as a result of hydrogen bonding between Meg and the other molecules (Figure 6.5). Meg was proven to be able to form such hydrogen bonds with polymers [209,253]. These findings were in line with the molecular dynamics simulation, which indicated a dense network of hydrogen bonds between the additive and NaCMC. The simplified view obtained from the molecular dynamics simulation also suggested that FE had the possibility to more strongly interact via hydrogen bonding with lysine side chains. It was also visualized that further polar and dispersive interactions may occur in a kind of pocket the polymer matrix was forming around FE (Figure 6.1). Such drug integration in the modified matrix was not observed in the same way in case of the Meg as additive where FE was rather located on the surface (Figure 6.2). Due to the simplified nature of the model, some care is needed to draw firm conclusions but the obtained molecular visualization provides insights into the likely drug interactions occurring in the different polymeric matrices. The qualitative differences may also have translated into different stabilization of supersaturated drug upon aqueous dispersion.

The FTIR pattern of the Lys formulation highlighted the interaction between the additive and NaCMC, in accordance with what was reported for the amino acid and a comparable substance in a previous study [144]. Such a pronounced matrix interaction with a drug (Figure 6.1) may thus result in superior

stabilization in the solid as well as in the solubilized form of the drug (Figure 6.7) [208]. The utility of molecular dynamics simulations and docking has previously been shown to be helpful in the evaluation of solid dispersion formulations and depending on the simulation details, qualitative or even quantitative predictions may be obtained [141]. While the ionic moieties of a polymer are especially important for its swelling in aqueous media, the interactions with a poorly soluble drug are often complex. An example is that even though ionic and polar interactions are more energetic than weaker Van der Waals interactions, the latter can in their summation result in a substantial contribution to how drug attaches to a polymer upon aqueous dispersion [171,183].

The dissolution profile of the Lys/NaCMC/FE formulation in contrast to the physical mixture underlined the stabilization properties of the polyelectrolyte matrix for the supersaturated state of FE. An initial high concentration of the physical mixture may have been caused by some surface amorphization during drug mixing or a direct excipient effect on solubilization. However, concentrations decreased rapidly to the saturation level, which was in contrast to the extruded formulation that was able to stabilize the supersaturated FE concentration over the time of the experiment. As such stabilization of supersaturated drug, another mechanism than the direct interaction within the polyelectrolyte matrix for the stabilization of the supersaturation is the increase in viscosity through NaCMC [254]. This could be a more general effect of a fast swelling polyelectrolyte and the viscosity measurements between the different samples showed barely differences except for slightly lower values for the physical mixture of the system with Meg (Table 6.1). The *in vitro* and the *in vivo* experiments were compatible with the NaCMC viscosity increase that may have led to some lag-time in release as well as it may have affected drug supersaturation. This would be in line with previous experiments investigating the influence of polymeric mixtures on the release [252] and the viscosity increase during aqueous dispersion through NaCMC [255].

In comparison, the amorphous formulations showed higher exposure in the rat study than their corresponding physical mixtures (Figure 6.9). Although the Lys formulation did show an increasing trend in AUC_{0-28h} compared to the physical mixture, this increase was not statistically significant. However, the C_{max} was statistically significantly increased in comparison to the physical mixture (Table 6.2). The comparatively good performance of the crystalline FE in combination with lysine and NaCMC was likely due to specific effects of the polyelectrolyte matrix combined with more general drug solubilization through phospholipids and bile salts [99]. Given these interesting result of the lysine physical mixture, more research should in the future also investigate the biopharmaceutical potential of crystalline formulations with polyelectrolytes and co-formers to enhance oral absorption.

The Meg formulation showed a faster release with a lower degree drug of supersaturation *in vitro* and was able to yield a significantly higher AUC and C_{max} when compared to its physical mixture. As for the *in vivo* comparison, the highest AUC and C_{max} were reported for the Lys formulation, which was in

line with the *in vitro* dissolution experiments. Therefore, the obtained results were encouraging to use a modified polyelectrolyte matrix for the solubility and bioavailability enhancement of poorly water-soluble drugs.

6.5 Conclusion

Amorphous formulations have become a key method to increase absorption of poorly water-soluble drugs. A limitation is here the selection of polymer because it has to fulfill different functionalities in the manufacturing of the formulation, for stability on the shelf as well regarding biopharmaceutical performance. This was addressed by the concept of modified polymeric matrices and the present study showed that addition of Lys and Meg enabled the amorphous formulation of FE in a new NaCMC polyelectrolyte matrix. The *in vitro* and *in vivo* results suggested advantages of the amorphous formulations compared to the physical mixture references. The amorphous formulations had significantly higher C_{max} values than their corresponding physical mixtures, which was in line with the dissolution experiments. This study presents the first animal study of the previously developed polyelectrolyte matrices [148]. The promising results show the potential of polyelectrolytes to enable supersaturating oral drug delivery. Future research on ASDs containing polyelectrolytes as a modified matrix for HME is needed to further investigate the specific advantages for a broad range of poorly water-soluble drugs.

Final remarks and outlook

In modern pharmaceutical development, poor aqueous solubility poses a major problem for numerous compounds in the pipeline as well as those on the market. Amorphous systems are an important part of overcoming such limitations. With an increasing number of newly developed drug candidates which exhibit low solubility and therefore present a problem for oral administration, approaches to increase the before mentioned solubility are of great interest. As discussed in this work, the formulation of a drug in its amorphous form does not present a "one-size-fits-all" solution to the problem since preparation and stabilization come with great difficulties. For an application of a newly developed drug product, pharmaceutical companies have to guarantee stability of the amorphous form at various stability settings defined by the regulatory agencies. In case the drug recrystallizes during the stability study, the biopharmaceutical performance would be affected, which may lead to insufficient drug exposure upon oral drug delivery and consequently insufficient therapeutic efficacy. As a result of the previously described risks, such a formulation approach is only applied if conventional formulation techniques fail to yield sufficient drug release and a bio-enabling formulation is needed.

At the start of the formulation development of an ASD, a combination of different excipients has to be assessed with regards to stabilization of the amorphous form. The most important compound in the formulation besides the drug is the polymer, which should not only stabilize the amorphous form of the API in the solid but also has a role in facilitating the manufacturing and should further enable and stabilize supersaturated drug following oral administration. Different concepts reaching from miniaturized assays to theoretical thermodynamic calculations can be applied in an excipient screening setup. As highlighted in the sections above, such concepts in combination with the careful selection of the manufacturing technique play an important role. Based on the multifunctional requirements of polymers in ASDs, this thesis presented the concept of modified polymer matrices for amorphous systems to broaden capabilities of formulators to formulate poorly water-soluble drugs. This work had a focus on HME even though it was not exclusive in that also solvent-based processes were part of the research.

The present work investigated the potential of small molecular interacting additives to specifically interact with the polymer and to improve formulation characteristics such as processability, amorphous stability, and drug release.

The studies described in Section 3, 4, and 6 supported the view that a molecularly oriented selection of an additive was crucial for successful formulation. During such a selection, certain properties of the

additive have to be considered starting with thermal properties like T_m and T_g, going on with functional groups for a possible molecular interaction, and ending with aqueous solubility. While these properties as well as miscibility and other structural consideration can be done during the theoretical assessment of the formulation design, this work has shown that practical trials with a preselected set of additives are still necessary, because even slight differences in structure between the molecules can have great influence on the interaction and therefore on the feasibility and performance of the formulation. In case differences cannot be detected between the selected additives, a more discriminative method has to be chosen. Such methods could be more demanding stability settings or more sensitive analytical methods like a synchrotron measurement as described in Section 4. Approaches like the SPADS screening (Section 2.2.3) are important improvements towards a more rational selection of excipients rather than an approach based on trial and error or restriction to commonly used compounds. It would also be possible to apply such a structured technique for the selection of an additive with a targeted molecular interaction. Theoretically, such an approach could start with the selection of a set of additives based on possible interactions and physico-chemical properties, which need to be tailored to the selected manufacturing technique. After the selection of specific additives, they have to be evaluated with the polymer selected in a miniaturized amorphization process, which should be closely related to the final manufacturing technique. In this experimental step, the type and amount of necessary additive should be identified.

Afterwards, small-scale manufacturing trials can be conducted, which include a drug-free formulation of the additive and the polymer. As seen in Section 4, the feasible amount of an additive might have to be balanced between suitability for the manufacturing process and with respect to the formation of a homogenous and stable glass. If the drug-free trials show sufficient manufacturability and glass formation of the polymeric matrix, it can be combined with the drug in a next step. The vision of the current research is that a broad range of such modified matrices should become available to formulators so that a broader choice is available to incorporate a drug candidate with its specific properties.

The trials in formulation development with the drug in the polymeric matrix have to be evaluated again with regards to amorphous stability. This evaluation should be done under controlled stability settings for example as described in ICH Q1 and if necessary with the most discriminative method to spot even minor differences between the formulations. When a stable formulation is found, the interactions within the formulation can be determined. As the most important factor at the end of the technical evaluation, biorelevant dissolution experiments have to be performed to prepare for possible *in vivo* studies.

After the successful development of a modified polymeric matrix, another aspect of such systems in the formulation development is the superiority over not only common formulation approaches but also over other conventional ASDs. For such a comparison the aspects described in Section 3,4,5, and 6 have to

be combined, which means a comparable ICH Q1 stability (Section 3,4 and 5), screening for interaction in the formulation (Section 3 and 4), and complete biopharmaceutical evaluation including first *in vivo* animal trials (Section 6).

As first step, an ASD comparison was made of HME with the modern and heavily investigated formulation technique of drug incorporation in mesoporous silica. This work highlighted that even after optimization of amorphous formulations for a given process technique, the individual drug properties may favor one particular approach. This work highlighted that a combination of mesoporous silica with a precipitation inhibiting polymer would be especially suited for drugs that are difficult to stabilize in amorphous form.

In light of the early stage research on modified matrices, one has to admit that currently, a fully structured development is still missing. Since even small changes in the additive selection may have a great impact on the formulation performance, the selection pool of new matrices should be as big as possible and should include a thorough evaluation of oral acceptability and regulatory restrictions.

These development considerations are not just exclusively true for modified polymeric matrices so also conventional ASDs have to present clear benefits in comparison to normal solid dosage forms like for example tablets obtain from direct compression. This is the reason why the formulation of a drug as ASD is currently only considered when other formulation approaches fail because of insufficient release behavior and *in vivo* performance.

The research presented in this work demonstrated clear benefits of focusing on targeted molecular interactions within the formulation between the polymer and an additive for ASDs. . In this way, different modified polymeric matrices were developed to investigate the improvement of polymer matrix properties and later on the stabilization of the drug in its amorphous and/or supersaturated state. On a small-scale amorphization technique, the polymeric matrices demonstrated promising results regarding amorphous stability, *in vitro* release and *in vivo* exposure of selected model systems. Future research would have to show how broadly the novel approach can be applied in formulation development and it will be interesting to see how the research findings are transferred to industrial pharmaceutical practice.

Bibliography

1. Amidon, G. L.; Lennernäs, H.; Shah, V. P.; Crison, J. R. A theoretical basis for a biopharmaceutic drug classification: the correlation of in vitro drug product dissolution and in vivo bioavailability. *Pharm. Res.* **1995**, *12*, 413–20.

2. Butler, J. M.; Dressman, J. B. The Developability Classification System: Application of Biopharmaceutics Concepts to Formulation Development. *J. Pharm. Sci.* **2010**, *99*, 4940–4954, doi:10.1002/jps.22217.

3. Kuentz, M.; Imanidis, G. In silico prediction of the solubility advantage for amorphous drugs – Are there property-based rules for drug discovery and early pharmaceutical development? *Eur. J. Pharm. Sci.* **2013**, *48*, 554–562, doi:10.1016/j.ejps.2012.11.015.

4. Rosenberger, J.; Butler, J.; Dressman, J. A Refined Developability Classification System. *J. Pharm. Sci.* **2018**, *107*, 2020–2032, doi:10.1016/j.xphs.2018.03.030.

5. Bergström, C. A. S.; Wassvik, C. M.; Johansson, K.; Hubatsch, I. Poorly soluble marketed drugs display solvation limited solubility. *J. Med. Chem.* **2007**, *50*, 5858–5862, doi:10.1021/jm0706416.

6. Wassvik, C. M.; Holmén, A. G.; Bergström, C. A. S.; Zamora, I.; Artursson, P. Contribution of solid-state properties to the aqueous solubility of drugs. *Eur. J. Pharm. Sci.* **2006**, *29*, 294–305, doi:10.1016/j.ejps.2006.05.013.

7. Van den Mooter, G. The use of amorphous solid dispersions: A formulation strategy to overcome poor solubility and dissolution rate. *Drug Discov. Today Technol.* **2012**, *9*, e79–e85, doi:10.1016/j.ddtec.2011.10.002.

8. Jain, N.; Yalkowsky, S. H. Estimation of the aqueous solubility I: Application to organic nonelectrolytes. *J. Pharm. Sci.* **2001**, *90*, 234–252, doi:10.1002/1520-6017(200102)90:2<234::AID-JPS14>3.0.CO;2-V.

9. Wassvik, C. M.; Holmén, A. G.; Draheim, R.; Artursson, P.; Bergström, C. A. S. Molecular Characteristics for Solid-State Limited Solubility. *J. Med. Chem.* **2008**, *51*, 3035–3039, doi:10.1021/jm701587d.

10. Abraham, M. H.; Grellier, P. L.; Mcgill, R. A. Determination of Olive Oil-Gas and Hexadecane-Gas Partition Coefficients, and Calculation of the Corresponding Olive Oil-Water and Hexadecane-Water Partition Coefficients. *J. CHEM. SOC. PERKIN TRANS* **1987**, *11*.

11. Abraham, M. H.; Le, J. The correlation and prediction of the solubility of compounds in water using an amended solvation energy relationship. *J. Pharm. Sci.* **1999**, *88*, 868–880, doi:10.1021/js9901007.

12.   Bergström, C. A. S.; Wassvik, C. M.; Johansson, K.; Hubatsch, I. Poorly Soluble Marketed Drugs Display Solvation Limited Solubility. *J. Med. Chem.* **2007**, *50*, 5858–5862, doi:10.1021/jm0706416.

13.   Edueng, K.; Mahlin, D.; Bergström, C. A. S. The Need for Restructuring the Disordered Science of Amorphous Drug Formulations. *Pharm. Res.* **2017**, *34*, 1754–1772, doi:10.1007/s11095-017-2174-7.

14.   Niederquell, A.; Kuentz, M. Biorelevant drug solubility enhancement modeled by a linear solvation energy relationship. *J. Pharm. Sci.* **2017**, *107*, 503–506.

15.   Lipinski, C. A.; Lombardo, F.; Dominy, B. W.; Feeney, P. J. Experimental and computational approaches to estimate solubility and permeability in drug discovery and development. *Adv. Drug Deliv. Rev.* **2001**, *46*, 3–26.

16.   Porter, C. J. H.; Trevaskis, N. L.; Charman, W. N. Lipids and lipid-based formulations: optimizing the oral delivery of lipophilic drugs. *Nat. Rev. Drug Discov.* **2007**, *6*, 231–248, doi:10.1038/nrd2197.

17.   Mu, H.; Holm, R.; Müllertz, A. Lipid-based formulations for oral administration of poorly water-soluble drugs. *Int. J. Pharm.* **2013**, *453*, 215–224, doi:10.1016/j.ijpharm.2013.03.054.

18.   Feeney, O. M.; Crum, M. F.; McEvoy, C. L.; Trevaskis, N. L.; Williams, H. D.; Pouton, C. W.; Charman, W. N.; Bergström, C. A. S.; Porter, C. J. H. 50years of oral lipid-based formulations: Provenance, progress and future perspectives. *Adv. Drug Deliv. Rev.* **2016**, *101*, 167–194, doi:10.1016/j.addr.2016.04.007.

19.   Savla, R.; Browne, J.; Plassat, V.; Wasan, K. M.; Wasan, E. K. Review and analysis of FDA approved drugs using lipid-based formulations. *Drug Dev. Ind. Pharm.* **2017**, *0*, 1–16, doi:10.1080/03639045.2017.1342654.

20.   Feeney, O. M.; Crum, M. F.; McEvoy, C. L.; Trevaskis, N. L.; Williams, H. D.; Pouton, C. W.; Charman, W. N.; Bergström, C. A. S.; Porter, C. J. H. 50 years of oral lipid-based formulations: Provenance, progress and future perspectives. *Adv. Drug Deliv. Rev.* **2016**, *101*, 167–194, doi:10.1016/j.addr.2016.04.007.

21.   Savla, R.; Browne, J.; Plassat, V.; Wasan, K. M.; Wasan, E. K. Review and analysis of FDA approved drugs using lipid-based formulations. *Drug Dev. Ind. Pharm.* **2017**, *43*, 1–16, doi:10.1080/03639045.2017.1342654.

22.   Fong, S. Y. K.; Ibisogly, A.; Bauer-Brandl, A. Solubility enhancement of BCS Class II drug by solid phospholipid dispersions: Spray drying versus freeze-drying. *Int. J. Pharm.* **2015**, *496*, 382–391, doi:10.1016/j.ijpharm.2015.10.029.

23.   Kossena, G. A.; Charman, W. N.; Wilson, C. G.; O'Mahony, B.; Lindsay, B.; Hempenstall, J. M.; Davison, C. L.; Crowley, P. J.; Porter, C. J. H. Low Dose Lipid Formulations: Effects on Gastric Emptying and Biliary Secretion. *Pharm. Res.* **2007**, *24*, 2084–2096, doi:10.1007/s11095-007-9363-8.

24.   Anby, M. U.; Williams, H. D.; McIntosh, M.; Benameur, H.; Edwards, G. A.; Pouton, C. W.;
       Porter, C. J. H. Lipid Digestion as a Trigger for Supersaturation: Evaluation of the Impact of
       Supersaturation Stabilization on the in Vitro and in Vivo Performance of Self-Emulsifying
       Drug Delivery Systems. *Mol. Pharm.* **2012**, *9*, 2063–2079, doi:10.1021/mp300164u.

25.   Bibi, H. A.; Holm, R.; Bauer-Brandl, A. Simultaneous lipolysis/permeation in vitro model, for
       the estimation of bioavailability of lipid based drug delivery systems. *Eur. J. Pharm.*
       Biopharm. **2017**, *117*, 300–307, doi:10.1016/j.ejpb.2017.05.001.

26.   Van Eerdenbrugh, B.; Van den Mooter, G.; Augustijns, P. Top-down production of drug
       nanocrystals: Nanosuspension stabilization, miniaturization and transformation into solid
       products. *Int. J. Pharm.* **2008**, *364*, 64–75, doi:10.1016/j.ijpharm.2008.07.023.

27.   Rabinow, B. E. Nanosuspensions in drug delivery. *Nat. Rev. Drug Discov.* **2004**, *3*, 785–796,
       doi:10.1038/nrd1494.

28.   Szejtli, J. *Cyclodextrin Technology*; Topics in Inclusion Science; Springer Netherlands:
       Dordrecht, 1988; Vol. 1; ISBN 978-90-481-8427-9.

29.   Szejtli, J. Chemistry, physical and biological properties of cyclodextrins. In *Cyclodextrines*;
       Szejtli, J., Osa, T., Eds.; Elsevier Science Ltd., 1996; pp. 189–204.

30.   Davis, M. E.; Brewster, M. E. Cyclodextrin-based pharmaceutics: past, present and future. *Nat.*
       Rev. Drug Discov. **2004**, *3*, 1023–1035, doi:10.1038/nrd1576.

31.   Goldberg, A. H.; Gibaldi, M.; Kanig, J. L. Increasing Dissolution Rates and Gastrointestinal
       Absorption of Drugs via solid Solutions and Eutectic mixtures II. *J. Pharm. Sci.* **1966**, *55*, 482–
       487, doi:10.1002/jps.2600550507.

32.   Chiou, W. L.; Riegelman, S. Preparation and dissolution characteristics of several fast-release
       solid dispersions of griseofulvin. *J. Pharm. Sci.* **1969**, doi:10.1002/jps.2600581218.

33.   Chiou, W. L.; Riegelman, S. Pharmaceutical Applications of Solid Dispersion Systems. *J.*
       Pharm. Sci. **1971**, *60*, 1281–1302, doi:10.1002/jps.2600600902.

34.   Mahlin, D.; Bergström, C. A. S. Early drug development predictions of glass-forming ability
       and physical stability of drugs. *Eur. J. Pharm. Sci.* **2013**, *49*, 323–332,
       doi:10.1016/j.ejps.2013.03.016.

35.   Ditzinger, F.; Price, D. J.; Ilie, A.-R.; Köhl, N. J.; Jankovic, S.; Tsakiridou, G.; Aleandri, S.;
       Kalantzi, L.; Holm, R.; Nair, A.; Saal, C.; Griffin, B.; Kuentz, M. Lipophilicity and
       hydrophobicity considerations in bio-enabling oral formulations approaches - a PEARRL
       review. *J. Pharm. Pharmacol.* **2019**, *71*, 464–482, doi:10.1111/jphp.12984.

36.   Baird, J. A.; Van Eerdenbrugh, B.; Taylor, L. S. A Classification System to Assess the
       Crystallization Tendency of Organic Molecules from Undercooled Melts. *J. Pharm. Sci.* **2010**,
       99, 3787–3806, doi:10.1002/jps.22197.

37.   Wyttenbach, N.; Kirchmeyer, W.; Alsenz, J.; Kuentz, M. Theoretical Considerations of the
       Prigogine–Defay Ratio with Regard to the Glass-Forming Ability of Drugs from Undercooled

Melts. *Mol. Pharm.* **2016**, *13*, 241–250, doi:10.1021/acs.molpharmaceut.5b00688.

38. Alhalaweh, A.; Alzghoul, A.; Mahlin, D.; Bergström, C. A. S. Physical stability of drugs after storage above and below the glass transition temperature: Relationship to glass-forming ability. *Int. J. Pharm.* **2015**, *495*, 312–317, doi:10.1016/j.ijpharm.2015.08.101.

39. Blaabjerg, L. I.; Bulduk, B.; Lindenberg, E.; Löbmann, K.; Rades, T.; Grohganz, H. Influence of glass forming ability on the physical stability of supersaturated amorphous solid dispersions. *J. Pharm. Sci.* **2019**, *108*, 2561–2569, doi:10.1016/j.xphs.2019.02.028.

40. Löbmann, K.; Grohganz, H.; Laitinen, R.; Strachan, C.; Rades, T. Amino acids as co-amorphous stabilizers for poorly water soluble drugs – Part 1: Preparation, stability and dissolution enhancement. *Eur. J. Pharm. Biopharm.* **2013**, *85*, 873–881, doi:10.1016/j.ejpb.2013.03.014.

41. Wyttenbach, N.; Kuentz, M. Glass-forming ability of compounds in marketed amorphous drug products. *Eur. J. Pharm. Biopharm.* **2017**, *112*, 204–208, doi:10.1016/j.ejpb.2016.11.031.

42. Rumondor, A. C. F.; Stanford, L. A.; Taylor, L. S. Effects of Polymer Type and Storage Relative Humidity on the Kinetics of Felodipine Crystallization from Amorphous Solid Dispersions. *Pharm. Res.* **2009**, *26*, 2599–2606, doi:10.1007/s11095-009-9974-3.

43. Indulkar, A. S.; Lou, X.; Zhang, G. G. Z.; Taylor, L. S. Insights into the Dissolution Mechanism of Ritonavir–Copovidone Amorphous Solid Dispersions: Importance of Congruent Release for Enhanced Performance. *Mol. Pharm.* **2019**, *16*, 1327–1339, doi:10.1021/acs.molpharmaceut.8b01261.

44. Saboo, S.; Mugheirbi, N. A.; Zemlyanov, D. Y.; Kestur, U. S.; Taylor, L. S. Congruent release of drug and polymer: A "sweet spot" in the dissolution of amorphous solid dispersions. *J. Control. Release* **2019**, *298*, 68–82, doi:10.1016/j.jconrel.2019.01.039.

45. Leuner, C.; Dressman, J. Improving drug solubility for oral delivery using solid dispersions. *Eur. J. Pharm. Biopharm.* **2000**, *50*, 47–60, doi:10.1016/S0939-6411(00)00076-X.

46. Vo, C. L.-N.; Park, C.; Lee, B.-J. Current trends and future perspectives of solid dispersions containing poorly water-soluble drugs. *Eur. J. Pharm. Biopharm.* **2013**, *85*, 799–813, doi:10.1016/j.ejpb.2013.09.007.

47. Chen, Y.; Wang, S.; Wang, S.; Liu, C.; Su, C.; Hageman, M.; Hussain, M.; Haskell, R.; Stefanski, K.; Qian, F. Initial Drug Dissolution from Amorphous Solid Dispersions Controlled by Polymer Dissolution and Drug-Polymer Interaction. *Pharm. Res.* **2016**, *33*, 2445–58, doi:10.1007/s11095-016-1969-2.

48. Newman, A.; Knipp, G.; Zografi, G. Assessing the performance of amorphous solid dispersions. *J. Pharm. Sci.* **2012**, *101*, 1355–1377, doi:10.1002/jps.23031.

49. Klug, H. P.; Alexander, L. E. *X-ray diffraction procedures for polycrystalline and amorphous materials*; John Wiley & Sons, 1974; ISBN 0471493694.

50. Kittel, C. Introduction to Solid State Physics, 8th edition. *Wiley Sons, New York, NY* **2004**.

51.   Bellantone, R. A. Fundamentals of Amorphous Systems: Thermodynamic Aspects. In *Amorphous Solid Dispersions*; Springer New York: New York, 2014; pp. 3–34.

52.   Gavezzotti, A. *Molecular Aggregation: Structure analysis and molecular simulation of crystals and liquids*; Oxford University Press: New York, 2006; ISBN 9780191718779.

53.   Hancock, B. C.; Shamblin, S. L. Molecular mobility of amorphous pharmaceuticals determined using differential scanning calorimetry. *Thermochim. Acta* **2001**, *380*, 95–107, doi:10.1016/S0040-6031(01)00663-3.

54.   Gupta, P.; Chawla, G.; Bansal, A. K. Physical Stability and Solubility Advantage from Amorphous Celecoxib: The Role of Thermodynamic Quantities and Molecular Mobility. *Mol. Pharm.* **2004**, *1*, 406–413, doi:10.1021/mp049938f.

55.   Hancock, B. C.; Parks, M. What is the True Solubility Advantage for Amorphous Pharmaceuticals? *Pharm. Res.* **2000**, *17*, 397–404, doi:10.1023/A:1007516718048.

56.   Mullin, J. W. *Crystallization*; 4th Editio.; Butterworth-Heinemann: Oxford, United Kingdom, 2001; ISBN 9780750648332.

57.   Ostwald, W. Studien über die Bildung und Umwandlung fester Körper. *Zeitschrift für Phys. Chemie* **1897**, *22U*, doi:10.1515/zpch-1897-2233.

58.   Schmelzer, J. W. P.; Gutzow, I. S.; Mazurin, O. V.; Priven, A. I.; Todorova, S. V.; Petroff, B. P. *Glasses and the Glass Transition*; Wiley-VCH Verlag GmbH & Co. KGaA: Weinheim, Germany, 2011; ISBN 9783527636532.

59.   Floudas, G.; Paluch, M.; Grzybowski, A.; Ngai, K. *Molecular Dynamics of Glass-Forming Systems*; Advances in Dielectrics; Springer Berlin Heidelberg: Berlin, Heidelberg, 2011; Vol. 1; ISBN 978-3-642-04901-9.

60.   Kawakami, K. Crystallization Tendency of Pharmaceutical Glasses: Relevance to Compound Properties, Impact of Formulation Process, and Implications for Design of Amorphous Solid Dispersions. *Pharmaceutics* **2019**, *11*, 202, doi:10.3390/pharmaceutics11050202.

61.   Tammann, G. *Der Glaszustand*; Leopold Voss Verlag: Leipzig, 1933;

62.   Kissi, E. O.; Grohganz, H.; Löbmann, K.; Ruggiero, M. T.; Zeitler, J. A.; Rades, T. Glass-Transition Temperature of the β-Relaxation as the Major Predictive Parameter for Recrystallization of Neat Amorphous Drugs. *J. Phys. Chem. B* **2018**, *122*, 2803–2808, doi:10.1021/acs.jpcb.7b10105.

63.   Paluch, M.; Roland, C. M.; Pawlus, S.; Zioło, J.; Ngai, K. L. Does the Arrhenius Temperature Dependence of the Johari-Goldstein Relaxation Persist above Tg? *Phys. Rev. Lett.* **2003**, *91*, 115701, doi:10.1103/PhysRevLett.91.115701.

64.   Brás, A. R.; Fonseca, I. M.; Dionísio, M.; Schönhals, A.; Affouard, F.; Correia, N. T. Influence of Nanoscale Confinement on the Molecular Mobility of Ibuprofen. *J. Phys. Chem. C* **2014**, *118*, 13857–13868, doi:10.1021/jp500630m.

65.   Mehta, M.; Kothari, K.; Ragoonanan, V.; Suryanarayanan, R. Effect of Water on Molecular

Mobility and Physical Stability of Amorphous Pharmaceuticals. *Mol. Pharm.* **2016**, *13*, 1339–1346, doi:10.1021/acs.molpharmaceut.5b00950.

66.   Bhattacharya, S.; Suryanarayanan, R. Local Mobility in Amorphous Pharmaceuticals—Characterization and Implications on Stability. *J. Pharm. Sci.* **2009**, *98*, 2935–2953, doi:10.1002/jps.21728.

67.   Zhu, D. (Alan); Zografi, G.; Gao, P.; Gong, Y.; Zhang, G. G. Z. Modeling Physical Stability of Amorphous Solids Based on Temperature and Moisture Stresses. *J. Pharm. Sci.* **2016**, *105*, 2932–2939, doi:10.1016/j.xphs.2016.03.029.

68.   Korhonen, O.; Bhugra, C.; Pikal, M. J. Correlation Between Molecular Mobility and Crystal Growth of Amorphous Phenobarbital and Phenobarbital with Polyvinylpyrrolidone and L-proline. *J. Pharm. Sci.* **2008**, *97*, 3830–3841, doi:10.1002/jps.21273.

69.   Newman, A.; Zografi, G. Commentary: Considerations in the Measurement of Glass Transition Temperatures of Pharmaceutical Amorphous Solids. *AAPS PharmSciTech* **2020**, *21*, 26, doi:10.1208/s12249-019-1562-1.

70.   Avramov, I.; Zanotto, E. D.; Prado, M. O. Glass-forming ability versus stability of silicate glasses. II. Theoretical demonstration. *J. Non. Cryst. Solids* **2003**, *320*, 9–20, doi:10.1016/S0022-3093(03)00081-4.

71.   Gutzow, I. S.; Schmelzer, J. W. P. Basic Properties and the Nature of Glasses: An Overview. In *Glasses and the Glass Transition*; Wiley-VCH Verlag GmbH & Co. KGaA: Weinheim, Germany, 2011; pp. 9–89.

72.   Blaabjerg, L. I.; Lindenberg, E.; Löbmann, K.; Grohganz, H.; Rades, T. Glass Forming Ability of Amorphous Drugs Investigated by Continuous Cooling and Isothermal Transformation. *Mol. Pharm.* **2016**, *13*, 3318–3325, doi:10.1021/acs.molpharmaceut.6b00650.

73.   Edueng; Bergström; Gråsjö; Mahlin Long-Term Physical (In)Stability of Spray-Dried Amorphous Drugs: Relationship with Glass-Forming Ability and Physicochemical Properties. *Pharmaceutics* **2019**, *11*, 425, doi:10.3390/pharmaceutics11090425.

74.   Panini, P.; Rampazzo, M.; Singh, A.; Vanhoutte, F.; Van den Mooter, G. Myth or Truth: The Glass Forming Ability Class III Drugs Will Always Form Single-Phase Homogenous Amorphous Solid Dispersion Formulations. *Pharmaceutics* **2019**, *11*, 529, doi:10.3390/pharmaceutics11100529.

75.   Patterson, J. E.; James, M. B.; Forster, A. H.; Lancaster, R. W.; Butler, J. M.; Rades, T. Preparation of glass solutions of three poorly water soluble drugs by spray drying, melt extrusion and ball milling. *Int. J. Pharm.* **2007**, *336*, 22–34, doi:10.1016/j.ijpharm.2006.11.030.

76.   Meng, F.; Gala, U.; Chauhan, H. Classification of solid dispersions: correlation to (i) stability and solubility (ii) preparation and characterization techniques. *Drug Dev. Ind. Pharm.* **2015**, *41*, 1401–1415, doi:10.3109/03639045.2015.1018274.

77.   Gurunath, S.; Pradeep Kumar, S.; Basavaraj, N. K.; Patil, P. A. Amorphous solid dispersion

method for improving oral bioavailability of poorly water-soluble drugs. *J. Pharm. Res.* **2013**, *6*, 476–480, doi:10.1016/j.jopr.2013.04.008.

78.   Sekiguchi, K.; Obi, N. Studies on Absorption of Eutectic Mixture. I. A Comparison of the Behavior of Eutectic Mixture of Sulfathiazole and that of Ordinary Sulfathiazole in Man. *Chem. Pharm. Bull. (Tokyo).* **1961**, *9*, 866–872, doi:10.1248/cpb.9.866.

79.   Repka, M. A.; Bandari, S.; Kallakunta, V. R.; Vo, A. Q.; McFall, H.; Pimparade, M. B.; Bhagurkar, A. M. Melt extrusion with poorly soluble drugs – An integrated review. *Int. J. Pharm.* **2018**, *535*, 68–85, doi:10.1016/j.ijpharm.2017.10.056.

80.   Paudel, A.; Worku, Z. A.; Meeus, J.; Guns, S.; Van den Mooter, G. Manufacturing of solid dispersions of poorly water soluble drugs by spray drying: Formulation and process considerations. *Int. J. Pharm.* **2013**, *453*, 253–284, doi:10.1016/j.ijpharm.2012.07.015.

81.   Shah, N.; Iyer, R. M.; Mair, H.-J.; Choi, D.; Tian, H.; Diodone, R.; Fahnrich, K.; Pabst-Ravot, A.; Tang, K.; Scheubel, E.; Grippo, J. F.; Moreira, S. A.; Go, Z.; Mouskountakis, J.; Louie, T.; Ibrahim, P. N.; Sandhu, H.; Rubia, L.; Chokshi, H.; Singhal, D.; Malick, W. Improved Human Bioavailability of Vemurafenib, a Practically Insoluble Drug, Using an Amorphous Polymer-Stabilized Solid Dispersion Prepared by a Solvent-Controlled Coprecipitation Process. *J. Pharm. Sci.* **2013**, *102*, 967–981, doi:10.1002/jps.23425.

82.   Shah, N.; Sandhu, H.; Phuapradit, W.; Pinal, R.; Iyer, R.; Albano, A.; Chatterji, A.; Anand, S.; Choi, D. S.; Tang, K.; Tian, H.; Chokshi, H.; Singhal, D.; Malick, W. Development of novel microprecipitated bulk powder (MBP) technology for manufacturing stable amorphous formulations of poorly soluble drugs. *Int. J. Pharm.* **2012**, *438*, 53–60, doi:10.1016/j.ijpharm.2012.08.031.

83.   Gerstein, B.; Dybowski, C. *Transient Techniques in NMR of Solids: An Introduction to Theory and Practice*; Academic Press: Cambridge, United States, 1985;

84.   Slichter, C. P. *Principles of Magnetic Resonance*; Springer Series in Solid-State Sciences; Springer Berlin Heidelberg: Berlin, Heidelberg, 1990; Vol. 1; ISBN 978-3-642-08069-2.

85.   Jenkins, R.; Snyder, R. L. *Introduction to X-ray Powder Diffractometry*; Wiley: New York, 1996;

86.   Bragg, W. L. Diffraction of Short Electromagnetic Waves by a Crystal. *Proc. Camb. Philol. Soc.* **1913**, *17*, 43–57.

87.   Lin, A. A.; Kwei, T. K.; Reiser, A. On the physical meaning of the Kwei equation for the glass transition temperature of polymer blends. *Macromolecules* **1989**, *22*, 4112–4119, doi:10.1021/ma00200a052.

88.   Paudel, A.; Meeus, J.; Mooter, G. Van den Structural Characterization of Amorphous Solid Dispersions. In *Amorphous solid dispersions*; Springer New York: New York, 2014; pp. 421–485.

89.   Tumuluri, V. S.; Kemper, M. S.; Lewis, I. R.; Prodduturi, S.; Majumdar, S.; Avery, B. A.;

Repka, M. A. Off-line and on-line measurements of drug-loaded hot-melt extruded films using Raman spectroscopy. *Int. J. Pharm.* **2008**, *357*, 77–84, doi:10.1016/j.ijpharm.2008.01.036.

90. Arnold, Y. E.; Imanidis, G.; Kuentz, M. T. Advancing in-vitro drug precipitation testing: new process monitoring tools and a kinetic nucleation and growth model. *J. Pharm. Pharmacol.* **2011**, *63*, 333–341, doi:10.1111/j.2042-7158.2010.01228.x.

91. Newman, A.; Reutzel-Edens, S. M.; Zografi, G. Coamorphous Active Pharmaceutical Ingredient–Small Molecule Mixtures: Considerations in the Choice of Coformers for Enhancing Dissolution and Oral Bioavailability. *J. Pharm. Sci.* **2018**, *107*, 5–17, doi:10.1016/j.xphs.2017.09.024.

92. Adler, C.; Teleki, A.; Kuentz, M. Multifractal Characterization of Pharmaceutical Hot-Melt Extrudates. *Pharm. Res.* **2017**, *34*, 321–332, doi:10.1007/s11095-016-2064-4.

93. Adler, C.; Schönenberger, M.; Teleki, A.; Kuentz, M. Molecularly designed lipid microdomains for solid dispersions using a polymer/inorganic carrier matrix produced by hot-melt extrusion. *Int. J. Pharm.* **2016**, *499*, 90–100, doi:10.1016/j.ijpharm.2015.12.057.

94. Grady, H.; Elder, D.; Webster, G. K.; Mao, Y.; Lin, Y.; Flanagan, T.; Mann, J.; Blanchard, A.; Cohen, M. J.; Lin, J.; Kesisoglou, F.; Hermans, A.; Abend, A.; Zhang, L.; Curran, D. Industry's View on Using Quality Control, Biorelevant, and Clinically Relevant Dissolution Tests for Pharmaceutical Development, Registration, and Commercialization. *J. Pharm. Sci.* **2018**, *107*, 34–41, doi:10.1016/j.xphs.2017.10.019.

95. Galia, E.; Nicolaides, E.; Hörter, D.; Löbenberg, R.; Reppas, C.; Dressman, J. B. Evaluation of various dissolution media for predicting in vivo performance of class I and II drugs. *Pharm. Res.* **1998**, *15*, 698–705.

96. Taylor, L. S.; Zhang, G. G. Z. Physical chemistry of supersaturated solutions and implications for oral absorption. *Adv. Drug Deliv. Rev.* **2016**, *101*, 122–142, doi:10.1016/j.addr.2016.03.006.

97. Friesen, D. T.; Shanker, R.; Crew, M.; Smithey, D. T.; Curatolo, W. J.; Nightingale, J. A. S. Hydroxypropyl Methylcellulose Acetate Succinate-Based Spray-Dried Dispersions: An Overview. *Mol. Pharm.* **2008**, *5*, 1003–1019, doi:10.1021/mp8000793.

98. Guzmán, H. R.; Tawa, M.; Zhang, Z.; Ratanabanangkoon, P.; Shaw, P.; Gardner, C. R.; Chen, H.; Moreau, J.; Almarsson, Ö.; Remenar, J. F. Combined Use of Crystalline Salt Forms and Precipitation Inhibitors to Improve Oral Absorption of Celecoxib from Solid Oral Formulations. *J. Pharm. Sci.* **2007**, *96*, 2686–2702, doi:10.1002/jps.20906.

99. Schwebel, H. J.; van Hoogevest, P.; Leigh, M. L. S.; Kuentz, M. The apparent solubilizing capacity of simulated intestinal fluids for poorly water-soluble drugs. *Pharm. Dev. Technol.* **2011**, *16*, 278–286, doi:10.3109/10837451003664099.

100. Ilevbare, G. A.; Taylor, L. S. Liquid–Liquid Phase Separation in Highly Supersaturated Aqueous Solutions of Poorly Water-Soluble Drugs: Implications for Solubility Enhancing

Formulations. *Cryst. Growth Des.* **2013**, *13*, 1497–1509, doi:10.1021/cg301679h.

101. Boyd, B. J.; Bergström, C. A. S.; Vinarov, Z.; Kuentz, M.; Brouwers, J.; Augustijns, P.; Brandl, M.; Bernkop-Schnürch, A.; Shrestha, N.; Préat, V.; Müllertz, A.; Bauer-Brandl, A.; Jannin, V. Successful oral delivery of poorly water-soluble drugs both depends on the intraluminal behavior of drugs and of appropriate advanced drug delivery systems. *Eur. J. Pharm. Sci.* **2019**, *137*, 104967, doi:10.1016/j.ejps.2019.104967.

102. Fong, S. Y. K.; Bauer-Brandl, A.; Brandl, M. Oral bioavailability enhancement through supersaturation: an update and meta-analysis. *Expert Opin. Drug Deliv.* **2017**, *14*, 403–426, doi:10.1080/17425247.2016.1218465.

103. Augustijns, P.; Brewster, M. E. Supersaturating Drug Delivery Systems: Fast is Not Necessarily Good Enough. *J. Pharm. Sci.* **2012**, *101*, 7–9, doi:10.1002/jps.22750.

104. Sironi, D.; Rosenberg, J.; Bauer-Brandl, A.; Brandl, M. PermeaLoop™, a novel in vitro tool for small-scale drug-dissolution/permeation studies. *J. Pharm. Biomed. Anal.* **2018**, *156*, 247–251, doi:10.1016/j.jpba.2018.04.042.

105. el-Egakey, M. A.; Soliva, M.; Speiser, P. Hot extruded dosage forms. I. Technology and dissolution kinetics of polymeric matrices. *Pharm. Acta Helv.* **1971**.

106. Breitenbach, J. Melt extrusion: from process to drug delivery technology. *Eur. J. Pharm. Biopharm.* **2002**, *54*, 107–117, doi:10.1016/S0939-6411(02)00061-9.

107. Thiry, J.; Krier, F.; Evrard, B. A review of pharmaceutical extrusion: Critical process parameters and scaling-up. *Int. J. Pharm.* **2015**, *479*, 227–240, doi:10.1016/j.ijpharm.2014.12.036.

108. Haser, A.; DiNunzio, J. C.; Martin, C.; McGinity, J. W.; Zhang, F. Melt Extrusion. In *Formulating Poorly Water Soluble Drugs*; Springer International Publishing, 2016; pp. 383–435.

109. FDA *Guidance for Industry: PAT – A Framework for Innovative Pharmaceutical Development, Manufacturing, and Quality Assurance*; 2005;

110. FDA *Guidance for Industry: Pharmaceutical cGMPs for the 21st Century: a risk-based approach*; 2004;

111. Martin, C. Twin Screw Extrusion for Pharmaceutical Processes. In *Melt Extrusion - Materials, Technology and Drug Product Design*; Springer New York: New York, 2013; pp. 47–79.

112. Shah, S.; Repka, M. A. Melt Extrusion in Drug Delivery: Three Decades of Progress. In *Melt Extrusion - Materials, Technology and Drug Product Design*; Springer New York: New York, 2013; pp. 3–46.

113. Shah, S.; Repka, M. A. Melt Extrusion in Drug Delivery: Three Decades of Progress. In *Melt Extrusion*; Springer New York, 2013; pp. 3–46.

114. Özgüney, I.; Shuwisitkul, D.; Bodmeier, R. Development and characterization of extended release Kollidon® SR mini-matrices prepared by hot-melt extrusion. *Eur. J. Pharm. Biopharm.*

2009, *73*, 140–145, doi:10.1016/j.ejpb.2009.04.006.

115. Prodduturi, S.; Urman, K. L.; Otaigbe, J. U.; Repka, M. A. Stabilization of hot-melt extrusion formulations containing solid solutions using polymer blends. *AAPS PharmSciTech* **2007**, *8*, E152–E161, doi:10.1208/pt0802050.

116. Price, D. J.; Ditzinger, F.; Koehl, N. J.; Jankovic, S.; Tsakiridou, G.; Nair, A.; Holm, R.; Kuentz, M.; Dressman, J. B.; Saal, C. Approaches to increase mechanistic understanding and aid in the selection of precipitation inhibitors for supersaturating formulations - a PEARRL review. *J. Pharm. Pharmacol.* **2019**, *71*, 483–509, doi:10.1111/jphp.12927.

117. Chokshi, R. J.; Shah, N. H.; Sandhu, H. K.; Malick, A. W.; Zia, H. Stabilization of Low Glass Transition Temperature Indomethacin Formulations: Impact of Polymer-Type and Its Concentration. *J. Pharm. Sci.* **2008**, *97*, 2286–2298, doi:10.1002/jps.21174.

118. Wyttenbach, N.; Janas, C.; Siam, M.; Lauer, M. E.; Jacob, L.; Scheubel, E.; Page, S. Miniaturized screening of polymers for amorphous drug stabilization (SPADS): Rapid assessment of solid dispersion systems. *Eur. J. Pharm. Biopharm.* **2013**, *84*, 583–598, doi:10.1016/j.ejpb.2013.01.009.

119. Repka, M. A.; Gerding, T. G.; Repka, S. L.; McGinity, J. W. Influence of Plasticizers and Drugs on the Physical-Mechanical Properties of Hydroxypropylcellulose Films Prepared by Hot Melt Extrusion. *Drug Dev. Ind. Pharm.* **1999**, *25*, 625–633, doi:10.1081/DDC-100102218.

120. Bookwala, M.; Thipsay, P.; Ross, S.; Zhang, F.; Bandari, S.; Repka, M. A. Preparation of a crystalline salt of indomethacin and tromethamine by hot melt extrusion technology. *Eur. J. Pharm. Biopharm.* **2018**, *131*, 109–119, doi:10.1016/j.ejpb.2018.08.001.

121. Singh, S.; Parikh, T.; Sandhu, H. K.; Shah, N. H.; Malick, A. W.; Singhal, D.; Serajuddin, A. T. M. Supersolubilization and Amorphization of a Model Basic Drug, Haloperidol, by Interaction with Weak Acids. *Pharm. Res.* **2013**, *30*, 1561–1573, doi:10.1007/s11095-013-0994-7.

122. Ditzinger, F.; Scherer, U.; Schönenberger, M.; Holm, R.; Kuentz, M. Modified Polymer Matrix in Pharmaceutical Hot Melt Extrusion by Molecular Interactions with a Carboxylic Coformer. *Mol. Pharm.* **2019**, *16*, 141–150, doi:10.1021/acs.molpharmaceut.8b00920.

123. Hildebrand, J.; Scott, R. The Solubility of Nonelectrolytes. *Reinhold, New York* **1950**, doi:10.1126/science.113.2938.450-a.

124. Laitinen, R.; Priemel, P. A.; Surwase, S.; Graeser, K.; Strachan, C. J.; Grohganz, H.; Rades, T. Theoretical Considerations in Developing Amorphous Solid Dispersions. In *Amorphous Solid Dispersions*; Springer New York, 2014; pp. 35–90.

125. Jankovic, S.; Tsakiridou, G.; Ditzinger, F.; Koehl, N. J.; Price, D. J.; Ilie, A.-R.; Kalantzi, L.; Kimpe, K.; Holm, R.; Nair, A.; Griffin, B.; Saal, C.; Kuentz, M. Application of the solubility parameter concept to assist with oral delivery of poorly water-soluble drugs - a PEARRL review. *J. Pharm. Pharmacol.* **2019**, *71*, 441–463, doi:10.1111/jphp.12948.

126. Van Krevelen, D. W. *Properties of Polymers, Their correlation with chemical structure; their numerical estimation and prediction from additive group contribution*; Elsevier, 1990; ISBN 9780080548197.

127. Niederquell, A.; Wyttenbach, N.; Kuentz, M. New prediction methods for solubility parameters based on molecular sigma profiles using pharmaceutical materials. *Int. J. Pharm.* **2018**, *546*, 137–144, doi:10.1016/j.ijpharm.2018.05.033.

128. Greenhalgh, D. J.; Williams, A. C.; Timmins, P.; York, P. Solubility parameters as predictors of miscibility in solid dispersions. *J. Pharm. Sci.* **1999**, *88*, 1182–1190, doi:10.1021/js9900856.

129. Forster, A.; Hempenstall, J.; Tucker, I.; Rades, T. Selection of excipients for melt extrusion with two poorly water-soluble drugs by solubility parameter calculation and thermal analysis. *Int. J. Pharm.* **2001**, *226*, 147–161, doi:10.1016/S0378-5173(01)00801-8.

130. Flory, P. J. *In Principles of polymer chemistry*; 1953; ISBN 0801401348.

131. Huggins, M. L. Some Properties of Solutions of Long-chain Compounds. *J. Phys. Chem.* **1942**, *46*, 151–158, doi:10.1021/j150415a018.

132. Pajula, K.; Taskinen, M.; Lehto, V.-P.; Ketolainen, J.; Korhonen, O. Predicting the Formation and Stability of Amorphous Small Molecule Binary Mixtures from Computationally Determined Flory−Huggins Interaction Parameter and Phase Diagram. *Mol. Pharm.* **2010**, *7*, 795–804, doi:10.1021/mp900304p.

133. Zhao, Y.; Inbar, P.; Chokshi, H. P.; Malick, A. W.; Choi, D. S. Prediction of the Thermal Phase Diagram of Amorphous Solid Dispersions by Flory–Huggins Theory. *J. Pharm. Sci.* **2011**, *100*, 3196–3207, doi:10.1002/jps.22541.

134. DeBoyace, K.; Wildfong, P. L. D. The Application of Modeling and Prediction to the Formation and Stability of Amorphous Solid Dispersions. *J. Pharm. Sci.* **2018**, *107*, 57–74, doi:10.1016/j.xphs.2017.03.029.

135. Tian, Y.; Booth, J.; Meehan, E.; Jones, D. S.; Li, S.; Andrews, G. P. Construction of Drug–Polymer Thermodynamic Phase Diagrams Using Flory–Huggins Interaction Theory: Identifying the Relevance of Temperature and Drug Weight Fraction to Phase Separation within Solid Dispersions. *Mol. Pharm.* **2013**, *10*, 236–248, doi:10.1021/mp300386v.

136. Gross, J.; Sadowski, G. Perturbed-Chain SAFT: An Equation of State Based on a Perturbation Theory for Chain Molecules. *Ind. Eng. Chem. Res.* **2001**, *40*, 1244–1260, doi:10.1021/ie0003887.

137. Anderson, B. D. Predicting Solubility/Miscibility in Amorphous Dispersions: It Is Time to Move Beyond Regular Solution Theories. *J. Pharm. Sci.* **2018**, *107*, 24–33, doi:10.1016/j.xphs.2017.09.030.

138. Prudic, A.; Ji, Y.; Luebbert, C.; Sadowski, G. Influence of humidity on the phase behavior of API/polymer formulations. *Eur. J. Pharm. Biopharm.* **2015**, *94*, 352–362, doi:10.1016/j.ejpb.2015.06.009.

139. Luebbert, C.; Huxoll, F.; Sadowski, G. Amorphous-Amorphous Phase Separation in API/Polymer Formulations. *Molecules* **2017**, *22*, 296, doi:10.3390/molecules22020296.

140. Karagianni, A.; Kachrimanis, K.; Nikolakakis, I. Co-Amorphous Solid Dispersions for Solubility and Absorption Improvement of Drugs: Composition, Preparation, Characterization and Formulations for Oral Delivery. *Pharmaceutics* **2018**, *10*, 98, doi:10.3390/pharmaceutics10030098.

141. Barmpalexis, P.; Karagianni, A.; Katopodis, K.; Vardaka, E.; Kachrimanis, K. Molecular modelling and simulation of fusion-based amorphous drug dispersions in polymer/plasticizer blends. *Eur. J. Pharm. Sci.* **2019**, *130*, 260–268, doi:10.1016/j.ejps.2019.02.004.

142. Barmpalexis, P.; Karagianni, A.; Kachrimanis, K. Molecular simulations for amorphous drug formulation: Polymeric matrix properties relevant to hot-melt extrusion. *Eur. J. Pharm. Sci.* **2018**, *119*, 259–267, doi:10.1016/j.ejps.2018.04.035.

143. Medarević, D.; Djuriš, J.; Barmpalexis, P.; Kachrimanis, K.; Ibrić, S. Analytical and Computational Methods for the Estimation of Drug-Polymer Solubility and Miscibility in Solid Dispersions Development. *Pharmaceutics* **2019**, *11*, 372, doi:10.3390/pharmaceutics11080372.

144. Laitinen, R.; Löbmann, K.; Grohganz, H.; Strachan, C.; Rades, T. Amino Acids as Co-amorphous Excipients for Simvastatin and Glibenclamide: Physical Properties and Stability. *Mol. Pharm.* **2014**, *11*, 2381–2389, doi:10.1021/mp500107s.

145. Laitinen, R.; Löbmann, K.; Grohganz, H.; Priemel, P.; Strachan, C. J.; Rades, T. Supersaturating drug delivery systems: The potential of co-amorphous drug formulations. *Int. J. Pharm.* **2017**, *532*, 1–12, doi:10.1016/j.ijpharm.2017.08.123.

146. Kasten, G.; Nouri, K.; Grohganz, H.; Rades, T.; Löbmann, K. Performance comparison between crystalline and co-amorphous salts of indomethacin-lysine. *Int. J. Pharm.* **2017**, *533*, 138–144, doi:10.1016/j.ijpharm.2017.09.063.

147. Dengale, S. J.; Grohganz, H.; Rades, T.; Löbmann, K. Recent advances in co-amorphous drug formulations. *Adv. Drug Deliv. Rev.* **2016**, *100*, 116–125, doi:10.1016/j.addr.2015.12.009.

148. Ditzinger, F.; Dejoie, C.; Sisak Jung, D.; Kuentz, M. Polyelectrolytes in Hot Melt Extrusion: A Combined Solvent-Based and Interacting Additive Technique for Solid Dispersions. *Pharmaceutics* **2019**, *11*, 174, doi:10.3390/pharmaceutics11040174.

149. Higashi, K.; Seo, A.; Egami, K.; Otsuka, N.; Limwikrant, W.; Yamamoto, K.; Moribe, K. Mechanistic insight into the dramatic improvement of probucol dissolution in neutral solutions by solid dispersion in Eudragit E PO with saccharin. *J. Pharm. Pharmacol.* **2016**, *68*, 655–664, doi:10.1111/jphp.12469.

150. Chavan, R. B.; Thipparaboina, R.; Kumar, D.; Shastri, N. R. Co amorphous systems: A product development perspective. *Int. J. Pharm.* **2016**, *515*, 403–415, doi:10.1016/j.ijpharm.2016.10.043.

151. Karimi-Jafari, M.; Padrela, L.; Walker, G. M.; Croker, D. M. Creating Cocrystals: A Review of

Pharmaceutical Cocrystal Preparation Routes and Applications. *Cryst. Growth Des.* **2018**, *18*, 6370–6387, doi:10.1021/acs.cgd.8b00933.

152. Desiraju, G. R. Crystal Engineering: A Holistic View. *Angew. Chemie Int. Ed.* **2007**, *46*, 8342–8356, doi:10.1002/anie.200700534.

153. Ueda, H.; Wu, W.; Löbmann, K.; Grohganz, H.; Müllertz, A.; Rades, T. Application of a Salt Coformer in a Co-Amorphous Drug System Dramatically Enhances the Glass Transition Temperature: A Case Study of the Ternary System Carbamazepine, Citric Acid, and L-Arginine. *Mol. Pharm.* **2018**, *15*, 2036–2044, doi:10.1021/acs.molpharmaceut.8b00174.

154. Löbmann, K.; Jensen, K. T.; Laitinen, R.; Rades, T.; Strachan, C. J.; Grohganz, H. Stabilized Amorphous Solid Dispersions with Small Molecule Excipients. In *Amorphous Solid Dispersions*; Springer New York: New York, 2014; pp. 613–636.

155. Seefeldt, K.; Miller, J.; Alvarez-Núñez, F.; Rodríguez-Hornedo, N. Crystallization Pathways and Kinetics of Carbamazepine–Nicotinamide Cocrystals from the Amorphous State by In Situ Thermomicroscopy, Spectroscopy, and Calorimetry Studies. *J. Pharm. Sci.* **2007**, *96*, 1147–1158, doi:10.1002/jps.20945.

156. Korhonen, O.; Pajula, K.; Laitinen, R. Rational excipient selection for co-amorphous formulations. *Expert Opin. Drug Deliv.* **2017**, *14*, 551–569, doi:10.1080/17425247.2016.1198770.

157. Pajula, K.; Lehto, V.-P.; Ketolainen, J.; Korhonen, O. Computational Approach for Fast Screening of Small Molecular Candidates To Inhibit Crystallization in Amorphous Drugs. *Mol. Pharm.* **2012**, *9*, 2844–2855, doi:10.1021/mp300135h.

158. Kasten, G.; Löbmann, K.; Grohganz, H.; Rades, T. Co-former selection for co-amorphous drug-amino acid formulations. *Int. J. Pharm.* **2019**, *557*, 366–373, doi:10.1016/j.ijpharm.2018.12.036.

159. Laitinen, R.; Löbmann, K.; Grohganz, H.; Priemel, P.; Strachan, C. J.; Rades, T. Supersaturating drug delivery systems: The potential of co-amorphous drug formulations. *Int. J. Pharm.* **2017**, *532*, 1–12, doi:10.1016/j.ijpharm.2017.08.123.

160. Jensen, K.; Löbmann, K.; Rades, T.; Grohganz, H. Improving Co-Amorphous Drug Formulations by the Addition of the Highly Water Soluble Amino Acid, Proline. *Pharmaceutics* **2014**, *6*, 416–435, doi:10.3390/pharmaceutics6030416.

161. Paluch, K. J.; McCabe, T.; Müller-Bunz, H.; Corrigan, O. I.; Healy, A. M.; Tajber, L. Formation and Physicochemical Properties of Crystalline and Amorphous Salts with Different Stoichiometries Formed between Ciprofloxacin and Succinic Acid. *Mol. Pharm.* **2013**, *10*, 3640–3654, doi:10.1021/mp400127r.

162. Dengale, S. J.; Hussen, S. S.; Krishna, B. S. M.; Musmade, P. B.; Gautham Shenoy, G.; Bhat, K. Fabrication, solid state characterization and bioavailability assessment of stable binary amorphous phases of Ritonavir with Quercetin. *Eur. J. Pharm. Biopharm.* **2015**, *89*, 329–338,

doi:10.1016/j.ejpb.2014.12.025.

163. Marks, J. A.; Wegiel, L. A.; Taylor, L. S.; Edgar, K. J. Pairwise Polymer Blends for Oral Drug Delivery. *J. Pharm. Sci.* **2014**, *103*, 2871–2883, doi:10.1002/jps.23991.

164. Ohyagi, N.; Ueda, K.; Higashi, K.; Yamamoto, K.; Kawakami, K.; Moribe, K. Synergetic Role of Hypromellose and Methacrylic Acid Copolymer in the Dissolution Improvement of Amorphous Solid Dispersions. *J. Pharm. Sci.* **2017**, *106*, 1042–1050, doi:10.1016/j.xphs.2016.12.005.

165. Serajuddin, A. T. M. Solid dispersion of poorly water-soluble drugs: Early promises, subsequent problems, and recent breakthroughs. *J. Pharm. Sci.* **1999**, *88*, 1058–1066, doi:10.1021/js980403l.

166. Hancock, B. C.; Zografi, G. Characteristics and Significance of the Amorphous State in Pharmaceutical Systems. *J. Pharm. Sci.* **1997**, *86*, 1–12, doi:10.1021/js9601896.

167. Janssens, S.; Van den Mooter, G. Review: physical chemistry of solid dispersions. *J. Pharm. Pharmacol.* **2009**, *61*, 1571–1586, doi:10.1211/jpp/61.12.0001.

168. Elder, D. P.; Kuentz, M.; Holm, R. Pharmaceutical excipients — quality, regulatory and biopharmaceutical considerations. *Eur. J. Pharm. Sci.* **2016**, *87*, 88–99, doi:10.1016/j.ejps.2015.12.018.

169. Desai, D.; Sandhu, H.; Shah, N.; Malick, W.; Zia, H.; Phuapradit, W.; Vaka, S. R. K. Selection of Solid-State Plasticizers as Processing Aids for Hot-Melt Extrusion. *J. Pharm. Sci.* **2018**, *107*, 372–379, doi:10.1016/j.xphs.2017.09.004.

170. Chavan, R. B.; Thipparaboina, R.; Kumar, D.; Shastri, N. R. Co amorphous systems: A product development perspective. *Int. J. Pharm.* **2016**, *515*, 403–415, doi:10.1016/j.ijpharm.2016.10.043.

171. Saal, W.; Ross, A.; Wyttenbach, N.; Alsenz, J.; Kuentz, M. Unexpected Solubility Enhancement of Drug Bases in the Presence of a Dimethylaminoethyl Methacrylate Copolymer. *Mol. Pharm.* **2018**, *15*, 186–192, doi:10.1021/acs.molpharmaceut.7b00804.

172. Saal, W.; Ross, A.; Wyttenbach, N.; Alsenz, J.; Kuentz, M. A Systematic Study of Molecular Interactions of Anionic Drugs with a Dimethylaminoethyl Methacrylate Copolymer Regarding Solubility Enhancement. *Mol. Pharm.* **2017**, *14*, 1243–1250, doi:10.1021/acs.molpharmaceut.6b01116.

173. Wu, W.; Löbmann, K.; Rades, T.; Grohganz, H. On the role of salt formation and structural similarity of co-formers in co-amorphous drug delivery systems. *Int. J. Pharm.* **2018**, *535*, 86–94, doi:10.1016/j.ijpharm.2017.10.057.

174. *Revolution Powder Analyzer User Manual*; Mercury Scientific Inc.: Newtown;

175. Tay, J. Y. S.; Liew, C. V.; Heng, P. W. S. Powder Flow Testing: Judicious Choice of Test Methods. *AAPS PharmSciTech* **2017**, *18*, 1843–1854, doi:10.1208/s12249-016-0655-3.

176. Meng, F.; Dave, V.; Chauhan, H. Qualitative and quantitative methods to determine miscibility

in amorphous drug–polymer systems. *Eur. J. Pharm. Sci.* **2015**, *77*, 106–111, doi:10.1016/j.ejps.2015.05.018.

177. Van Eerdenbrugh, B.; Taylor, L. S. An ab initio polymer selection methodology to prevent crystallization in amorphous solid dispersions by application of crystal engineering principles. *CrystEngComm* **2011**, *13*, 6171, doi:10.1039/c1ce05183k.

178. Kojima, T.; Higashi, K.; Suzuki, T.; Tomono, K.; Moribe, K.; Yamamoto, K. Stabilization of a Supersaturated Solution of Mefenamic Acid from a Solid Dispersion with EUDRAGIT® EPO. *Pharm. Res.* **2012**, *29*, 2777–2791, doi:10.1007/s11095-011-0655-7.

179. Parikh, T.; Serajuddin, A. T. M. Development of Fast-Dissolving Amorphous Solid Dispersion of Itraconazole by Melt Extrusion of its Mixture with Weak Organic Carboxylic Acid and Polymer. *Pharm. Res.* **2018**, *35*, 127, doi:10.1007/s11095-018-2407-4.

180. Baranska, H.; Kuduk-Jaworska, J.; Szostak, R.; Romaniewska, A. Vibrational spectra of racemic and enantiomeric malic acids. *J. Raman Spectrosc.* **2003**, *34*, 68–76, doi:10.1002/jrs.953.

181. Lauer, M. E.; Siam, M.; Tardio, J.; Page, S.; Kindt, J. H.; Grassmann, O. Rapid Assessment of Homogeneity and Stability of Amorphous Solid Dispersions by Atomic Force Microscopy— From Bench to Batch. *Pharm. Res.* **2013**, *30*, 2010–2022, doi:10.1007/s11095-013-1045-0.

182. Qian, F.; Huang, J.; Zhu, Q.; Haddadin, R.; Gawel, J.; Garmise, R.; Hussain, M. Is a distinctive single Tg a reliable indicator for the homogeneity of amorphous solid dispersion? *Int. J. Pharm.* **2010**, *395*, 232–235, doi:10.1016/j.ijpharm.2010.05.033.

183. Saal, W.; Wyttenbach, N.; Alsenz, J.; Kuentz, M. Interactions of dimethylaminoethyl methacrylate copolymer with non-acidic drugs demonstrated high solubilization in vitro and pronounced sustained release in vivo. *Eur. J. Pharm. Biopharm.* **2018**, *125*, 68–75, doi:10.1016/j.ejpb.2018.01.006.

184. Persson, L. C.; Porter, C. J. H.; Charman, W. N.; Bergström, C. A. S. Computational prediction of drug solubility in lipid based formulation excipients. *Pharm. Res.* **2013**, *30*, 3225–3237, doi:10.1007/s11095-013-1083-7.

185. Li, S.; Tian, Y.; Jones, D. S.; Andrews, G. P. Optimising Drug Solubilisation in Amorphous Polymer Dispersions: Rational Selection of Hot-melt Extrusion Processing Parameters. *AAPS PharmSciTech* **2016**, *17*, 200–213, doi:10.1208/s12249-015-0450-6.

186. Qi, S.; Gryczke, A.; Belton, P.; Craig, D. Q. M. Characterisation of solid dispersions of paracetamol and EUDRAGIT® E prepared by hot-melt extrusion using thermal, microthermal and spectroscopic analysis. *Int. J. Pharm.* **2008**, *354*, 158–167, doi:10.1016/j.ijpharm.2007.11.048.

187. Hurychová, H.; Kuentz, M.; Šklubalová, Z. Fractal Aspects of Static and Dynamic Flow Properties of Pharmaceutical Excipients. *J. Pharm. Innov.* **2018**, *13*, 15–26, doi:10.1007/s12247-017-9302-0.

188. Hancock, B. C.; Vukovinsky, K. E.; Brolley, B.; Grimsey, I.; Hedden, D.; Olsofsky, A.; Doherty, R. A. Development of a robust procedure for assessing powder flow using a commercial avalanche testing instrument. *J. Pharm. Biomed. Anal.* **2004**, *35*, 979–990, doi:10.1016/j.jpba.2004.02.035.

189. Nalluri, V. R.; Puchkov, M.; Kuentz, M. Toward better understanding of powder avalanching and shear cell parameters of drug–excipient blends to design minimal weight variability into pharmaceutical capsules. *Int. J. Pharm.* **2013**, *442*, 49–56, doi:10.1016/j.ijpharm.2012.08.010.

190. Schram, C. J.; Beaudoin, S. P.; Taylor, L. S. Impact of Polymer Conformation on the Crystal Growth Inhibition of a Poorly Water-Soluble Drug in Aqueous Solution. *Langmuir* **2015**, *31*, 171–179, doi:10.1021/la503644m.

191. Vertzoni, M.; Fotaki, N.; Nicolaides, E.; Reppas, C.; Kostewicz, E.; Stippler, E.; Leuner, C.; Dressman, J. Dissolution media simulating the intralumenal composition of the small intestine: physiological issues and practical aspects. *J. Pharm. Pharmacol.* **2004**, *56*, 453–462, doi:10.1211/0022357022935.

192. Wilson, M. R.; Jones, D. S.; Andrews, G. P. The development of sustained release drug delivery platforms using melt-extruded cellulose-based polymer blends. *J. Pharm. Pharmacol.* **2017**, *69*, 32–42, doi:10.1111/jphp.12656.

193. Repka, M. A.; Bandari, S.; Kallakunta, V. R.; Vo, A. Q.; McFall, H.; Pimparade, M. B.; Bhagurkar, A. M. Melt extrusion with poorly soluble drugs – An integrated review. *Int. J. Pharm.* **2018**, *535*, 68–85, doi:10.1016/j.ijpharm.2017.10.056.

194. Calcagnile, P.; Cacciatore, G.; Demitri, C.; Montagna, F.; Esposito Corcione, C. A Feasibility Study of Processing Polydimethylsiloxane–Sodium Carboxymethylcellulose Composites by a Low-Cost Fused Deposition Modeling 3D Printer. *Materials (Basel).* **2018**, *11*, 1578, doi:10.3390/ma11091578.

195. Cho, H.-J.; Jee, J.-P.; Kang, J.-Y.; Shin, D.-Y.; Choi, H.-G.; Maeng, H.-J.; Cho, K. Cefdinir Solid Dispersion Composed of Hydrophilic Polymers with Enhanced Solubility, Dissolution, and Bioavailability in Rats. *Molecules* **2017**, *22*, 280, doi:10.3390/molecules22020280.

196. Sahbaz, Y.; Williams, H. D.; Nguyen, T.-H.; Saunders, J.; Ford, L.; Charman, S. A.; Scammells, P. J.; Porter, C. J. H. Transformation of Poorly Water-Soluble Drugs into Lipophilic Ionic Liquids Enhances Oral Drug Exposure from Lipid Based Formulations. *Mol. Pharm.* **2015**, *12*, 1980–1991, doi:10.1021/mp500790t.

197. Stoimenovski, J.; MacFarlane, D. R.; Bica, K.; Rogers, R. D. Crystalline vs. Ionic Liquid Salt Forms of Active Pharmaceutical Ingredients: A Position Paper. *Pharm. Res.* **2010**, *27*, 521–526, doi:10.1007/s11095-009-0030-0.

198. Rowe, R. C.; Sheskey, P. J.; Fenton, M. E. Handbook Of Pharmaceutical Excipients: Pharmaceutical Excipients. In *American Pharmacists Association*; Washington D.C., USA, 2012 ISBN 0853696187.

199. Löbmann, K.; Laitinen, R.; Strachan, C.; Rades, T.; Grohganz, H. Amino acids as co-amorphous stabilizers for poorly water-soluble drugs – Part 2: Molecular interactions. *Eur. J. Pharm. Biopharm.* **2013**, *85*, 882–888, doi:10.1016/j.ejpb.2013.03.026.

200. Jensen, K. T.; Larsen, F. H.; Cornett, C.; Löbmann, K.; Grohganz, H.; Rades, T. Formation Mechanism of Coamorphous Drug–Amino Acid Mixtures. *Mol. Pharm.* **2015**, *12*, 2484–2492, doi:10.1021/acs.molpharmaceut.5b00295.

201. Li, L.; AbuBaker, O.; Shao, Z. J. Characterization of Poly(Ethylene Oxide) as a Drug Carrier in Hot-Melt Extrusion. *Drug Dev. Ind. Pharm.* **2006**, *32*, 991–1002, doi:10.1080/03639040600559057.

202. Ashiotis, G.; Deschildre, A.; Nawaz, Z.; Wright, J. P.; Karkoulis, D.; Picca, F. E.; Kieffer, J. The fast azimuthal integration Python library: pyFAI. *J. Appl. Crystallogr.* **2015**, *48*, 510–519, doi:10.1107/S1600576715004306.

203. Lu, Q.; Zografi, G. Phase behavior of binary and ternary amorphous mixtures containing indomethacin, citric acid, and PVP. *Pharm. Res.* **1998**, *15*, 1202–6.

204. Yadollahi, M.; Namazi, H. Synthesis and characterization of carboxymethyl cellulose/layered double hydroxide nanocomposites. *J. Nanoparticle Res.* **2013**, *15*, 1563, doi:10.1007/s11051-013-1563-z.

205. Fan, L.; Peng, M.; Zhou, X.; Wu, H.; Hu, J.; Xie, W.; Liu, S. Modification of carboxymethyl cellulose grafted with collagen peptide and its antioxidant activity. *Carbohydr. Polym.* **2014**, *112*, 32–38, doi:10.1016/j.carbpol.2014.05.056.

206. Ellenberger, D.; O'Donnell, K. P.; Williams, R. O. Optimizing the Formulation of Poorly Water-Soluble Drugs. In *Formulating Poorly Water Soluble Drugs*; Springer International Publishing: Cham, 2016; pp. 41–120.

207. Gupta, P.; Bansal, A. K. Molecular interactions in celecoxib-PVP-meglumine amorphous system. *J. Pharm. Pharmacol.* **2005**, *57*, 303–310, doi:10.1211/0022357055597.

208. Edueng, K.; Mahlin, D.; Larsson, P.; Bergström, C. A. S. Mechanism-based selection of stabilization strategy for amorphous formulations: Insights into crystallization pathways. *J. Control. Release* **2017**, *256*, 193–202, doi:10.1016/j.jconrel.2017.04.015.

209. Telang, C.; Mujumdar, S.; Mathew, M. Improved physical stability of amorphous state through acid base interactions. *J. Pharm. Sci.* **2009**, *98*, 2149–2159, doi:10.1002/jps.21584.

210. Heinz, A.; Strachan, C. J.; Gordon, K. C.; Rades, T. Analysis of solid-state transformations of pharmaceutical compounds using vibrational spectroscopy. *J. Pharm. Pharmacol.* **2009**, *61*, 971–988, doi:10.1211/jpp.61.08.0001.

211. Mankova, A. A.; Borodin, A. V.; Kargovsky, A. V.; Brandt, N. N.; Kuritsyn, I. I.; Luo, Q.; Sakodynskaya, I. K.; Wang, K. J.; Zhao, H.; Chikishev, A. Y.; Shkurinov, A. P.; Zhang, X.-C. Terahertz time-domain and FTIR spectroscopy of tris-crown interaction. *Chem. Phys. Lett.* **2012**, *554*, 201–207, doi:10.1016/j.cplett.2012.10.039.

212. Hebeish, A.; Sharaf, S. Novel nanocomposite hydrogel for wound dressing and other medical applications. *RSC Adv.* **2015**, *5*, 103036–103046, doi:10.1039/C5RA07076G.

213. Rams-Baron, M.; Jachowicz, R.; Boldyreva, E.; Zhou, D.; Jamroz, W.; Paluch, M. Physical Instability: A Key Problem of Amorphous Drugs. In *Amorphous Drugs*; Springer International Publishing: Cham, 2018; pp. 107–157.

214. Van Eerdenbrugh, B.; Baird, J. A.; Taylor, L. S. Crystallization Tendency of Active Pharmaceutical Ingredients Following Rapid Solvent Evaporation—Classification and Comparison with Crystallization Tendency from Under cooled Melts. *J. Pharm. Sci.* **2010**, *99*, 3826–3838, doi:10.1002/jps.22214.

215. Sliwinska-Bartkowiak, M.; Dudziak, G.; Gras, R.; Sikorski, R.; Radhakrishnan, R.; Gubbins, K. E. Freezing behavior in porous glasses and MCM-41. *Colloids Surfaces A Physicochem. Eng. Asp.* **2001**, *187–188*, 523–529, doi:10.1016/S0927-7757(01)00637-9.

216. McCarthy, C. A.; Ahern, R. J.; Dontireddy, R.; Ryan, K. B.; Crean, A. M. Mesoporous silica formulation strategies for drug dissolution enhancement: a review. *Expert Opin. Drug Deliv.* **2016**, *13*, 93–108, doi:10.1517/17425247.2016.1100165.

217. Azaïs, T.; Tourné-Péteilh, C.; Aussenac, F.; Baccile, N.; Coelho, C.; Devoisselle, J.-M.; Babonneau, F. Solid-State NMR Study of Ibuprofen Confined in MCM-41 Material. *Chem. Mater.* **2006**, *18*, 6382–6390, doi:10.1021/cm061551c.

218. Müller, R. H.; Wei, Q.; Keck, C. M. CapsMorph: >4 Years long-term stability of industrially feasible amorphous drug formulations. In *Int. Symp. Control. Rel. Bioact. Mater. 40*; Honolulu/Hawai, 2013.

219. Mellaerts, R.; Houthoofd, K.; Elen, K.; Chen, H.; Van Speybroeck, M.; Van Humbeeck, J.; Augustijns, P.; Mullens, J.; Van den Mooter, G.; Martens, J. A. Aging behavior of pharmaceutical formulations of itraconazole on SBA-15 ordered mesoporous silica carrier material. *Microporous Mesoporous Mater.* **2010**, *130*, 154–161, doi:10.1016/j.micromeso.2009.10.026.

220. Salonen, J.; Kaukonen, A. M.; Hirvonen, J.; Lehto, V.-P. Mesoporous Silicon in Drug Delivery Applications. *J. Pharm. Sci.* **2008**, *97*, 632–653, doi:10.1002/jps.20999.

221. Williams, H. D.; Trevaskis, N. L.; Charman, S. A.; Shanker, R. M.; Charman, W. N.; Pouton, C. W.; Porter, C. J. H. Strategies to address low drug solubility in discovery and development. *Pharmacol. Rev.* **2013**, *65*, 315–499.

222. Knopp, M. M.; Wendelboe, J.; Holm, R.; Rades, T. Effect of amorphous phase separation and crystallization on the in vitro and in vivo performance of an amorphous solid dispersion. *Eur. J. Pharm. Biopharm.* **2018**, *130*, 290–295, doi:10.1016/j.ejpb.2018.07.005.

223. Brough, C.; Miller, D. A.; Keen, J. M.; Kucera, S. A.; Lubda, D.; Williams, R. O. Use of Polyvinyl Alcohol as a Solubility-Enhancing Polymer for Poorly Water Soluble Drug Delivery (Part 1). *AAPS PharmSciTech* **2016**, *17*, 167–179, doi:10.1208/s12249-015-0458-y.

224. Price, D. J.; Nair, A.; Kuentz, M.; Dressman, J.; Saal, C. Calculation of drug-polymer mixing enthalpy as a new screening method of precipitation inhibitors for supersaturating pharmaceutical formulations. *Eur. J. Pharm. Sci.* **2019**, *132*, 142–156, doi:10.1016/j.ejps.2019.03.006.

225. ICH Expert Working Group ICH Guideline Q1A(R2) Stability Testing of New Drug Substances and Products. In *International Conference on Harmonization*; 2003 ISBN 0269-4727.

226. Dressman, J. B.; Amidon, G. L.; Reppas, C.; Shah, V. P. Dissolution testing as a prognostic tool for oral drug absorption: immediate release dosage forms. *Pharm. Res.* **1998**, *15*, 11–22.

227. Edueng, K.; Mahlin, D.; Gråsjö, J.; Nylander, O.; Thakrani, M.; Bergström, C. A. S. Supersaturation Potential of Amorphous Active Pharmaceutical Ingredients after Long-Term Storage. *Molecules* **2019**, *24*, 2731, doi:10.3390/molecules24152731.

228. Paudel, A.; Geppi, M.; Mooter, G. Van den Structural and Dynamic Properties of Amorphous Solid Dispersions: The Role of Solid-State Nuclear Magnetic Resonance Spectroscopy and Relaxometry. *J. Pharm. Sci.* **2014**, *103*, 2635–2662, doi:10.1002/jps.23966.

229. Lee, H. L.; Vasoya, J. M.; Cirqueira, M. de L.; Yeh, K. L.; Lee, T.; Serajuddin, A. T. M. Continuous Preparation of 1:1 Haloperidol–Maleic Acid Salt by a Novel Solvent-Free Method Using a Twin Screw Melt Extruder. *Mol. Pharm.* **2017**, *14*, 1278–1291, doi:10.1021/acs.molpharmaceut.7b00003.

230. Djuris, J.; Nikolakakis, I.; Ibric, S.; Djuric, Z.; Kachrimanis, K. Preparation of carbamazepine–Soluplus® solid dispersions by hot-melt extrusion, and prediction of drug–polymer miscibility by thermodynamic model fitting. *Eur. J. Pharm. Biopharm.* **2013**, *84*, 228–237, doi:10.1016/j.ejpb.2012.12.018.

231. Zheng, M.; Bauer, F.; Birk, G.; Lubda, D. Polyvinyl Alcohol in Hot Melt Extrusion to Improve the Solubility of Drugs Available online: https://www.sigmaaldrich.com/content/dam/sigma-aldrich/0/content/pdf/PS-PVA-HME-Improve-Solubility-03-2017_EN_MS.pdf (accessed on May 2, 2019).

232. Loschen, C.; Klamt, A. COSMO quick : A Novel Interface for Fast σ-Profile Composition and Its Application to COSMO-RS Solvent Screening Using Multiple Reference Solvents. *Ind. Eng. Chem. Res.* **2012**, *51*, 14303–14308, doi:10.1021/ie3023675.

233. Greenspan, L. Humidity fixed points of binary saturated aqueous solutions. *J. Res. Natl. Bur. Stand. Sect. A Phys. Chem.* **1977**, *81A*, 89–96, doi:10.6028/jres.081a.011.

234. Kissi, E. O.; Ruggiero, M. T.; Hempel, N.-J.; Song, Z.; Grohganz, H.; Rades, T.; Löbmann, K. Characterising glass transition temperatures and glass dynamics in mesoporous silica-based amorphous drugs. *Phys. Chem. Chem. Phys.* **2019**, doi:10.1039/C9CP01764J.

235. Patel, D. D.; Anderson, B. D. Effect of Precipitation Inhibitors on Indomethacin Supersaturation Maintenance: Mechanisms and Modeling. *Mol. Pharm.* **2014**, *11*, 1489–1499,

doi:10.1021/mp400658k.

236. Mehta, M.; Suryanarayanan, R. Accelerated Physical Stability Testing of Amorphous Dispersions. *Mol. Pharm.* **2016**, *13*, 2661–2666, doi:10.1021/acs.molpharmaceut.6b00218.

237. Cordeiro, T.; Castiñeira, C.; Mendes, D.; Danède, F.; Sotomayor, J.; Fonseca, I. M.; Gomes da Silva, M.; Paiva, A.; Barreiros, S.; Cardoso, M. M.; Viciosa, M. T.; Correia, N. T.; Dionisio, M. Stabilizing Unstable Amorphous Menthol through Inclusion in Mesoporous Silica Hosts. *Mol. Pharm.* **2017**, *14*, 3164–3177, doi:10.1021/acs.molpharmaceut.7b00386.

238. Dahan, A.; Beig, A.; Lindley, D.; Miller, J. M. The solubility–permeability interplay and oral drug formulation design: Two heads are better than one. *Adv. Drug Deliv. Rev.* **2016**, *101*, 99–107, doi:10.1016/j.addr.2016.04.018.

239. Buckley, S. T.; Frank, K. J.; Fricker, G.; Brandl, M. Biopharmaceutical classification of poorly soluble drugs with respect to "enabling formulations." *Eur. J. Pharm. Sci.* 2013.

240. Chavan, R. B.; Thipparaboina, R.; Kumar, D.; Shastri, N. R. Evaluation of the inhibitory potential of HPMC, PVP and HPC polymers on nucleation and crystal growth. *RSC Adv.* **2016**, *6*, 77569–77576, doi:10.1039/C6RA19746A.

241. Williams, H. D.; Trevaskis, N. L.; Charman, S. A.; Shanker, R. M.; Charman, W. N.; Pouton, C. W.; Porter, C. J. H. Strategies to Address Low Drug Solubility in Discovery and Development. *Pharmacol. Rev.* **2013**, *65*, 315–499, doi:10.1124/pr.112.005660.

242. Barmpalexis, P.; Syllignaki, P.; Kachrimanis, K. A study of water uptake by selected superdisintegrants from the sub-molecular to the particulate level. *Pharm. Dev. Technol.* **2018**, *23*, 476–487, doi:10.1080/10837450.2017.1280827.

243. Moser, K.; Kriwet, K.; Kalia, Y. N.; Guy, R. H. Stabilization of supersaturated solutions of a lipophilic drug for dermal delivery. *Int. J. Pharm.* **2001**, *224*, 169–176, doi:10.1016/S0378-5173(01)00762-1.

244. Hancock, B. C.; Shamblin, S. L.; Zografi, G. Molecular Mobility of Amorphous Pharmaceutical Solids Below Their Glass Transition Temperatures. *Pharm. Res. An Off. J. Am. Assoc. Pharm. Sci.* **1995**, doi:10.1023/A:1016292416526.

245. Bevernage, J.; Forier, T.; Brouwers, J.; Tack, J.; Annaert, P.; Augustijns, P. Excipient-Mediated Supersaturation Stabilization in Human Intestinal Fluids. *Mol. Pharm.* **2011**, *8*, 564–570, doi:10.1021/mp100377m.

246. Markopoulos, C.; Andreas, C. J.; Vertzoni, M.; Dressman, J.; Reppas, C. In-vitro simulation of luminal conditions for evaluation of performance of oral drug products: Choosing the appropriate test media. *Eur. J. Pharm. Biopharm.* **2015**, *93*, 173–182, doi:10.1016/j.ejpb.2015.03.009.

247. Berthelsen, R.; Holm, R.; Jacobsen, J.; Kristensen, J.; Abrahamsson, B.; Müllertz, A. Kolliphor Surfactants Affect Solubilization and Bioavailability of Fenofibrate. Studies of in Vitro Digestion and Absorption in Rats. *Mol. Pharm.* **2015**, *12*, 1062–1071,

doi:10.1021/mp500545k.

248.   Negrini, R.; Aleandri, S.; Kuentz, M. Study of Rheology and Polymer Adsorption Onto Drug Nanoparticles in Pharmaceutical Suspensions Produced by Nanomilling. *J. Pharm. Sci.* **2017**, *106*, 3395–3401, doi:10.1016/j.xphs.2017.07.006.

249.   Krieger, E.; Vriend, G. YASARA View – molecular graphics for all devices from smartphones to work stations. *Bioinformatics* **2014**, *30*, 2981–2982.

250.   Do, T. T.; Van Speybroeck, M.; Mols, R.; Annaert, P.; Martens, J.; Van Humbeeck, J.; Vermant, J.; Augustijns, P.; Van den Mooter, G. The conflict between in vitro release studies in human biorelevant media and the in vivo exposure in rats of the lipophilic compound fenofibrate. *Int. J. Pharm.* **2011**, *414*, 118–124, doi:10.1016/j.ijpharm.2011.05.009.

251.   Fagerberg, J. H.; Karlsson, E.; Ulander, J.; Hanisch, G.; Bergström, C. A. S. Computational Prediction of Drug Solubility in Fasted Simulated and Aspirated Human Intestinal Fluid. *Pharm. Res.* **2015**, *32*, 578–589, doi:10.1007/s11095-014-1487-z.

252.   Kalivoda, A.; Fischbach, M.; Kleinebudde, P. Application of mixtures of polymeric carriers for dissolution enhancement of fenofibrate using hot-melt extrusion. *Int. J. Pharm.* **2012**, *429*, 58–68, doi:10.1016/j.ijpharm.2012.03.009.

253.   Liu, X.; Zhou, L.; Zhang, F. Reactive Melt Extrusion To Improve the Dissolution Performance and Physical Stability of Naproxen Amorphous Solid Dispersions. *Mol. Pharm.* **2017**, *14*, 658–673, doi:10.1021/acs.molpharmaceut.6b00960.

254.   Warren, D. B.; Benameur, H.; Porter, C. J. H.; Pouton, C. W. Using polymeric precipitation inhibitors to improve the absorption of poorly water-soluble drugs: A mechanistic basis for utility. *J. Drug Target.* **2010**, *18*, 704–731, doi:10.3109/1061186X.2010.525652.

255.   Barbucci, R.; Magnani, A.; Consumi, M. Swelling Behavior of Carboxymethylcellulose Hydrogels in Relation to Cross-Linking, pH, and Charge Density. *Macromolecules* **2000**, *33*, 7475–7480, doi:10.1021/ma0007029.

List of abbreviations

AFM	Atomic force microscopy
API	Active pharmaceutical ingredient
ATR-FTIR	Attenuated total reflectance Fourier-transform infrared spectroscopy
BCS	Biopharmaceutics classification system
CLSM	Confocal laser scanning microscopy
DCS	Development classification system
DMSO	Dimethyl sulfoxide
DSC	Differential scanning calorimetry
DVS	Dynamic vapor sorption
EDX	Energy dispersive X-ray analysis
EE	Eudragit E PO
FaSSIF	Fasted state simulated intestinal fluid
FE	Fenofibrate
GFA (I/II/III)	Glass forming ability class (I/II/III)
GI	Gastro intestinal
HPLC	High performance liquid chromatography
HME	Hot melt extrusion
HSM	Hot stage microscopy
HSQC	Heteronuclear single quantum coherence spectroscopy
LC	Liquid chromatography

Lys	Lysine
MA	Malic acid
Meg	Meglumine
MPB	Micro-precipitated bulk powder
NaCMC	Sodium carboxymethyl cellulose
PAT	Process analytical technology
PDF	Pair distribution function
PLM	Polarized light microscopy
PVA	Polyvinyl alcohol
PXRD	Powder X-ray diffraction
RH	Relative humidity
RT	Room temperature
TRIS	Trometamol
SEM	Scattering electron microscopy
(SS)-NMR	(Solid-state) nuclear magnetic resonance spectroscopy
UV/VIS	Ultra violet / visible light
UHPLC	Ultra high pressure liquid chromatography

List of figures

List of tables

List of symbols

δ_d	Partial solubility parameter atomic nonpolar forces
δ_h	Partial solubility parameter hydrogen bonding
δ_p	Partial solubility parameter polar forces
δ_{total}	Total solubility parameter
E_d	Energy atomic nonpolar forces
E_h	Energy hydrogen bonding
E_p	Energy polar forces
E_{total}	Total cohesive energy
$\Delta G^{a,c}{}_T$	Difference in Gibbs free energy between the amorphous and the crystalline form at a given temperature
ΔG_{mix}	Gibbs free energy of mixing
$\log P$	Partitioning constant
$\varphi_{d/p}$	Volume fraction of drug or polymer
$n_{d/p}$	Molar amount of drug or polymer
$\log S_w$	Water solubility of a drug
R	Ideal gas constant
$\sigma^a{}_T$	Chemical potential of the amorphous form at a given temperature
$\sigma^c{}_T$	Chemical potential of the crystalline form at a given temperature
T_g	Glass transition temperature
T_{dec}	Degradation temperature

T_m	Melting point
V_m	Molar Volume
X_{dp}	Flory-huggins interaction parameter for a drug-polymer mixture